InSTREAM

In Situ Turbulence Replication and Measurement

FINAL REPORT

October 1, 2015 to January 31, 2018

OERA Project Number: 300-173-1

Rockland Scientific International

Peter Stern, Fabian Wolk

Submitted on January 31, 2018

Contents

1. Executive Summary

The In Situ Turbulence Replication and Measurement (InSTREAM) project was conceived to address some fundamental questions about the turbulence physics in tidal energy sites and laboratory tanks used to simulate these sites. The objective was to develop a sensor system that could measure across the full spectral range of turbulent motion found in these tidal energy generation sites. This system would combine traditional acoustic and electro-magnetic sensors with the Rockland Scientific shear sensor technology, used in traditional physical oceanography turbulence research. By deploying this sensor system in a laboratory test tank and tidal energy sites the data sets can be compared between the real-world and the laboratory and insights into the scaling effects can be obtained.

The project consortium was funded by the Offshore Energy Research Association of Nova Scotia and Innovate UK. The partners are:

Rockland Scientific International (Rockland), Victoria, BC, Canada
Dalhousie University (Dalhousie), Halifax, NS, Canada
BlackRock Tidal Power (BlackRock), NS, Canada
FloWave Ocean Energy Research Facility (FloWave), University of Edinburgh, UK
European Marine Energy Center (EMEC), Orkney, UK
Ocean Array Systems (OAS), now Octue, Cambridge, UK

The project started in November 2015 and was completed in November 2017. The sensors were designed and deployed in the FloWave tank in early 2016. A similar sensor suite and a novel datalogging and data handling system was created for the EMEC deployment at the Fall of Warness tidal test site in Orkney, Scotland. This was to be a long term deployment on the EMEC Instrumentation Pod, which is placed on the seabed. The third deployment was in the Black Rock Tidal Power berth at the FORCE site in Minas Passage, Bay of Fundy, Nova Scotia. The FORCE deployment used two *Nemo* moorings used previously in the TiME project and in other research conducted by Prof. Alex Hay, Dalhousie University.

Data was successfully collected from FloWave and FORCE. Unfortunately, the combination of a software bug and simultaneous failure of the IMP shore cable precluded the collection of useful scientific data from the EMEC deployment. However, the EMEC deployment was successful in proving the novel system design and data handling architecture, as well as the long-term survivability of the Rockland sensors.

All available data from the various deployments was pre-processed by Rockland Scientific and Dalhousie University and this was presented together with the raw data to Ocean Array Systems for analysis and numerical modelling. Using and extending the methodology from the TiME project, OAS characterized the turbulent flow in the FloWave tank and at the FORCE site. This was used to create simulations of a typical tidal energy turbine, and an array of turbines, in these two environments. This analysis work is invaluable for the engineering and scientific understanding of the turbulent flow effects on devices. The recent and future publications based on these data sets are key-stone work, and both Rockland and OAS will continue to educate the Tidal Energy Conversion community using the InSTREAM data.

The new sensor system allows point-based and multi-point measurements of the flow, which is essential for extracting turbulent structure. As a result, the reliability of analysis when scaling results from tank to real-world environments, based on the full characterization of the flow dynamics, is now achievable with a greater level of confidence than with existing acoustic techniques.

Despite minor technical and operational setbacks, we consider the InSTREAM project as success, resulting in numerous technical and commercial outcomes. For the Canadian project partners these can be summarized as follows:

- Developed and tested measurement instrumentation and methodology for accurately, repeatedly, and reliably characterize turbulent flow in laboratory and field.
- Generated a wealth of turbulent flow data sets from tidal energy test sites in Canada and the UK that will inform scientific and engineering work aimed at understanding of the impact of turbulence on tidal energy converters, as well as describing and understanding site specific flow conditions.
- Completed a case-study of turbine performance analysis and comparative numerical modeling of turbine wake effects in laboratory and field conditions.

2. Project Introduction

Background

In the marine environment tidal channels are an active region of interest for electrical power generation using turbines and other types of energy conversion machines. Tidal races are inherently turbulent. This variability of the water flow speed, direction and intensity affects the reliability and efficiency of energy extraction machines, typically turbines situated on the sea floor. As well, the turbulent wakes downstream of the turbines complicate the efficiency of energy capture at array installations, and the wake may have environmental effects (scouring).

To properly understand the turbulent regime in these locations it is necessary to measure the mean current speeds and velocity fluctuations across a range of length scales. Furthermore, these tidal dependent parameters have a time dependency over the tidal cycle. The predictability of tidal currents is limited by: (i) fluctuations over time scales on the order of hours are observed that cannot be replicated in standard ocean models; (ii) device-scale turbulent fluctuations over time scales of seconds are significant and inherently unpredictable; and (iii) predictions are localized within 100 m from the measurement location.

Current practice heavily relies on Acoustic Doppler Current Profilers (ADCPs) located several meters away from the point location of interest in tidal energy sites. These acoustic devices are impractical to use in the shallow depths of laboratory test tanks and they have considerable uncertainty in their measurements because of intrinsic noise and their divergent beam geometry. Commercially available ADCPs are resolution limited O(10+ m) ranges – their sampling rates are less then 100 Hz, and the maximum spatial resolution is less then 25 cm. Furthermore, because they consolidate the measurement into a single, instantaneous velocity they do not directly resolve the actual quantities of interest. Namely the Cartesian components of that velocity (u, v, w). Instead, estimates are given for u, v, w based on measurements of V along the different beam axes, and because the beams diverge only time-averaged quantities can be estimated and homogeneity on the spatial scale of beam separation – O(10 m) at 10+ m range – must be assumed. Thus, only second order turbulence statistics can be estimated.

Acoustic Doppler Velocimeters (ADVs) can provide point measurements with a high temporal resolution. However, they rely on acoustic scatterers in the water, especially in rapidly changing flows. There is often a lack of particles in tidal channels and this hinders the usefulness of ADVs. Using ADVs in laboratory setups also requires scatters which can be problematic in test flumes and tanks. As well, laboratory grade ADVs are usually not rugged enough for field work.

Velocity shear probes have long been used in the physical oceanography community for direct turbulence measurements (microstructure), specifically turbulent kinetic energy dissipation. These sensors have proven to be robust and reliable. They are in direct contact with the water and deform microscopically under the influence of the cross-stream (turbulent u,v,w) flow vectors.

These challenges and limitations in existing measurement practice point to a need for a measurement capability that can capture continuous full-spectrum turbulence in high-speed tidal flows. Both in the real world of tidal energy sites and in laboratory settings to allow for scale modelling.

The InSTREAM project was conceived to address these questions. The project consortium consisted of:

Rockland Scientific International (Rockland), Victoria, BC, Canada

Dalhousie University (Dalhousie), Halifax, NS, Canada

BlackRock Tidal Power (BlackRock), NS, Canada

FloWave Ocean Energy Research Facility (FloWave), University of Edinburgh, UK

European Marine Energy Center (EMEC), Orkney, UK

Ocean Array Systems (OAS), now Octue, Cambridge, UK

Objectives and Methodology

Given the shortcomings of existing measurement technology, the **main goal** of the project is to develop a **system for measuring, understanding, and describing turbulent velocity fluctuations in tidal flows, on all length scales that are pertinent for tidal energy generation**. The system will comprise sensor technology and experiment methodology such that results are directly 'translatable' between test tank and real-world environments and can be relied upon as a legitimate and recognised basis for standards-compliant and bank-grade performance analyses and predictions.

The **first key objective** is to develop existing non-acoustic shear probe technology–already proven in the real marine environment–into laboratory grade instrumentation. Thus, identical sensors can be used in both the laboratory and the in-field environments, eliminating the 'disconnect' between the present laboratory and ocean-ready sensor technologies. Furthermore, these previously disparate measurement results can be compared directly and without the uncertainty of using different sensor technologies in the two environments.

The **second key objective** is to use field-deployable versions of the laboratory instrument at the EMEC and FORCE sites. Field data from EMEC and FORCE enable real-world measurements to be down translated to tank scale, and vice versa. The measurements system at EMEC will connect directly to the existing Integrated Monitoring Pod (IMP). The location of the measurements at EMEC will be in the centre of the site, providing the maximum benefit to all EMEC test berths. At FORCE, the measurement

system will be connected to a mid-water-column floating platform previously tested at Grand Passage (Dalhousie University). The FORCE Bay of Fundy test site was provided by project partner Black Rock Tidal Power and the experiment was undertaken with project partner Alex Hay from Dalhousie University, using their Nemo mooring buoy and the Rockland Scientific mooring buoy.

Finally, the **third key objectiv**e is to characterise the measurement results according to their turbulent structural content using the new tools and descriptors being demonstrated by OAS in the MRCF TiME project.

To conduct the work the project was divided into several work packages and a master schedule established using project management software. This schedule was revised several times throughout the project to reflect actual progress and delays. The final version is Revision 3.9 and is found in Appendix A along with a summary timeline.

The first two work packages relate to the FloWave laboratory instrumentation and experimental measurements. Work package 1 covered the instrumentation design, development and functional testing to verify that the system worked. Work package two comprised the experimental measurement campaign to characterize the flow in the tank.

Work package 3 covered the EMEC system design, construction, integration and deployment and recovery. This was the riskiest experimental field work because of the many unknowns regarding the system integration onto the EMEC Instrumentation Monitoring Pod (IMP) and the planned long term deployment of six months or more.

Work package 4 was the deployment of two “Nemo” mooring buoys outfitted with Rockland MicroRider turbulence measurement instruments and ADCPs. This work was done in partnership with Black Rock Tidal Power and Dalhousie University Professor Alex Hay and his team. BRTP provided the logistical support and the use of their site within the FORCE area. The Dalhousie group provided their mooring buoy, on-site support to help with the preparations, deployment and recovery and first pass processing of the ADCP data. The FORCE experiment fell into work package 4. This included the upgrades to the mooring buoys, MicroRider turbulence measurement instrument, selecting the test sites, and the deployment and recovery with Dalhousie and Black Rock Tidal Power.

Data analysis and numerical modeling was the next step, work package 5. First pass analysis was done by Rockland Scientific, Ocean Array Systems and Dalhousie to verify and qualify the data and prepare the data sets for the numerical modelling. Ocean Array Systems (now Octue) took all the data and did the numerical modelling.

Work packages 1, 2 and 3 were done in parallel as much as possible. The FloWave work was begun first, followed soon thereafter by the design work for the EMEC and FORCE systems.

3. Scientific Objectives

The key objectives of the project are to:

1. Develop laboratory grade instrumentation based on existing Rockland technology and use it in the FloWave tank

2. Make a field deployable version of the laboratory instrument and use them at the EMEC and FORCE sites
3. Characterize the measurement results from all three sites using the software tools and techniques demonstrated by OAS

There have been no changes to these objectives compared to the original project plan.

4. Description of Work

WP 1 Tidal Tank Measurement System

The key objectives of developing laboratory grade turbulence instrumentation by Rockland and characterizing the FloWave tank using this equipment was the focus of the first two work packages. The characterization experimental plan was generated through several meetings and discussions between Rockland, FloWave, Ocean Array Systems with some comments provided by the other partners.

Rockland Scientific leveraged its core shear probe technology and expertise in analog electronics to design the MicroPod-Shear instrument. This is a modular, single sensor package that uses the shear probe as the sensor, with the signal output as either 4-20mA analog (an industry standard) or 0-5VDC analog.

The other technology that Rockland developed was the MicroPod-EM. A modular, one-dimensional electro-magnetic current sensor. For this unit Rockland had JFE Advantech, the manufacturer of the base EM sensor, created an OEM version for Rockland that was purpose built for incorporation into Rockland's small form factor MicroPod sensor packages, and also for Rockland's other instrumentation. The MicroPod-EM outputs data either in 0-5VDC analog or RS232 serial.

The purpose of the MicroPod-EM is to measure the mean flow velocity while the MicroPod-Shears measure the cross-stream variance (turbulence). In order to properly process the shear probe data the simultaneous mean flow velocity is required. Both of these MicroPod sensors are solid state devices that do not rely on acoustics and sound scatters. They will work in very clean water conditions.

The project proposal indicated that an intermediate Rockland data logger would be part of the system. This was never implemented. Instead, the sensors were connected directly to the FloWave data systems. This was an excellent demonstration of the readiness of the Rockland sensors for laboratory "plug and play".

The FloWave team designed and fabricated the sensor mounting equipment for the experimental work. They also undertook some preliminary trials with an off the shelf EM sensor to demonstrate that it would be suitable for the project. Once these trials were complete and had shown that the EM sensor worked as expected, Rockland completed the development and construction of the MicroPod-EM sensor unit.

FloWave integrated the two MicroPod-Shear sensors and the MicroPod-EM plus the Nortek Vectrino ADV into their facility systems for power and data. The data streams were logged into the FloWave industrial Ni-DAQ data acquisition system together with other tank system parameters. Data files were analyzed onsite to verify system operation and quality of the data sets.

System testing showed excellent agreement between the Nortek ADV and the MicroPod-EM when they are located closely together on the mounting frame. As the separation increases, they do not correlate as well. The shear turbulence data agreed with the ADV data quite well. And, the shear data could be used to estimate the flow velocities with good coherency and correlation to the Nortek Vectrino ADV.

When the project started Rockland had been using the shear probe as its core turbulence measurement sensor in its standard oceanographic profiling instruments for many years. The challenge was repackaging the shear probe into a small size suitable for laboratory work in an industrial environment where there is elevated electro-magnetic interference (EMI) and unpredictable mechanical vibrations. EMI can introduce excessive noise into the signal stream and distort the measurements to the point of rendering them useless. Mechanical vibrations will be detected by the shear sensor. To compensate for these induced vibrations a vibrations sensor is mounted inside the MicroPod housing. The vibration sensor signal is logged simultaneously with the shear signal so that the vibrations can be removed during processing to reveal the actual turbulence data.

Challenges encountered in the system development:

- Initial system commissioning showed excessive mechanical vibrations in the mounting system for the MicroPods. The mounting system was redesigned and made more rigid, with better sensor vibration mounts.
- Rockland wrote custom Matlab translation scripts to take the Ni-DAQ data files and convert them into file formats that could be processed using standard Rockland software. This was a minor obstacle and increased Rockland's data ingestion capabilities.
- The noise floor on the shear probe signals was higher than expected, at first this was thought to be due to the poor EMI rejection of the 4-20mA signal being carried in a long cable that was not sufficiently shielded. Further investigation found that it was the ambient building vibrations caused by the motors and machinery that were inducing the background noise into the shear probe signals. Fortunately, the signals being measured are very strong such that this elevated noise floor is not a factor in the data quality.
- Another delay resulted from commissioning a second Nortek Vectrino ADV to use in the experiment. Integrating this sensor proved problematic as it was generating interference in the original ADV. It was decided that this second ADV was not necessary as previous experimental work had shown that the shear probes matched the ADV data well enough that the shear data could be used with confidence to estimate velocities.

Work Package 1 was completed as scheduled and the instrumentation was put into use in Work Package 2. The MicroPod-EM that was developed was also part of Work Package 3, the EMEC instrumentation. The MicroPod-Shear and MicroPod-EM sensors are both now part of Rockland Scientific's standard product offering.

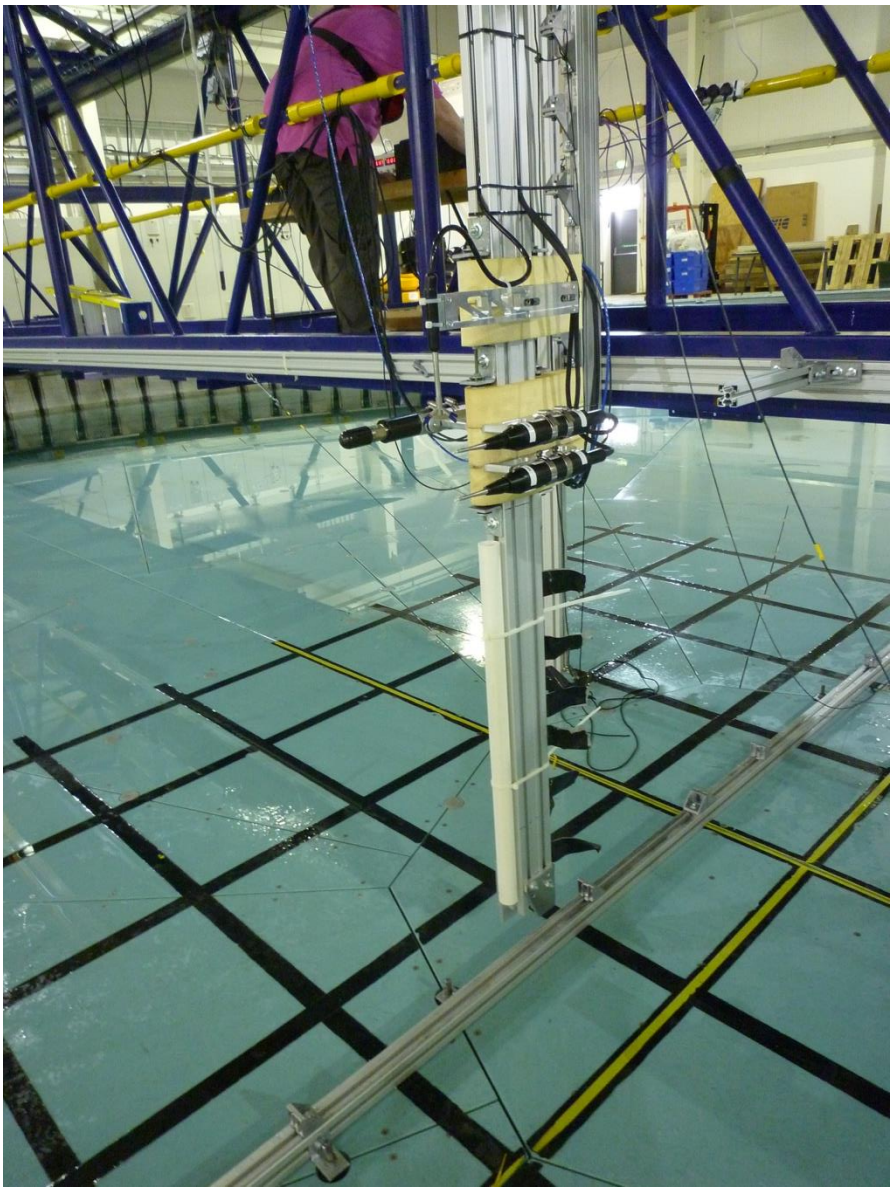

Figure 1: FloWave experiment setup. The two MicroPod-Shear units are on the right, vertically aligned with the downward facing Vectrino. The MicroPod-EM is on the other side of the vertical strut.

WP2 – FloWave Characterization

The FloWave test tank is a 1:20 scale experimental facility for ocean energy research. The tank is 20 m in diameter and 2 m deep, corresponding to a real-world depth of 40 m. As a symmetrical, circular facility with 28 current generating impellers and 168 wave making paddles arranged around the circumference. This allows for any combination of direction of waves and current.

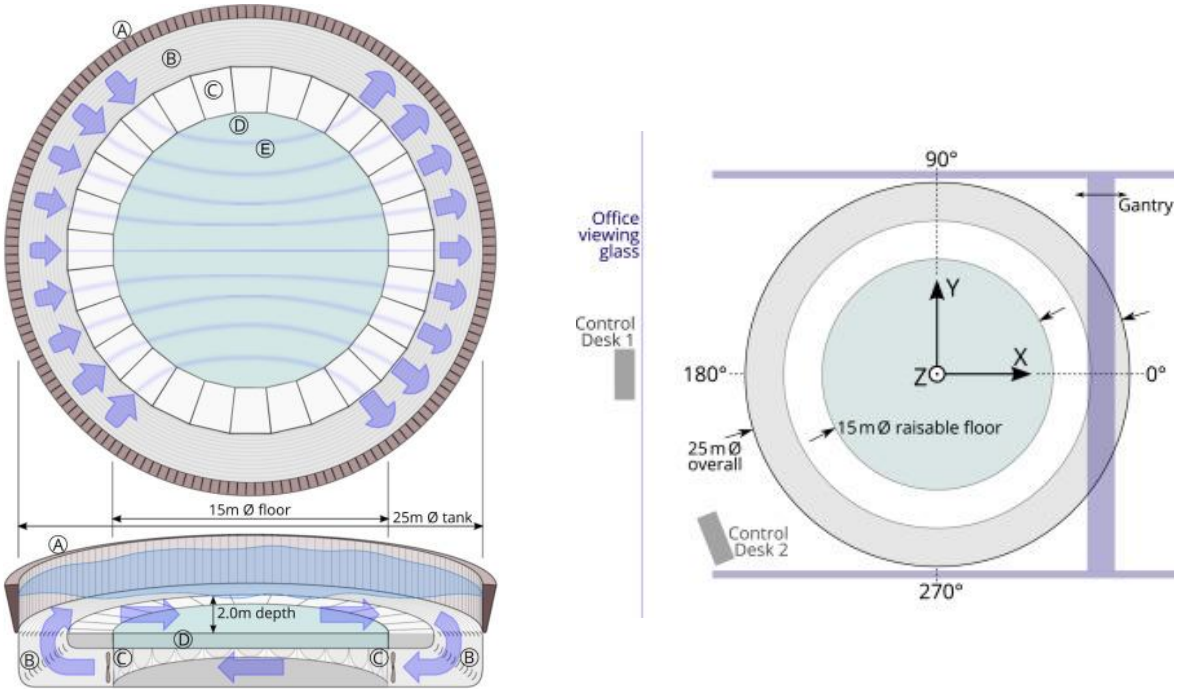

Figure 2: Overview drawings of the FloWave test tank.

For the purposes of the experiment the tank was set to generate a horizontal current running in the positive X direction (standard FloWave coordinates) with a width of approximately 6 meters centered on the X-axis. Flow speeds of 0.6 m/s, 0.8 m/s, 1.0 m/s and 1.2 m/s were all used at various times during the experiments.

The tank experiments had two purposes:

1. Characterize the turbulent regimes in the tank
2. Investigate the turbulent regime with relation to real world data from FORCE and EMEC

Five questions were set to answer:

1. What is the Large Eddy size (length scales) in vertical and horizontal?
2. Is the Reynolds Stress profile coupled to the mean velocity profile?
3. What is the degree of anisotropy at different length scales?
4. How do the spectra of Turbulent Kinetic Energy (TKE) vary through the tank?
5. Is there any influence of surface waves on the measurements?

To answer these questions, six experimental scenarios were created:

1. Functional checks at nominal flow and depth to confirm proper operation of the measurement equipment.
2. Down-channel measurements at 1m height (the tank uses height instead of depth, as it is referenced from the floor of the tank) to investigate measurement convergence at different stations.
3. What are the large eddy length scales? Horizontal spacing of two instrument packages, each package with a ADV and Shear, one package has EM
4. Similarly, change the vertical spacing to gauge large eddy length scales.
5. Mapping of vertical profiles of Reynolds stresses.
6. What effects do waves have on turbulence in the tank? This was a bonus experiment, if there was time.

The test plan matrix can be found in Appendix B. A sketch showing the locations in the tank where measurements were made is also in Appendix B.

The functional checks revealed that the sensor suite worked as expected. However, there were two sources of noise interfering with the shear probe signals. One was electro-magnetic interference (EMI), and re-configuring the way the electrical grounds were wired resolved this issue. The second was due to mechanical vibrations being picked up by the shear sensors. This was eventually traced to the ambient vibrations generated by the electrical motors, switchgear and other building functions. This noise was not a showstopper as the measured signals were significantly higher in strength.

The original mounting arrangement created for the preliminary tests was found to be too compliant. FloWave redesigned the mounting framework to couple to both the floor and the gantry making a more rigid structure and they improved the sensor cradles with vibration mounts. These changes resulted in a suitable arrangement that was not too onerous to change when moving stations.

Other challenges encountered in the experimental work:

- Test programme was delayed because of other demands on the tank.
- Delays in getting tank time were created by an unexpected maintenance shutdown period.
- The second Nortek Vectrino ADV resulted in interference with the first ADV when they were mounted close to each other. For those experiments only one ADV was used.

After the delays due to lack of access to the tank the test programme was completed in February 2017. Because of time constraints the original test plan was condensed after discussion amongst the project partners concluded that this could be done without detriment to the quality of the data set. But the team did manage to get the wave experiment completed, albeit on a more simplified basis.

The data quality from the FloWave work was of overwhelming good quality and quantity. This data set will facilitate study beyond the original project deliverables and should be considered an asset to the Tidal Sectors of Canada and the UK.

The results of this study were published by Clark et al. (2017), attached in the appendix. The conclusions of the tank measurements will be discussed in Section 7.

WP3: EMEC Installation

The EMEC field work involved designing a turbulence measurement system incorporating:

- a Rockland MicroRider customized for the site conditions
- a MicroPod-EM sensor
- a data logging computer and interfaces to the EMEC equipment.

These instruments were mounted on the EMEC Instrument Monitoring Pod (IMP) which was deployed at the EMEC Tidal Energy test area in the Fall of Warness, Orkney, Scotland. The intention was to have the system deployed for at least six months so that a massive data set could be acquired, and the longevity of the instrumentation could be tested.

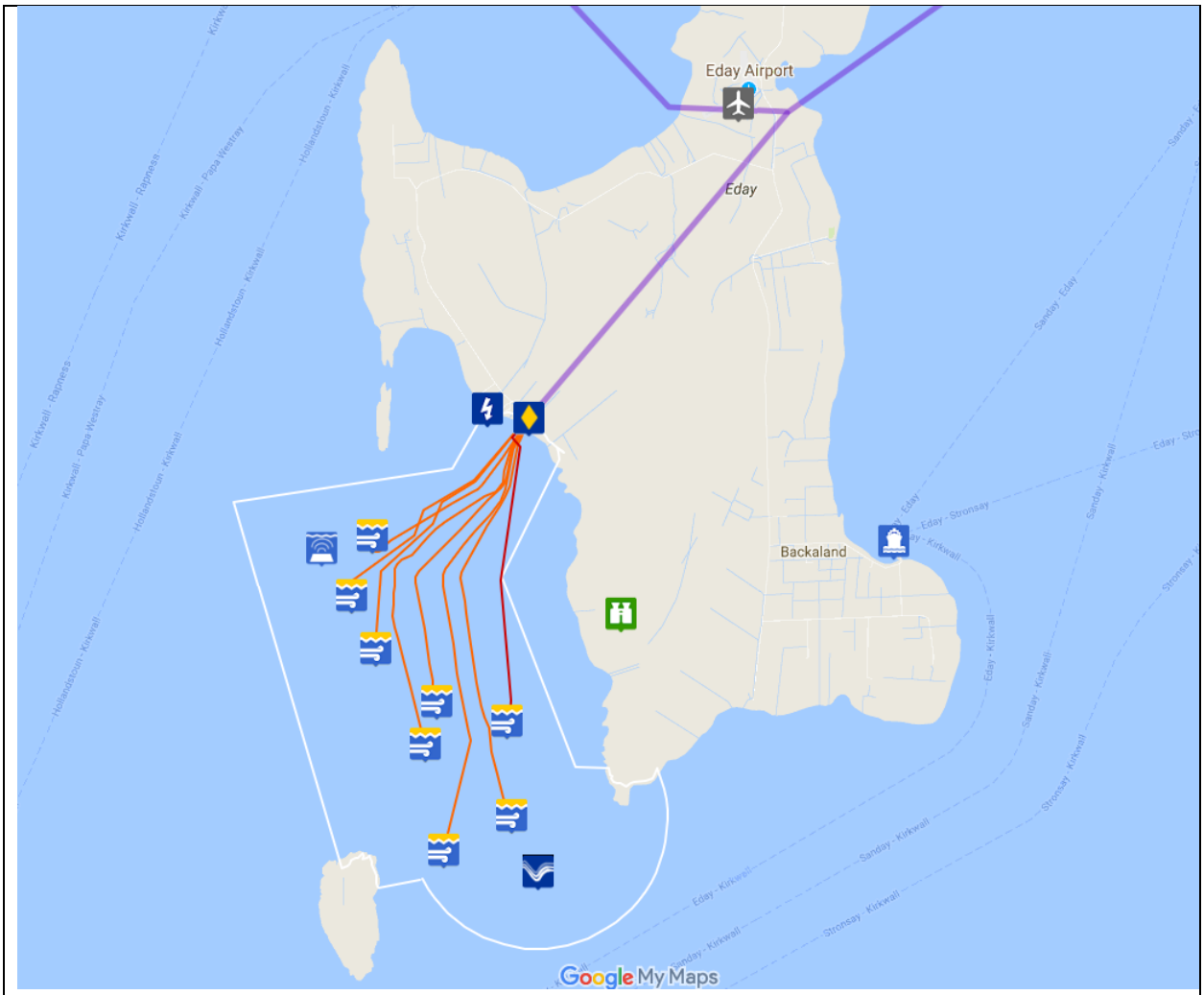

Figure 3: Simplified map of the Fall of Warness Tidal Energy test site next to Eday island.

The EMEC system design began in February 2016 with a preliminary meeting between EMEC and Rockland at Stromness. EMEC had recovered the Instrumentation Pod and was having its shore cable repaired. Rockland designed the MicroRider mounting frame with advice from the EMEC team. The frame carries the customized MicroRider and a MicroPod-EM.

The MicroRider was outfitted with 4 shear sensors, 2 FP07 thermistor sensors, a two-axis precision inclinometer, and a magnetometer. The MicroPod-EM sent its analog signal out to the MicroRider where it was added to the data stream sent to the logging computer in the sea chest on the IMP. The data streaming and data logging was a customized hybrid of the Rockland real-time and internal recording systems. The real-time data transceiver boards (RTrans and UTrans) were used to send the data stream to the logging computer as in any Rockland real-time system. In the place of the ODAS-RealTime(RT) data logging software (which requires human operation) a customized ODAS-InternalRecording(IR) package was made by Rockland for this special application.

The data logging system was also designed by Rockland. This consisted of a data logging computer and interface located inside the IMP communications seachest. This computer logged the data stream from the MicroRider. It also connected to the IMP Ethernet system. This enables remote access to the computer for file transfer and remote diagnostics. The data files would be transferred from the onboard storage to the EMEC shore station on the island of Eday. From Eday they are sent via the microwave link to the main servers in Kirkwall. Here they may be downloaded from anywhere in the world for processing.

The system design went through a few iterations as Rockland worked through the design requirements. At first a PC104 based system was considered as Rockland had experience with these in the past. However, this was rejected as not being powerful or flexible enough for this project. The system was designed around an Intel NUC running Linux. A small, fully featured computer more than capable of interfacing with the EMEC Ethernet and act as the real time data logger for the MicroRider and MicroPod-EM. At first it was thought that the data could be streamed in real time to the shore station. But this was not practical given the data volumes involved and the specialized requirements of the Rockland real-time data streaming hardware. The solution was to log the data onboard the IMP on the Rockland data logging NUC computer. The Rockland recording software was customized for the specific demands of this installation. By running the Linux operating system, it became very simple to have quasi realtime data available at the shore station and on the EMEC servers using remote syncing. The data files were stored by the data logging computer on a 1TB solid state hard drive located in the IMP seachest with the NUC. The remote server could access these data files using the EMEC Ethernet and copy them to the shore servers. First, they would be moved to the Eday shore station and then transferred via the microwave link to the main servers at Kirkwall.

The original project plan called for the deployment in April 2016. This was conditional on EMEC having the IMP ready. The IMP shore cable required major repairs, and this took longer than expected, which led to the deployment being re-scheduled for late summer or early fall 2016.

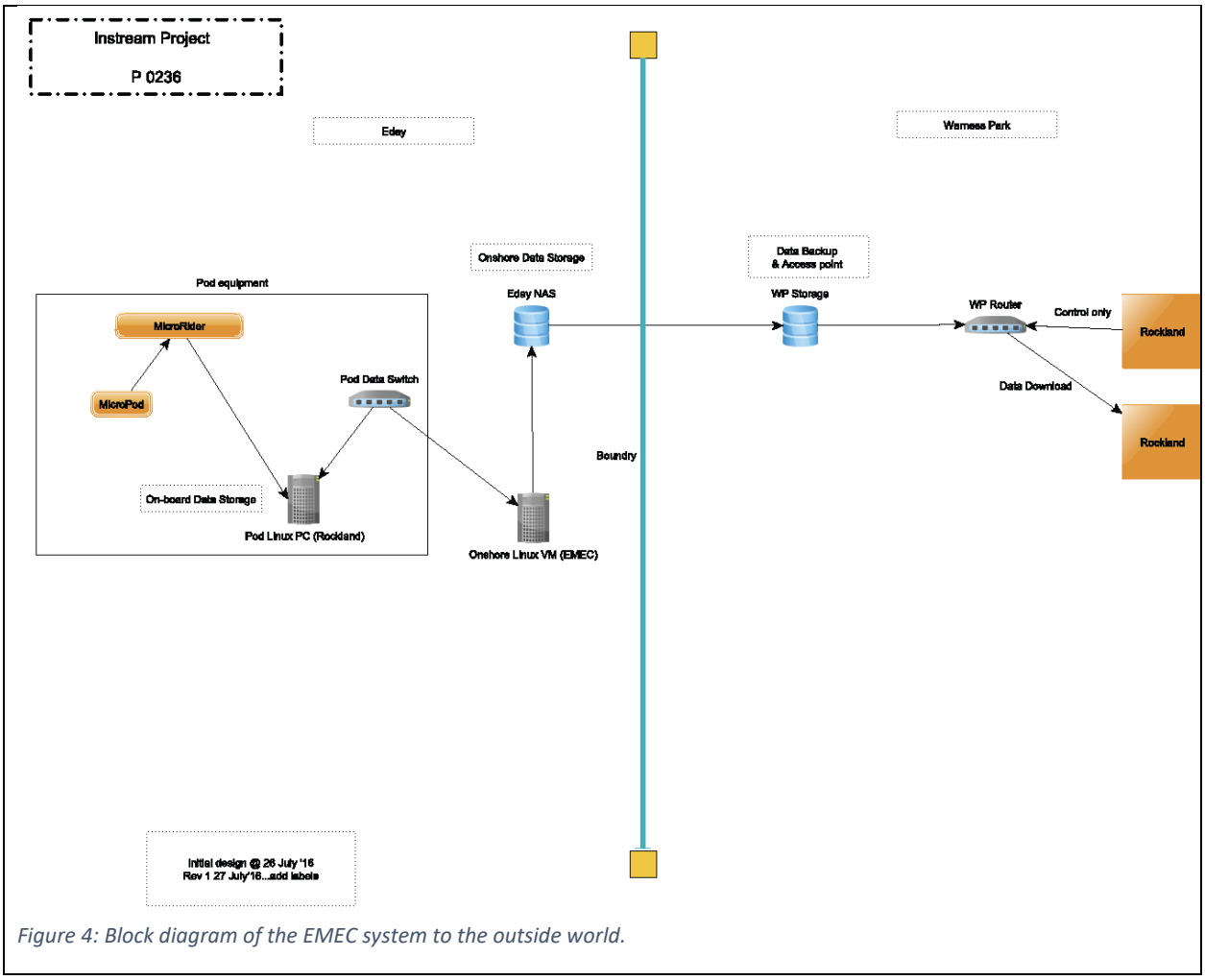

Figure 4: Block diagram of the EMEC system to the outside world.

The system was successfully integrated and tested in August 2016 in preparation for deployment. EMEC challenges with the shore cable repair together with the winter weather and difficulty securing ship time meant the deployment was delayed until April 2017.

Mechanically the MicroRider and MicroPod were installed on custom frame designed by Rockland in collaboration with EMEC. The instruments had to be as far above the IMP as possible so as to be in flow not affected by the structure. At the same time, they could not be so high as to interfere with the deployment and recovery operations. The frame is rigidly fixed to the top of the IMP with the instruments pointing into the Ebb flow. Unlike the Nemo floats, the EMEC installation only allows for measurements on the Ebb tide, not both Ebb and Flood.

The EMEC Instrumentation Pod with the Rockland MicroRider and MicroPod-EM instruments was deployed successfully at the Fall of Warness Tidal test site on April 18, 2017. The equipment survived the deployment and logged data which was transferred to the shore station as planned. We gained access through the Team Viewer application to our data logging computer on May 4 and had diagnosed a problem in the data logging software streaming implementation. A software bug, which was not detected during the system testing, meant that the data was unusable. On May 5 when we tried to

update the software to resolve the problem we found that the POD had lost its connection to the shore station. Attempts to make connection failed. The POD was recovered on August 3. Preliminary tests indicate problems with the shore cable. The Rockland MicroRider and MicroPod survived intact, albeit with some biofouling.

The bug was in the way the Rockland data logging software was compiled. It was compiled for a 32-bit system and the data logging computer was a 64-bit system. This was not caught because the software ran properly on the computer except that it was looping the data stream in a one second loop. This was not noticed in the testing because bench testing is done using fixed output test sensors. It was assumed that because the software was running properly, and the correct size test data files were generated that the system was logging properly.

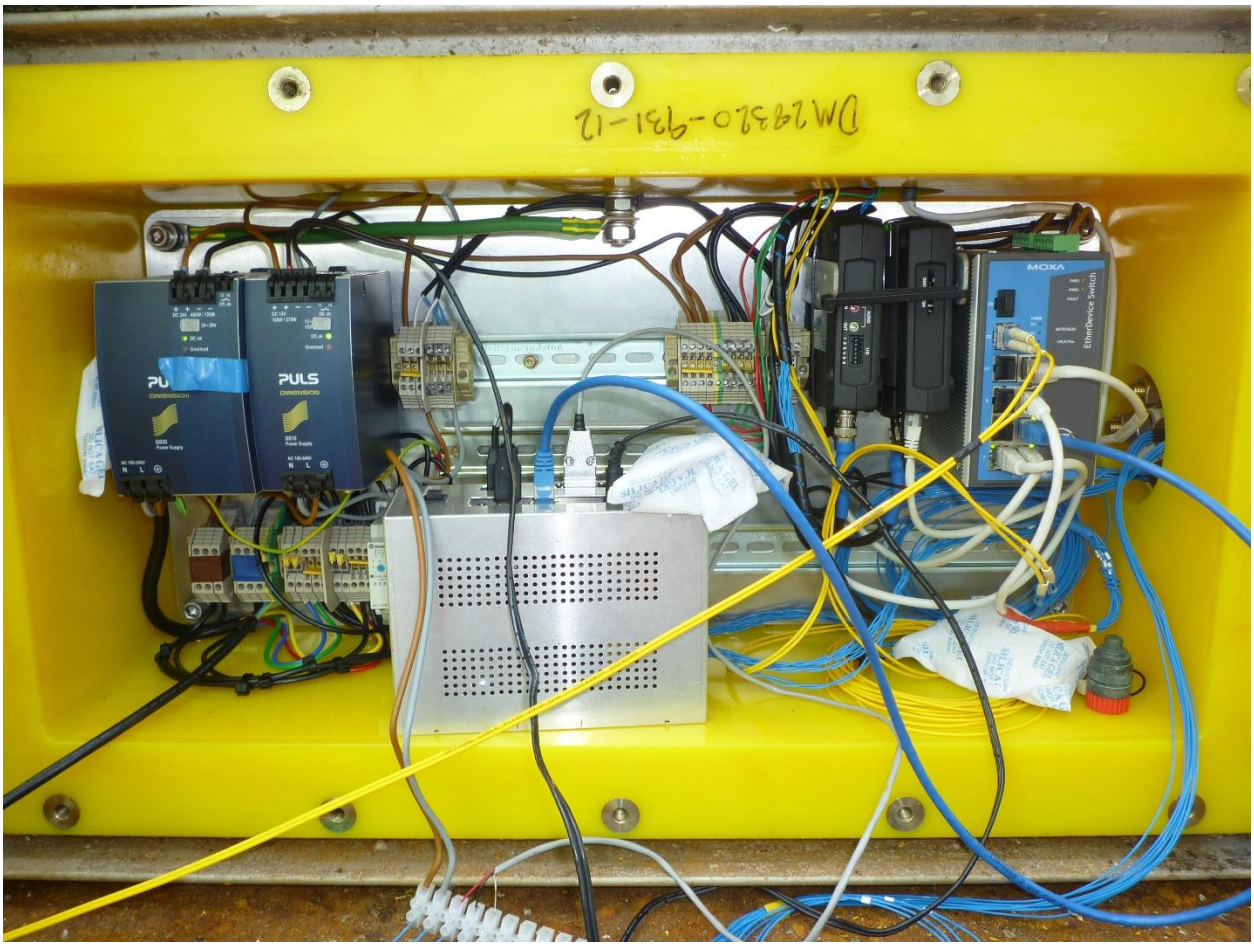

Figure 5: Inside of the sea chest during integration testing. The Rockland electronics are in the silver box in the middle. In the final assembly the box is mounted onto the DIN rails in the back of the box in between the terminal blocks.

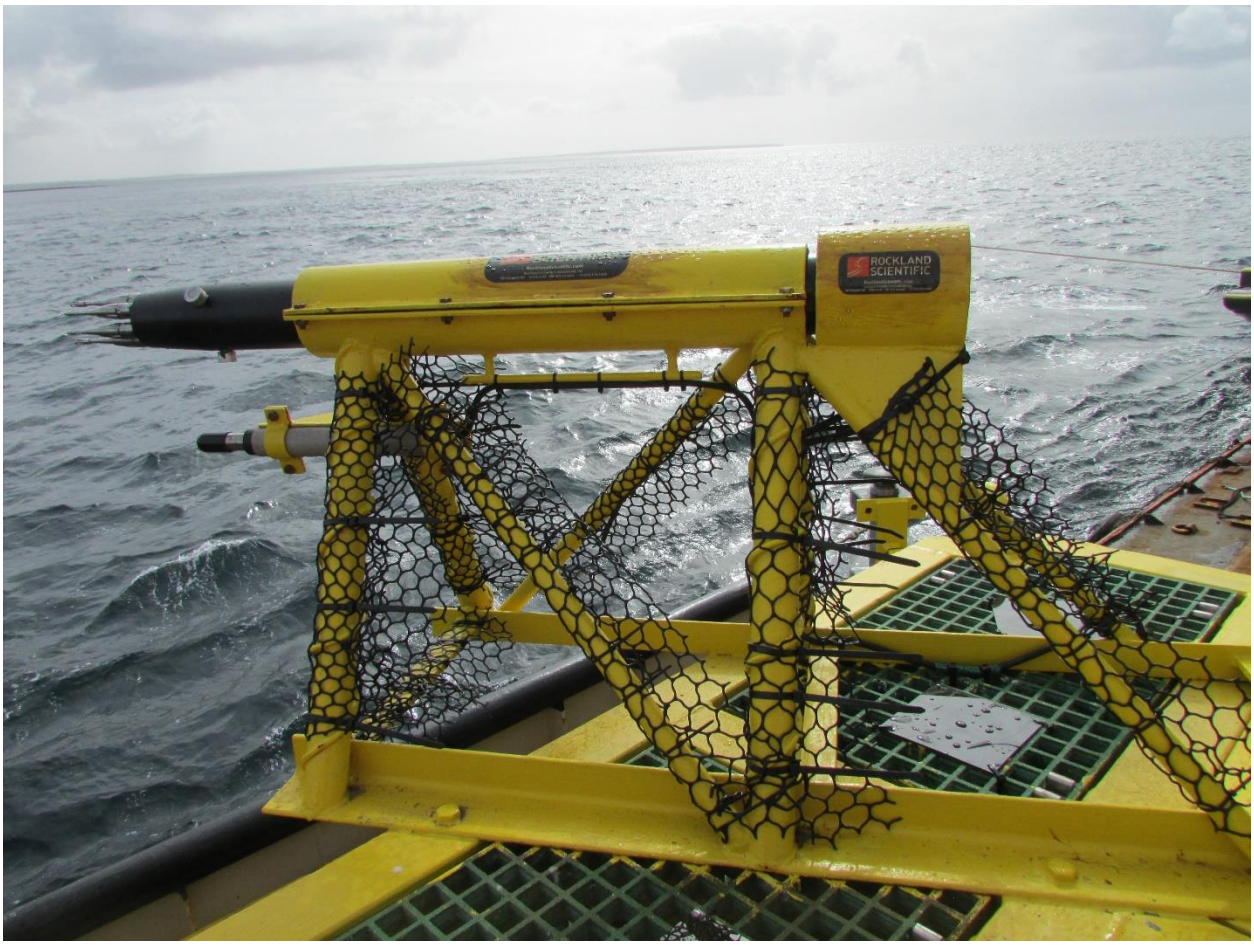

Figure 6: MicroRider and MicroPod on EMEC Instrumentation Pod ready for Deployment, April 18 2017.

Figure 7: Sensors on MicroRider after recovery on August 3, 2017.

The data obtained from the EMEC deployment is not usable for scientific analysis, however, it does indicate that everything functioned properly. In any case the deployment was too late to allow for inclusion of this data into the numerical modelling work package as planned. The 14-week deployment was a good test for the long-term survival of our equipment. All six turbulence sensors survived, which is quite remarkable given their inherent fragility. There was barnacle growth on the rear bulkhead of the MicroRider and on the metal base of the EM sensor. As well there was some growths and entrained vegetation on the MicroRider sensor holders. The ADCP data from EMEC has been collected and can be used in part in the numerical modelling if needed in the future.

At this time there are no plans to redeploy under the auspices of the InSTREAM project. EMEC is holding the equipment while they explore other opportunities to use it on the IMP in the future.

Based on the condition of the equipment after recovery it is recommended that biofouling protection be added to the MicroRider and MicroPod-EM to stop marine growth (barnacles) from adhering to the instruments. These could possibly cause irreparable damage and compromise a long-term deployment

WP4: FORCE system and deployment

The FORCE field work was the most predictable. Rockland and Dalhousie had both done this type of work before with the “Nemo” buoys outfitted with the Rockland MicroRider and ADCP instruments. This experience allowed Rockland and Dalhousie to upgrade the Nemo buoys for InSTREAM by improving the mounting of the MicroRider and optimizing the trim and balance of the floats.

The goal of this experiment was to collect field data from an active Tidal Energy research site over the course of a full two-week tidal cycle. The deployment was scheduled for August 2016 and this was completed as planned, with minor schedule changes to accommodate tides and ship availability.

The Nemo floats are a torpedo shaped body anchored to the sea floor through an acoustic release. The floats are self-contained systems with batteries, sensors and instruments. The floats are free to swivel a full 360 degrees, allowing for measurements in all flow directions. The bridle and axle that connect the float body to the mooring line allow for the floats to self-level in the flow, under high flows the floats will experience “blow-down” as the flow pushes them back.

Rockland designed and fabricated the improved instrument guards, mounting plates and other components. Rockland provided instructions and parts to Dalhousie, so they could prepare their buoy for the new assembly methods and parts.

Each Nemo float was equipped with a MicroRider carrying 4 shear probes, 1 thermistor, a pressure transducer, a two-axis precision inclinometer, a 6DOF gyro, and a magnetometer. Also installed on the float was a Nortek Vector ADV that recorded data internally and sent analog velocity data to the MicroRider; and an upward looking ADCP (acoustic Doppler current profiler) that recorded its data internally.

Dalhousie supplied the ADCP acoustic current profilers for both floats. Dalhousie made available the Aquatron tank for the final trim testing and ballasting of the floats so they would be level in slack water. BlackRock and Dalhousie coordinated the vessel used for the deployments. As the vessel chartered could only manage one float, the deployments were carried out over two days. A team from Rockland went to Nova Scotia to assist with the trim testing, setup and deployments. The recovery of the two

floats was handled by Dalhousie and BlackRock. A representative from Rockland performed a first pass data check in Halifax in the week after the floats were recovered.

The Nemo floats were deployed in Minas Passage approximately 2km west of Black Rock Island within the Black Rock Tidal Power berth at the FORCE site. The two floats were separated by approximately 200m. With Nemo East being the Dalhousie float and Nemo West the Rockland-Nemo.

INSTRUMENT	PARAMETER	VALUES
Nemo East (Dalhousie)	Deployment time	2016-08-27 11:43 UTC
	Recovery time	2016-09-11 10:36 UTC
	Longitude	64°26.310’ E
	Latitude	45°22.149’ N
	Water depth	55 m
	Height above bottom	14.8 m
	Data file names	MP2_XXX.p
	Data file deployment	MP2_002.p
	Data file recovery	MP2_360.p
Nemo West (Rockland)	Deployment time	2016-08-28 12:41 UTC
	Recovery time	2016-09-11 10:19 UTC
	Longitude	64°26.401’ E
	Latitude	45°22.115’ N
	Water depth	55 m
	Height above bottom	39.8 m
	Data file names	MP1_XXX.p
	Data file deployment	MP1_003.p
	Data file recovery	MP1_336.p

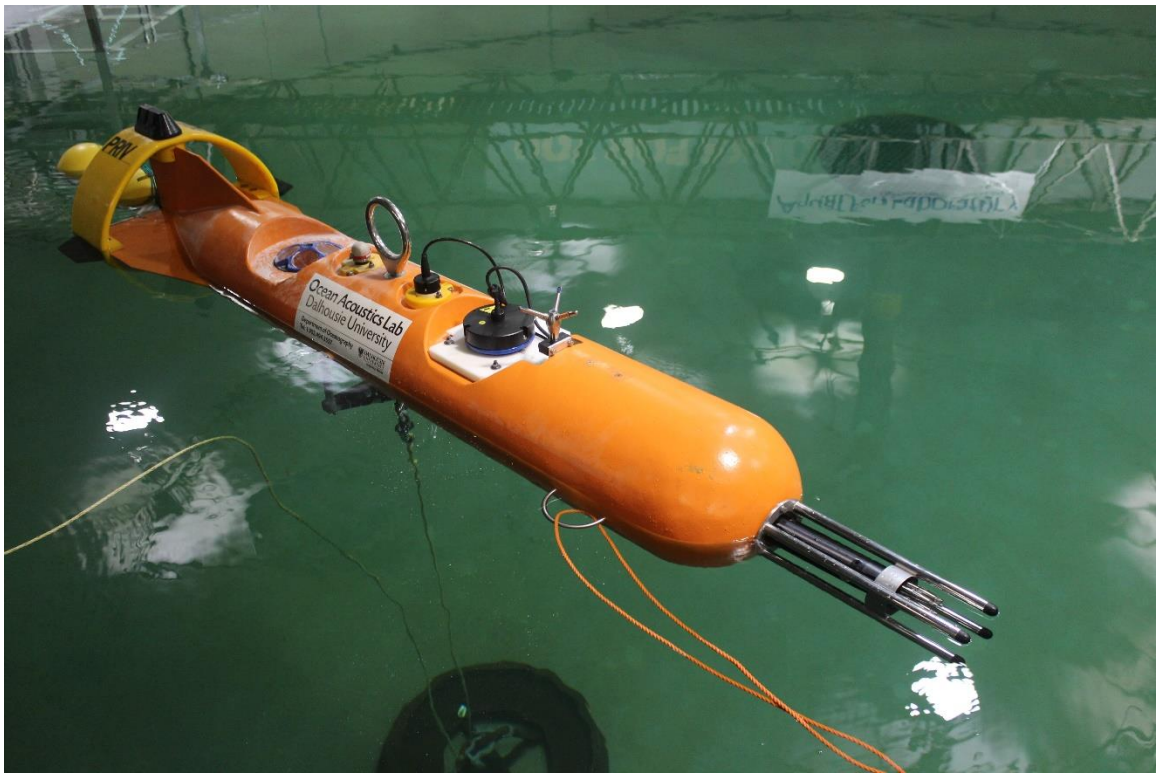

Figure 8: The Dalhousie Nemo float being trimmed in the Dalhousie Aquatron facility.

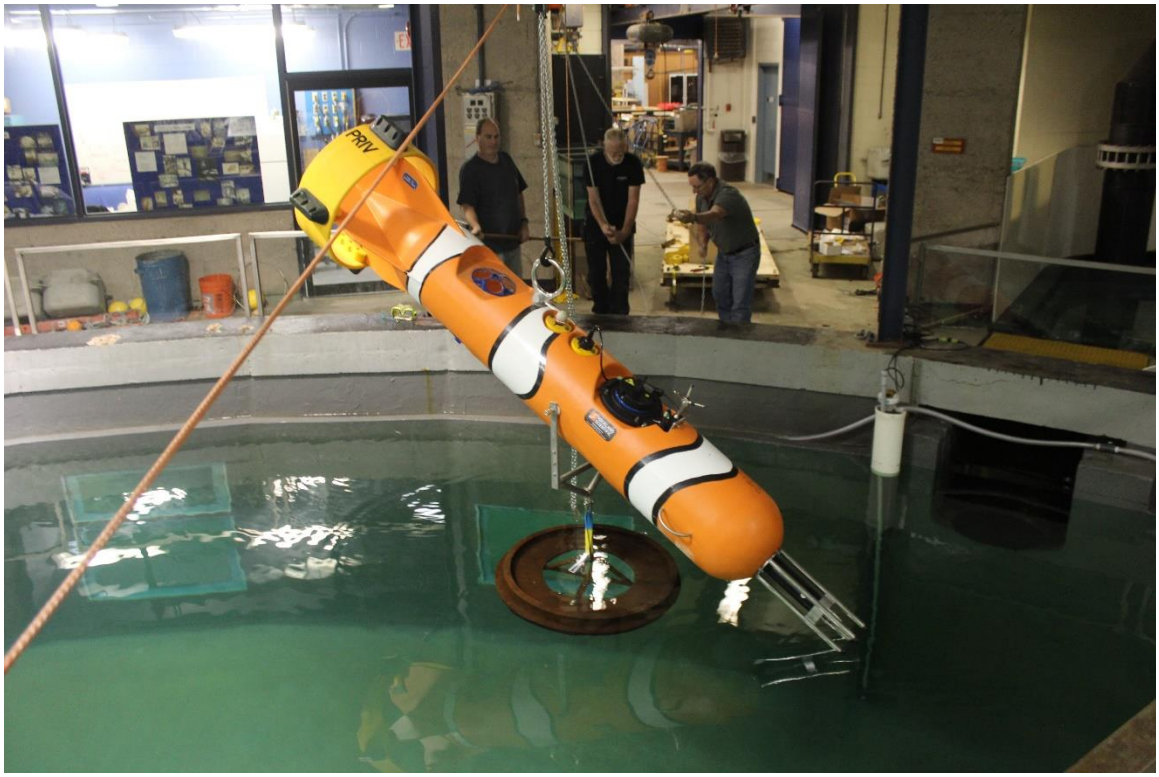

Figure 9: Trim testing the Rockland Scientific Nemo in the Dalhousie Aquatron tank.

Figure 10: Launching the Dalhousie Nemo float in Minas Passage.

WP5: Numerical Modelling

Data Processing by Dalhousie (Rachel Horwitz and Alex Hay)

Velocity profiles

Velocity profiles were calculated from the upward looking ADCPs on each Nemo float. The Nemo East float was moored closer to the bottom, so the profiles at this site span a greater portion of the water column. Where Nemo West measured velocities (30-50m elev.), the two profiles are comparable.

The Nemo East velocity profiles exhibit increased shear toward the bed and are log-shaped up to about 30m above the bed, indicating Nemo East is within the log-layer of the boundary layer flow, but Nemo West was above it. Values of friction velocity were obtained from the Nemo East velocity profiles and the corresponding drag coefficients, $Cd = 8.7 \times 10^{-3}$ on flood and 4.0×10^{-3} on ebb, exhibit ebb-flood asymmetry similar to that found in other Bay of Fundy tidal passages (Hay et al., 2013; McMillan et al., 2013).

Dissipation rates from Second order structure functions

Dissipation rates were estimated from spatial differences in velocity along each ADCP beam using the 2nd order structure function method (Kolmogorov, 1941c). This method avoids biases that may be induced by instrument motion when applying a more common spectral method to estimate dissipation rates, and estimates from upstream and downstream facing beam pairs were averaged to further remove bias from shear in the mean flow. Dissipation rates were calculated for each 5-min time record over 5-m elevation ranges.

As expected, dissipation rates increase with increasing mean speed on both ebb and flood tides. At any speed and tide direction, the highest dissipation rates are found closest to the bed, and values decrease upwards. Profiles above Nemo West had a much shorter vertical extent due to the longer mooring line length, but where data were available, dissipation rates from Nemo West are comparable to those from Nemo East, and exhibit similar variations with flow speed and elevation. Dissipation rates are higher for a given mean speed on ebb than flood.

We found that the direction of flow (ebb vs flood) had a much greater effect on dissipation rate than the difference between the two mooring sites, 200m apart in the cross-channel direction, indicating that the along-channel variation in bathymetry, rather than cross-channel variation, has the greater effect on the evolution of the marine boundary layer at this site.

Comparison between ADCP and MicroRider results

The MicroRider turbulence sensor on each buoy made measurements at buoy height, which varied with flow speed due to the blowdown. To compare ADCP results to those of the MicroRider, dissipation rates were computed over the nearest 5 m range above each ADCP for all flow speeds in both tide direction. Dissipation rates compare well between the two very different instruments/ methods, and were within 50% of each other for both sites and tide direction. The ADCP-based method found a smaller difference between the East and West sites than the MicroRider-based estimates for both tide directions.

Reynolds stresses

The well-established “variance method” to calculate Reynolds stresses from beams of a fixed, level ADCP cannot be applied here because non-zero pitch and roll, and vertical instrument velocities cause

apparent contributions to the Reynolds stresses, as described by early developers of this method (e.g., Lohrmann et al., 1990; vanHaren et al., 1994; Lu and Lueck, 1999b).

Dalhousie developed a new method to estimate profiles of Reynolds stress from an ADCP mounted on a compliant mooring (subsurface buoy). This method uses structure functions computed along the ADCP beams, and the difference between estimates from upstream and downstream facing beams. This method is not sensitive buoy motion. Preliminary results show maximum stresses of 0.25 m^2/s^2 at mid-water depth (the lowest elevation we could measure) at max flood with lower stresses at slower flow speeds, and values decreasing upwards from mid-water depth at all flow speeds, consistent with lower shear observed in the velocity profiles far above the bed. We anticipate submitting a manuscript on this topic for publication in 2018.

Data Processing by Rockland

MicroRider and ADV (Nortek Vector) data from the FORCE deployment was processed by Rockland. This work is documented in Rockland Scientific Internal Note 060, included in Appendix C. This was done for both Nemo East and Nemo West. The data were corrected to account for actual calibration coefficients of certain sensors. As well those sensors that have reference axes were all aligned and referenced to a common coordinate system. The data sets are very large and one-minute averages are made to get an overall picture of the data. The data is converted from raw to physical units for the overview plots.

Data Processing & Modelling by OAS

In March 2017 Ocean Array Systems had the data from the FloWave experiments and the FORCE deployment. The EMEC deployment had not occurred yet and it was decided to carry on with the analysis and numerical modeling without the EMEC data. At this time the EMEC deployment was scheduled for April 2017 and we were optimistic that at the very least we would get some data to help validate the modelling. OAS and the analysis team were confident that the FORCE data was sufficient to reach the project deliverables and goals. To accommodate the delays on the EMEC deployment, the FloWave experiments and to allow for enough analysis time, a change request was submitted to extend the project end date and scope. The end date was changed from July 2017 as on the original project schedule to November 31, 2017.

OAS reported that “the data from Flowave is of overwhelmingly good quality and quantity (all proposed tests, including the “wish list” were completed), which will facilitate study beyond the original project deliverables. This dataset should be considered an excellent asset to the UK Tidal Sector - it is usable not just within this project but for future commercial and academic research, addressing several key questions - the whole team and Flowave in particular should be proud.”

The OAS/Octue summary report is included in Appendix D.

WP6: Reporting and dissemination

Besides the regular interim reports required by the various funding bodies, the project has been active in generating press releases, conference papers and other publicity. Here is the current log of activity:

InSTREAM PR and Results dissemination log

Documents

- Hancyk, February 2016: Project Summary, InSTREAM. Presented at ICOE Conference Edinburgh and Marine Renewables Canada Open House Ottawa, also disseminated as a press release to TEC related media outlets
- Wolk, F and A. Hay, 2016: Measuring Flow Turbulence. In Horizon 2020 Project Portals, Vol 9, p 193.
- Hay, A., 2016: Going beyond TKE. In Horizon 2020 Project Portals, Vol 9, p 192.
- Wolk, F. 2016: InSTREAM – Sensors and methods for measuring turbulence in laboratory and field, Abstract submitted to AWTEC conference Nov 2016, Singapore.
- Clark T. et al, InSTREAM: Measurement, Characterisation and Simulation of Turbulence from Test Tank to Ocean. Abstract submitted to EWTEC conference Jan 2017, Cork.

Events

- Marine Renewables Canada Conference 2016, November 2015, Montreal QC
- ICOE 2016, February 2016, Edinburgh UK
- Marine Renewables Canada Open House and Members Roundtable, June 2016, Victoria, BC
- AWTEC 2016, October 2016, Singapore
- Project exhibited by EMEC on their stand at 13th Renewables UK Wave & Tidal Conf, London, Feb 2017.
- US DoE NREL 3rd Marine Hydrokinetic Instrumentation Workshop, February 28 - March 1, 2017, Fort Lauderdale, FL
- IEC TC114 Ad Hoc Group #7 Meeting, April 3, 2017, London, UK

Press Releases & Articles

- July 2016: FloWave/EMEC/OAS press release 'Trans-Atlantic research funding package to focus on measuring & understanding tidal turbulence'
- August 2016: Black Rock Tidal Power press release regarding deployment in Minas Passage
- October 2016: Canada – UK collaboration set to make a splash in tidal technology innovation, http://www.era-can.net/collaboration/story1-tidal-technology/
- June 2017: Collaboration Brings Tidal Power to Light
  in *CanadaExport*, online magazine of the Canadian Trade Commissioner Service

5. Risks

Besides some of the challenges and risks already described in this report there were several risks identified in the project. These were captured in the project risk log, as shown here:

INSTREAM PROJECT				DATE CREATED: 2016 May 1
RISK LOG				REVISION: 2. Edited 2016 Nov 22
RISK NUMBER	WP SECTION	DESCRIPTION OF RISK	IMPACT OF RISK	MEDIATION OF RISK
1	4.1, 4.4, 4.14	EMEC - Corrosion of instrumentation	failure of instrument	large active aluminum anodes, painting over hard anodized aluminum
2	4.3	EMEC - delay in development of internal recording/data file transfer system	delay of deployment	Not a Risk Anymore
3	4.3	EMEC - delay in development of automated scripts for data file transfer and system monitor	delay of deployment	Not a Risk Anymore
4	4.12	EMEC - damage to equipment during deployment	failure of instrument	very clear and careful deployment & handling plans. design mounting scheme to minimize risk from rigging
5	4.12,4.14	EMEC - damage to equipment (sensors) during operations	reduced data set	redundant sensors
6	4.14	EMEC - power interruption to Rockland equipment	loss of data	EMEC has backup generators
7	4.14	EMEC - data file transfer errors	loss of data	backup datafiles stored on a SSD on the IMP side. data files are in 1 hour chunks.
8	4.2,4.9.4.14	EMEC - interference with measurements - body vibrations, acoustic interference, power surges, debris covering sensors.	poor data	Careful design to minimize these effects. we will have to live with some aspects of this risk (for example the debris on sensors). The EMEC deployment is the highest risk and most experimental aspect of the project. Because there is no way to perform a fully functional test of our equipment and the IMP equipment operating under water prior to deployment we do not know what, if any, acoustic of electro-magnetic (EMI) interference issues may occur. We have implemented in our design our best practices as known at the time of design to minimize

				the EMI issue. The acoustic issue may be less of a concern because of the geometry of the assembly. It is possible that the signals we are measuring will not be unduly influenced because they are so strong that the interference gets buried into the overall "noise floor"
9	4.12	EMEC - delay in deployment causing delays in rest of project deliverables	overall project delay	the risk to the overall project of a delayed EMEC deployment is not great. EMEC is a fixed site and will stream data continuously once operational. data can be analyzed very soon after deployment and can be analyzed on an ongoing basis afterwards.
10	5.12	FORCE - mooring blowdown and dynamic performance	poor data, damage to equipment	Not a Risk Anymore
11	5.12	FORCE - poor dataset from first 2 week deployment	poor data	Not a Risk Anymore
12	5.12	FORCE - deployment delays due to weather	delay to project	Not a Risk Anymore
13	3.4, 3.6	FLOWAVE - mounting system results in poor quality data	poor data	Not a Risk Anymore
14		Data Processing delays	overall project delay	delay in project timelines due to lack of resources to complete all data processing tasks in a timely fashion. A meeting of the data processing principals will be scheduled where the allocation of resources; clear definition of requirements will be laid out; and a more realistic assessment of time required will be assessed

6. Outcomes & Conclusions

General observations:

The project was successful in meeting its key goals and objectives. Rockland's shear probe technology was adapted for the laboratory environment along with an electro-magnetic current meter. The shear sensor was the core sensor technology used in the FloWave test tank and in the field experiments at FORCE and EMEC.

There were delays in the FloWave work because of other demands on the facility and un-scheduled maintenance. This resulted in the simplification of the original test plan; nevertheless the partners were able to create a thorough and high-quality set of data.

The EMEC work was the riskiest, because this type of turbulence installation had been attempted on a fixed platform. An entirely new system design was developed to handle the data files and the control of the Rockland turbulence instruments. Despite some setbacks, the EMEC installation was successful on all other counts.

The Bay of Fundy experiment at the FORCE site went according to plan. A full two-week data set was obtained from two moored instrument systems deployed 200 m apart at the Black Rock site.

The data processing and numerical modeling has resulted in the first direct comparison of the FloWave tank environment to a real-world tidal energy site (FORCE). This is unique and unprecedented. The data set obtained in InSTREAM is very large and there is great potential for future processing and modelling.

The international collaboration was, on the whole, very positive. This project has enabled the partners to make contacts and establish good working relationships with organizations and individuals that will stand them all in good stead in the long-term as the tidal energy industry advances. There were challenges because of the time differences, and geographic separation. The use of the Basecamp online platform, email, meeting at conferences and direct travel all helped to maintain the flow of information and keep abreast of the project activities.

Technical Outcomes

Technical outcomes for the project partners are summarized in the following list. Details are given below

Rockland

- Validated laboratory sensor technology and integration into industrial lab data acquisition system
- Designed and integrated quasi-real-time sensor system onto the EMEC IMP sea bottom platform
- Demonstrated the long-term survivability of Rockland's turbulence sensors
- Improved the design and manufacturing capability of sensor systems for Tidal Energy applications
- Created additional contracts and partnerships for future opportunities (e.g., Rockland is now pursuing a small project with OAS)

Dalhousie

- Collected data from the Bay of Fundy, specifically the FORCE site in Minas Passage for use in lateral studies in tidal energy research

- Created opportunities for academic papers
- Created opportunities for young scientists
- Refined the Dalhousie *Nemo* buoy and upgraded its capability for turbulence measurements.

Black Rock

- Collected pertinent turbulence data from their berth at FORCE

EMEC

- Demonstrated successful integration of complex, yet fragile, sensors onto their IMP platform
- Demonstrated a new diver-less deployment and recovery system
- Looking for future opportunities to deploy the turbulence payload
- Added capability of providing live data streams to external users

FloWave

- Successfully integrated turbulence sensor system into industry Labview DAQ
- Generated excellent data sets of the FloWave tank
- Increased understanding of the physics of the flow in the tank
- Gained insights into the scaling factors in the tank and the limitations of modelling

OAS

- Created online repository of all data sets for future work
- Extended the TiME project methodology
- Completed case-study of the capability of OAS to provide turbine performance analysis

Laboratory versus Field Environment

Measurements at FloWave and the FORCE sites show that there is a significant difference between the turbulent velocity fluctuations observed in a tidal channel and the turbulence that can be generated in a laboratory setting, such as the FloWave facility. The discrepancy arises from the difference in size of the largest three-dimensional eddies of the turbulence. The largest eddies that are generated in an unstratified channel type of flow is determined by the distance to the nearest boundary, such as the bottom or the free surface. At the FORCE site, Nemo was approximately 15m above the bottom during moderate currents, and its height above the bottom was larger than 7m even during the strongest flows. Thus, we expect eddy sizes of ∼10m at FORCE. The FloWave tank is 2m deep and we expect eddies of ∼1m at mid depth.

At the FORCE site, the shear probes provide two estimates of vertical velocity fluctuations, w, and two of the lateral fluctuations v. Five-hundred seconds of data, collected during a current of 1.3 m s^{-1}, were used to estimate four spectra, and these were averaged in to a single spectrum of velocity (blue). The spectrum follows the $k^{-5/3}$ Kolmogorov spectrum down to the smallest wavenumber of 0.05 cpm – a wavelength of 20m or an eddy size of about one-half of that length. Similar measurements taken at FloWave, using two shear probes that were oriented to sense $\partial w/\partial x$, provide a velocity spectrum that has a much more limited inertial (k−5/3) subrange. The spectrum of vertical velocity departs from the Kolmogorov spectrum at ∼1 cpm – eddies larger than 0.5m have suppressed velocity. Concurrent vertical velocity measurements taken with an ADV show identical results, but the high wavenumber portion of the spectrum is absent, due to the sampling rate of 100 s^{-1}, and there may be some aliasing

due to the nature of the ADV measurements. The shear-probe signals are never aliased. Thus, measurements collected in a laboratory facility replicate the high-wavenumber portion of the turbulence spectrum only – the inertial subrange to the dissipation range. Measurements for lower wavenumbers must be carefully scaled to account for the under-representation of the largest scales – scales that may be very important for assessing hydrodynamic loading forces.

Modeling and Simulation

Data analysis and simulation was carried out by OAS between March and October 2017. For the turbulence characterization and scaling metrics for FloWave and FORCE, the length scale and intensity values were used to create load cases for the scaling investigation. The integral length scales for FloWave and FORCE were calculated. Using these numbers and other parameters allows for a simulation to be built to compare the tank against the real-world.

The second part of the simulation of a turbine in the flow. The Schottel Hydro (Black Rock) turbine geometry was used to build a representative model. Artificial turbulent fields for the simulation were generated based on the integral length scales determined by measurements at FORCE and FloWave using the microstructure sensors from Rockland and the standard acoustic ADCP and ADV data. Thus, integrating the InSTREAM methodology to build the final model. The results are captured in two videos:

Single turbine comparison, FORCE and FloWave

https://vimeo.com/253207151

The video shows the evolution of the turbine wake in conditions found at the FORCE eastern site (upper part of the video). A smooth floor and level sea surface is chosen for simplicity and for comparison to the FloWave simulation. There is a significant difference in wake evolution, power coefficient and thrust coefficient between the two sites. Turbulent Kinetic Energy at the FORCE site exists at much longer length scales than the turbine diameter leading to significant off-axis meandering of the wake. In FloWave, the TKE is concentrated at length scales of a similar order to the turbine diameter leading to rapid breakdown in the wake and much less meandering.

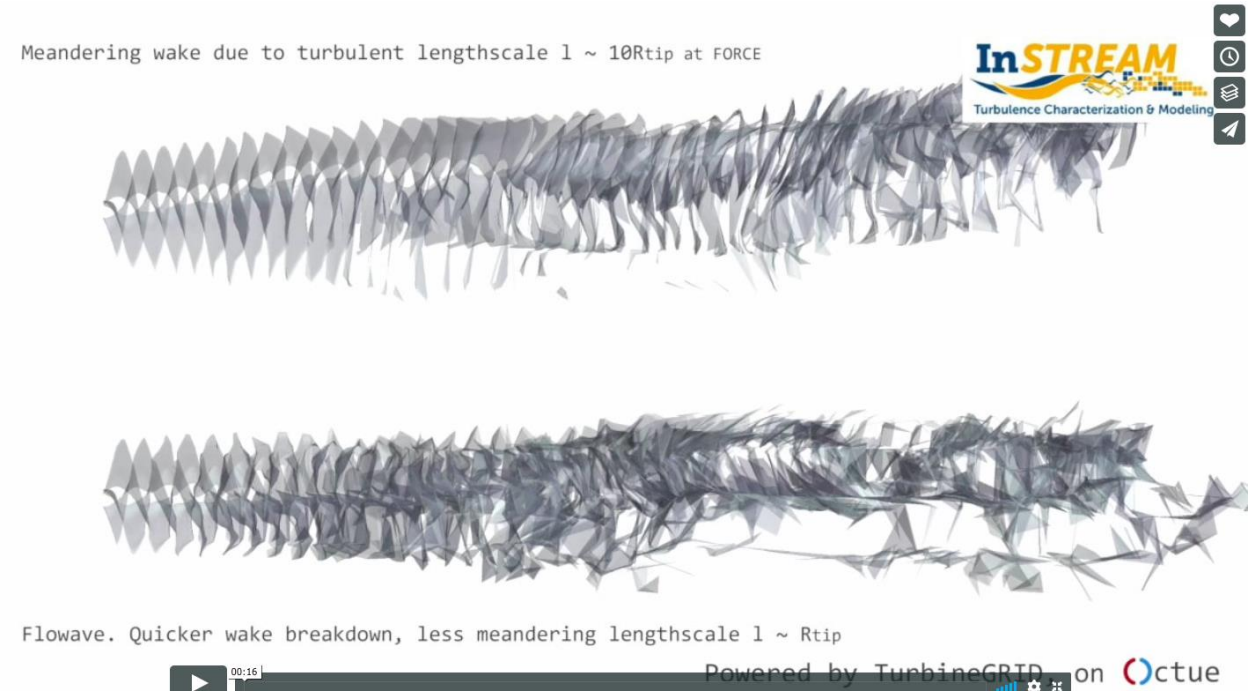

Turbine array simulation, FORCE and FloWave
https://vimeo.com/253204915

In this simulation, a small array was simulated by adding two more turbines, for a total of three. The additional two were placed eight turbine diameters downstream and offset two turbine diameters in the cross-stream direction. All other parameters were the same as in Simulation 1. It is obvious that the meandering wake cone in the FORCE model has a large impact on downstream turbines. This suggests that scale model studies in the FloWave facility may not replicate wake interaction effects properly in array modelling in the tank.

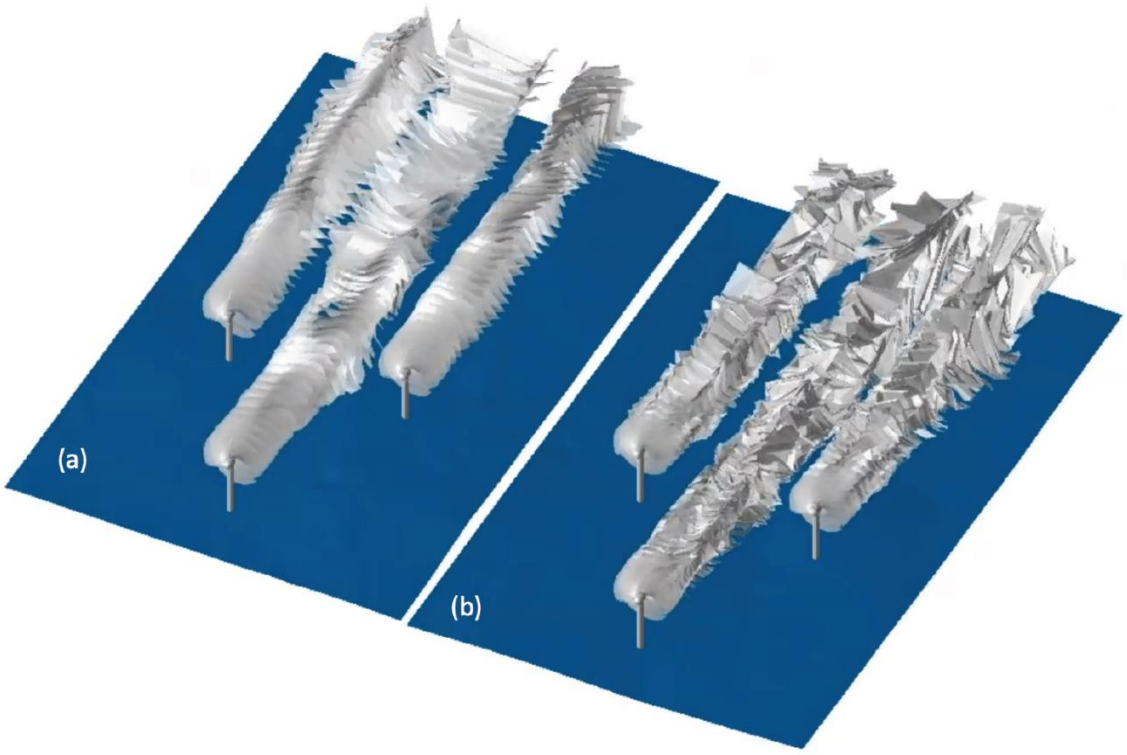

Figure 11: Snapshots from numerical simulations of realistic tidal flow past a turbine array. Inputs were chosen to best represent (a) field conditions and (b) laboratory conditions.

Online Data Processing Platform

A related initiative, which ran alongside the InSTREAM work, partially funded by Rockland, OAS, and the UK's Global Co-Operation fund, was the development of a data analytics platform. The general platform was developed by OAS, allowing for quick and easy generation of analysis 'apps' in the cloud. For the InSTREAM work, Rockland's turbulence processing library (ODASLib) was developed into one of the apps running inside analytics platform. The InSTREAM project was chosen as a showcase for the platform, which is approaching an open Beta version at the time of writing. Within InSTREAM, the platform was used to manage the diverse range of data sources, and to host execution of the numerical analyses discussed in the previous chapter.

The development of the processing platform provided a mutual benefit to all InSTREAM partners, particularly since the platform provides a route to leveraging cloud-based data processing services out of the sensor technology that designed and validated as part of InSTREAM.

Commercial Outcomes

One of the proposed downstream benefits of the InSTREAM project was the development and validation of new commercial, exportable products. The scope of the funding and measurement objectives required instrumentation packages and deployment/recovery techniques that reflected the lab testing and field operation realities of the tidal energy conversion industry.

Prior to InSTREAM, Rockland had a suite of existing oceanographic instruments that was applied to measurement gaps for tidal energy applications. The InSTREAM project permitted Rockland to engage

in research and development for instrumentation packages purpose-built for the TEC industry. Collaboration with new trans-Atlantic partners provided invaluable R&D value-add for improvements.

FloWave provided equipment optimized for an advanced tidal test tank facility. Feedback on instrument orientation, environmental 'noise' from operating electrical machinery e.g. wave paddles, and vibrations, permitted Rockland engineers to make incremental improvements to optimize the performance of the laboratory instrumentation.

The collaboration with Dalhousie and BlackRock for the field work of the Nemo platforms provided more experience with long-term deployments in tidal channels, a service offering now offered by Rockland commercially.

While the data at the EMEC site was unusable, the collaboration provided an education and experience on mounting instrumentations on fixed platforms to operate and transmit high bandwidth data autonomously.

Collaboration with Ocean Array Systems resulted in a better understanding of how to 'bridge' the gap between oceanographic science and engineering. This allows Rockland to present a clear value proposition to TEC device and project developers.

Rockland is leveraging the product improvements, experience, and prestige of the InSTREAM project and is actively working on several "pre-commercial" opportunities in Canada, UK and France to characterize turbulent flow in laboratories and the field sites, using the equipment and solutions that were developed in this project. In addition, InSTREAM resulted in a series of peer-reviewed papers—presented at industry conferences—that describe best practices for the characterization of turbulence for device and project development. In this regard, Rockland disagrees with the statement of the UK partners that the "whole consortium has no further plans to cooperate in the deployment of instrumentation or the exploitation of its measurements at present until a time when the market conditions change."

The aforementioned product improvements, specifically the fixed platform systems have generated opportunities in adjacent operational markets for long-term autonomous time-series measurements of turbulence. Rockland has received a large equipment sales contract, for a defence research application, that utilizes elements of the Nemo platform used during the Bay of Fundy deployments for InSTREAM. There are also other pending commercial contracts for the aquaculture and oil and gas industries featuring a fixed platform equipment sale and a multi-year field service program, respectively.

Commercial outcomes for the InSTREAM partners include, but are not limited to:

- New markets
- New customers
- New products
- New capabilities and knowledge that provides value both inherent and direct (can sell for profit)

Specifically:

Rockland: conference and peer-reviewed research papers, products, new partners for R&D, improvements to equipment, more experience with long term deployments in tidal channels, adjacent commercial applications of equipment and field service to defence, oil & gas and aquaculture industries.

Dalhousie University: unique data sets that could be published in peer-reviewed research journals, improvements to Nemo mooring flotation,

BlackRock: a comprehensive data set of turbulence flow conditions at their deployment site in the Bay of Fundy. This could be leveraged a competitive advantage for siting, device design, array layout and operational decision making.

EMEC – although the data was unusable, good practical experience was gained in collaboration with research partners, including the mounting and handling custom instrumentation on the IMP, and streaming and moving large data sets for 3rd party access.

FloWave – now has a first pass characterization of the tank for turbulence and an understanding of the scaling to be considered in flow modelling and testing. This is a unique advantage that can be leveraged as a differentiator from competing offerings in Continental Europe and East Asia.

Ocean Array Systems – have produced and validated a software including data ingestion, processing, analysis and simulation tools that can be offered commercially. Ocean Array Systems have developed a product niche that can turn the turbulence data collected into information for device designers and project developers.

7. Challenges and Limitations

While successful, the project partners had to deal with the following minor challenges.

- It was difficult for Rockland to stay on top of the UK partners' progress. While Rockland was the stated project lead partner, there was no formal mechanism that compelled the UK project partners to report budget and technical progress details, as well as operational decisions, to Rockland. Essentially, the UK partners were responsible to report only to Innovate UK, particularly on the budget and financing side.
- A project like InSTREAM that involves operations in an unpredictable and unforgiving environment (tidal energy sites and weather) must have sufficient flexibility in schedule and large contingencies for budget to accommodate the inherent delays and costs of working in the marine environment (especially tidal energy sites, which are particularly challenging). While these risks have been acknowledged prior to the project start, and risk-mitigation strategies were put in place, it was still difficult to deal with this, because of the significant geographic separation of the partners. For example, the coordination of efforts between EMEC (in the Orkneys) and Rockland (in Victoria) was particularly disruptive to the day-to-day operations of Rockland, those that are not related to InSTREAM.

8. Recommendations & Future Work

- Further processing of the FORCE site data into "engineering" data for BlackRock and Schottel. This work will be ongoing and likely not completed in the short term, because the scientific implications and understanding of the data sets collected during InSTREAM still requires analysis, which is outside of the scope of this project. Rockland staff scientist continue to be

engaged with the scientific and engineering community to further the methods and conclusions that locked in the mysteries of the data from FORCE.

- Long term deployment (of more than six months) is still lacking. Rockland intends to continue the collaboration with EMEC and support them in the operation of the long-term turbulence measurement system mounted on the IMP sea bottom platform. Such a data set will be of great value to the scientific and engineering community
- As scientific interpretation of the FORCE and EMEC data sets progresses, there remains the need to collect more site-specific data at other locations, because local conditions vary strongly between sites. It is not clear yet if one can generalize conditions across different sites or if local measurement will always have to be performed.
- Allow much larger travel budget for partners in these multi-jurisdiction schemes

9. Bibliography

- Collaboration agreement
- Project proposal
- AWTEC paper
- EWTEC paper

10. Appendices

APPENDIX A – Summary timeline and Project Schedule

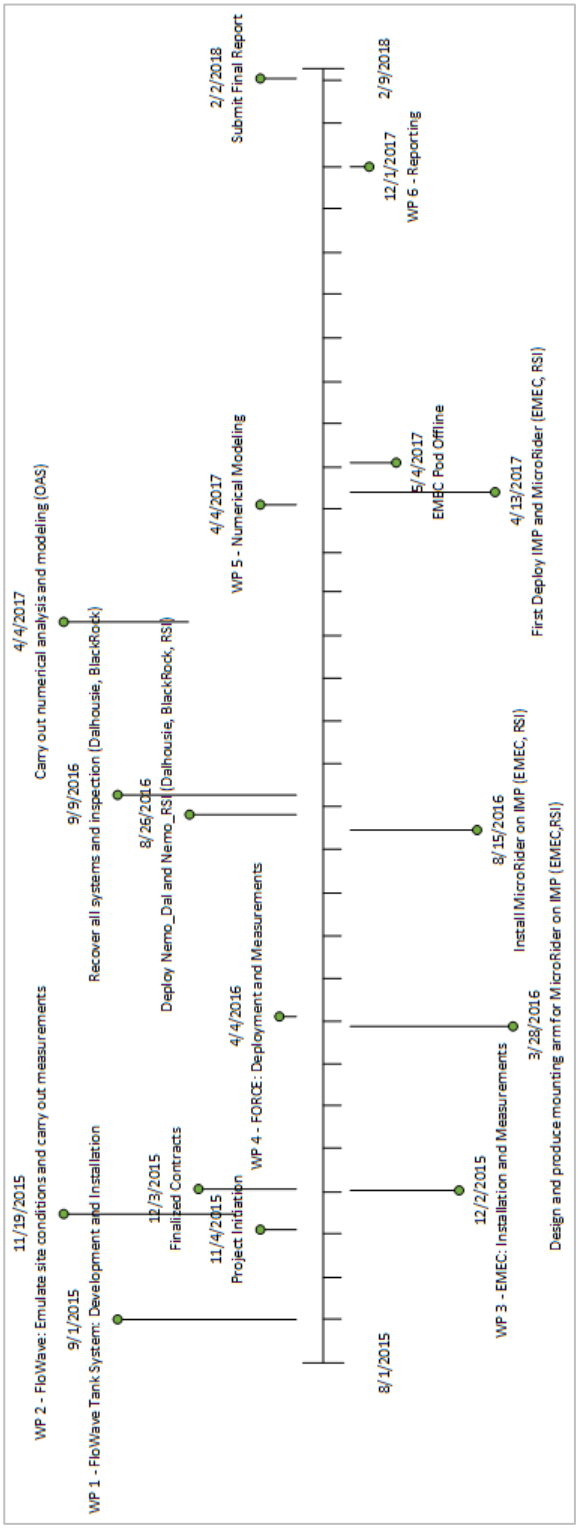

Title
1) Project Initiation
• 1.1) Negotiate Contract
• 1.2) Sign OERA Contract
• 1.3) Sign InnovateUK Contracts
• 1.4) Sign Collaboration Agreement
◆ 1.5) Finalized Contracts
2) WP 1 - FloWave Tank System: Development and Installation
• 2.1) Design and produce MicroPod for two-node tank measurement system (RSI)
• 2.2) Test demo EM current meter at FloWave (FloWave)
• 2.3) Acquire MicroPod-EM current meter system (RSI)
• 2.4) Design data interface and software for Flowave NiDAQ (RSI,FloWave)
• 2.5) Turbulence system testing and troubleshooting (RSI)
◆ 2.6) Completed construction of tank measurement system (RSI)
• 2.7) Transport to FloWave (RSI)
• 2.8) Generate test plan (OAS, RSI, FloWave & other partners as needed)
• 2.9) Integrate and test at FloWave (RSI, Flowave)
◆ 2.10) Commission turbulence system at FloWave (RSI, Flowave)
3) WP 2 - FloWave: Emulate site conditions and carry out measurements
• 3.1) Provide met-ocean data from EMEC site to Flowave (EMEC)
• 3.2) Provide met-ocean data from FORCE site to Flowave (BlackRock)
• 3.3) Program met-ocean conditions in tank and emulate site conditions (Flowave,OAS)
• 3.4) Conduct turbulence measurements at Flowave (Flowave, RSI) Phase 1
• 3.5) Process, collate and summarize test data (Flowave, RSI,OAS) Phase 1
• 3.6) Conduct turbulence measurements at Flowave Phase 2
• 3.7) Process, collate and summarize test data (Flowave, RSI,OAS) Phase 2
◆ 3.8) Interim Progress Report (RSI, all partners)
4) WP 3 - EMEC: Installation and Measurements
• 4.1) Design MicroRider-EMEC (RSI)
• 4.2) Design and produce mounting arm for MicroRider on IMP (EMEC,RSI)
• 4.3) Develop data & power interface for MicroRider on IMP (RSI,EMEC)
• 4.4) Build MicroRider_EMEC package (RSI)
• 4.5) Compile method statement and risk assessment for marine ops (EMEC)
• 4.6) Transport MicroRider to EMEC (RSI)
• 4.7) Generate data collection plan (EMEC, RSI, OAS & other partners as needed)
• 4.8) Install MicroRider on IMP (EMEC, RSI)
• 4.9) Check Mechanical Mounting
• 4.10) Check Electrical Power interface
• 4.11) Check communications between MR-EMEC and shore station. Verify Scripts
▶ **4.12) First Deploy IMP and MicroRider (EMEC, RSI)**
• 4.13) EMEC Pod Recovery & Repair
5) WP 4 - FORCE: Deployment and Measurements
• 5.1) Arrange ship charter (BlackRock,Dalhousie)
• 5.2) Build two MicroRiders for Nemo_Dalhouse and Nemo_RSI
• 5.3) Transport Nemo_RSI, 2xMicroRiders & ancillary equipment from RSI to Dalhousie (RSI)
• 5.4) Acquire ADV for installation on Nemo_RSI
◆ 5.5) Interim Progress Report (all partners)
• 5.6) Generate data collection plan (Dalhousie, RSI, OAS & other partners as needed)
• 5.7) Integrate Nemo_RSI measurement system (RSI)
• 5.8) Prepare Nemo_Dal for deployment (Dalhousie)
• 5.9) Prepare ancillary ADCP for deployment (Dalhousie)
• 5.10) Check trim of Nemo floats at Dalhousie Tank (Dalhousie, RSI)
• 5.11) Transport 2x Nemo equipment and ancillary systems from YHZ to deployment site (Dalhousie)
• 5.12) Deploy Nemo_Dal and Nemo_RSI (Dalhousie, BlackRock, RSI)
• 5.13) Recover all systems and inspection (Dalhousie, BlackRock)
• 5.14) Data processing and validation (Dalhousie, RSI)
◆ 5.15) Interim Progress Report (all partners)
6) WP 5 - Numerical Modeling
• 6.1) Ongoing Data Processing by Dalhousie
• 6.2) Collect data from FloWave, FORCE deployments (OAS)
• 6.3) Carry out numerical analysis and modeling (OAS)
◆ 6.4) Interim Progress Report (RSI, all partners)
7) WP 6 - Reporting
• 7.1) Collect reports from partners
• 7.2) Compile Final Report
• 7.3) Internal review
◆ 7.4) Submit Final Report

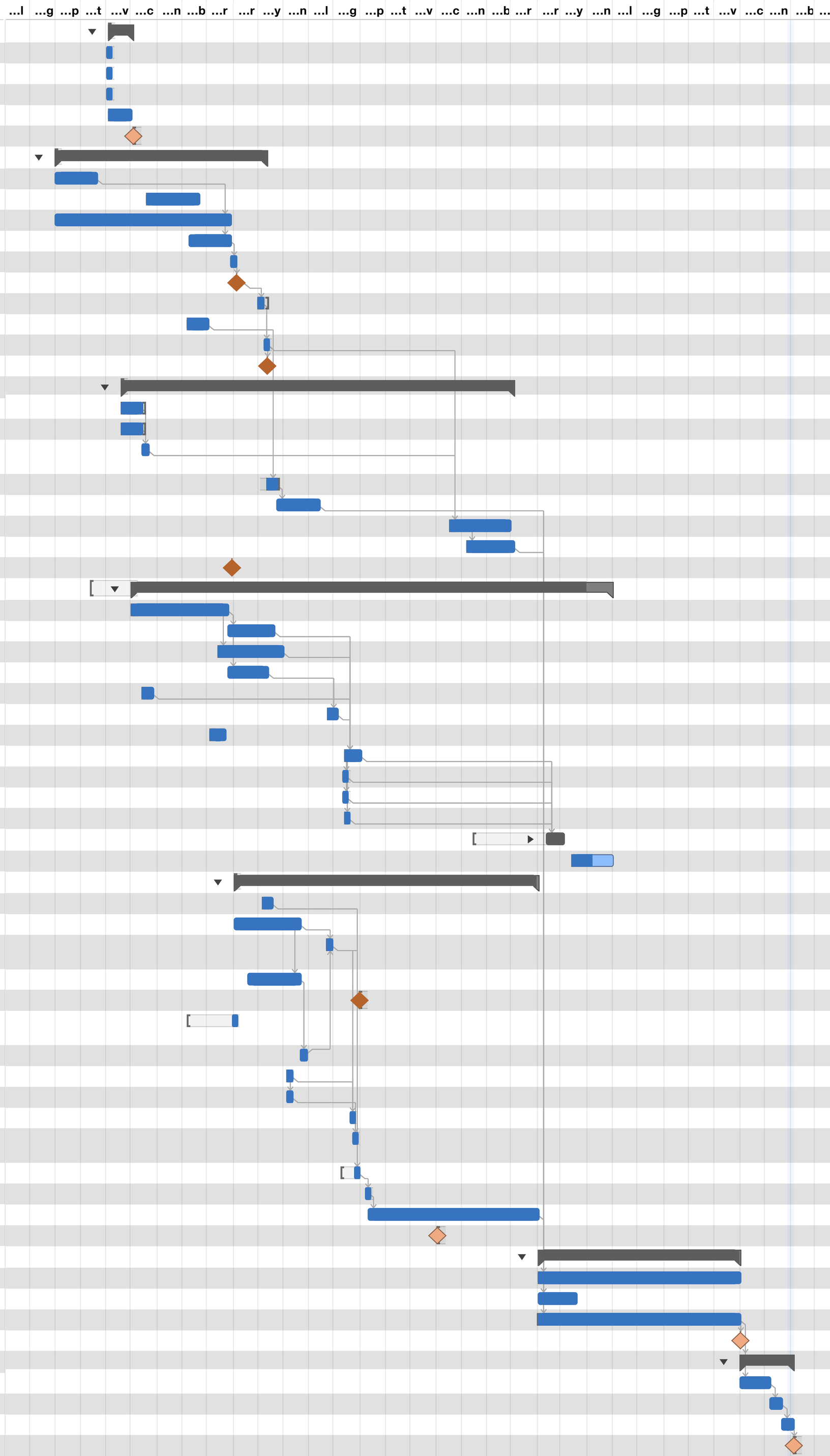

APPENDIX B – FloWave: Sketch of measurement locations and Experiment Test Matrix

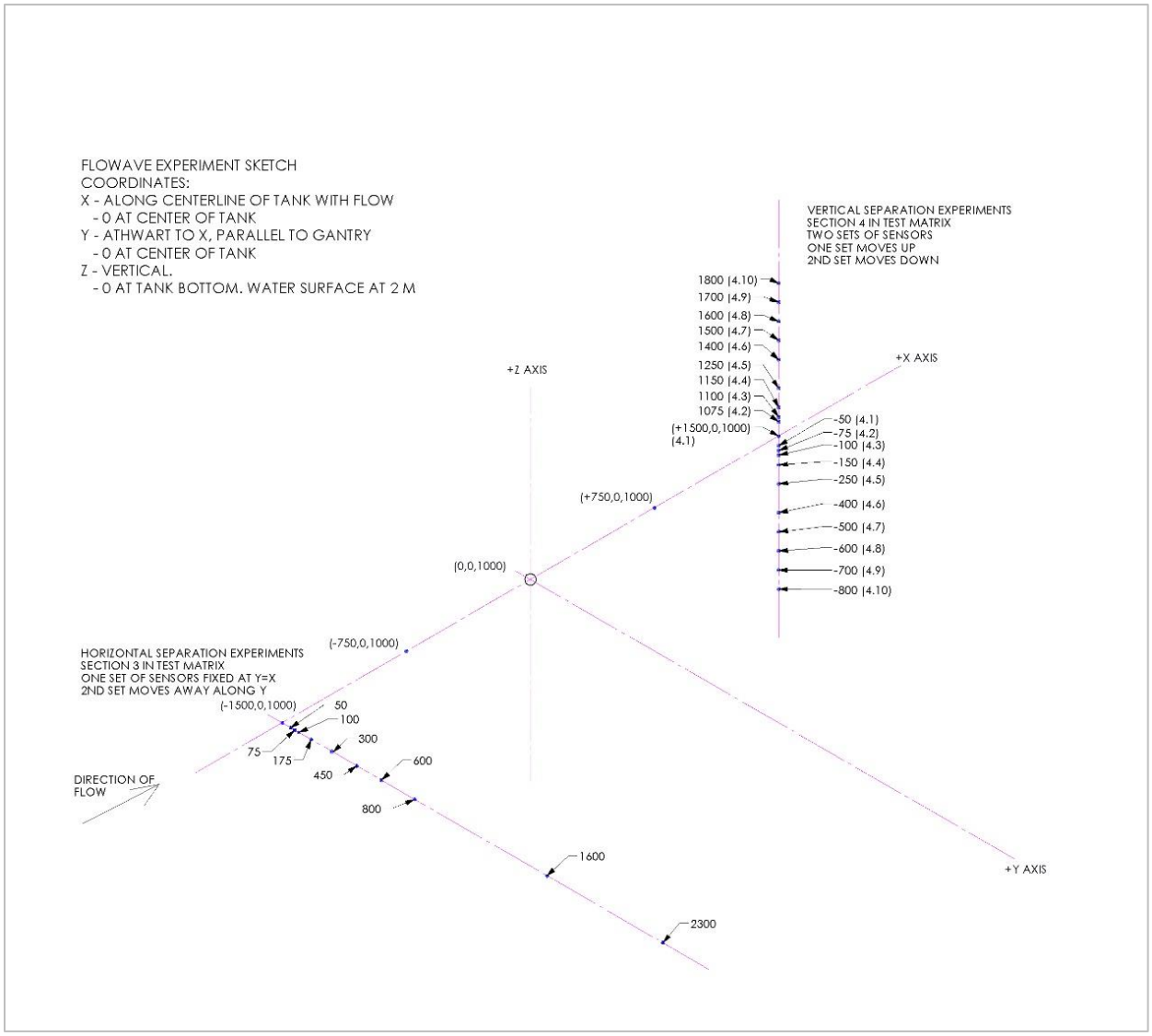

Sketch showing the measurement locations in the FloWave tank.

FloWave test Matrix

Flowave Turbulence Test Schedule

T. Clark (OAS), J. Steynor and T. Davey (Flowave), P. Stern (RSI)
23 February 2016

OCEAN ARRAY SYSTEMS

Questions to answer:

1. Does it work - functional checks
2. Large Eddy Size (lengthscales) in vertical and horizontal?
3. Is the Reynolds Stress profile coupled to the mean velocity profile
4. Degree of anisotropy at 3 different lengthscales:
   - 1m - blade length
   - 1cm - blade chord length
   - 1mm - skin effects
5. How does the spectra of TKE vary through the tank
6. Wave effects

TESTS

Number	Description
1	Functional Check - does it work and convergence test using vectrino
2	Down channel at 1m height to investigate convergence at different stations
3	What are the large eddy lengthscales? Horizontal spacing of Two instrument packages, each having a vector and a shear probes, with package 1 containing an EM meter too.
4	What are the large eddy lengthscales? Vertical spacing of the same two instrument packages (but oriented horizontally to get closer to the floor)
5	Vertical Profiles of Reynolds Stresses. One instrument package, Shear_z, Shear_y, Vector, EM. Transect down constant Y coord of load cell.
6	What effect do waves have on turbulence?

OUTSTANDING QUESTIONS

Are we confident integrating shear back to velocity (from a nominally stationary probe)?

Are we likely to see coherence in shear as well as in velocity?

Tom's thoughts: Yes, but it'll be quite difficult to recognise structural properties from it.

NOTES

Coordinate system:

+x is the flow direction, parallel to the gantry tracks, with 0 in the centre of the tank.
+y is cross-stream, forming a right handed set with x and z, with its origin at the tank centre
+z is upward, with 0 at the floor
.'lc' denotes load cell location

Assumptions:

flow is symmetrical around the x-axis (direction of flow). that is, flow at y=+1m is the same as at y=-1m

Sensor 2 position:

is given in mm relative to Sensor 1 position

Profiles:

z coordinate is given as 'profile', a series of points from floor to free-surface (or vice-versa) is required.
Duration is per point through the profile.
Spacing worked out in meeting 23 Feb - Peter/Jeff, do you have this or should I re-derive?
Peter - We had Horizontal profiles with Sensor1 fixed on the centerline (x-axis) and S2 at 10-12 data points along +y out to 2.3m.
Peter - For the Vertical profiles we had S1 and S2 packages on a vertical riser at the centerline. Both starting at 1m (center of depth) and then moving apart in z 10-12 data points over 1.9 meters (nominal depth and get as close to floor and surface)
PETER - refer to the scanned sketches for all the doodles of spacing and location

Test Order

The days on which tests were done became corrupted (or dummy here did something to overwrite).
I've indicated a general order by letter of the runs within each test.
I believe Peter and Jeff had a record of which tests were to be run in which sequence?
Peter - I don't recall having set days or schedule of testing. I think it was a to be determined based on Tom D. and Jeff's tank experience in how to do things efficiently.

Wave tests:

Sinusoidal waves only (no sense complicating thigs with spectrum)
Attempt to be made to adjust wave amplitude to the values defined in the table below. Wave amplitude varies across the pool - we're only concerned with wave height at the measurement location.

Airy analysis:

An airy assumption can be used to determine wave orbital velocities as a function of wave height and frequency
Assumptions and parameters:

Linear wave - current superposition (nonlinearity due to fetch or breaking negligible)

Floor z	0	mm
Free surface z	2000	mm
Current speed	0.8	m/s
TI @ z = 1000mm	0.05	-

Turbulent fluctuation - velocity x component (CRUDE!!!! But O() correct)

u'	0.04	m/s

The figure on the right shows u' as resulting from wave orbital velocities, under an airy approximation, at z = 1000mm.
We want the fluctuation due to wave orbitals to be of similar order to turbulent fluctuations, therefore want to be in the top right
The crease at Period 1.6s is a result of transition between intermediate (above the crease) and deep water (below the crease) airy approximations.
Airy analysis will be unreliable close to the crease

Wave test parameterisation

Attached MATLAB files have been used to deduce the test points in red, in the figure on the right.
The primary rationale is to do a sweep of wave period and determine the effect of period on turbulence.
To do this, I've attempted to control the orbital velocities seen at the sensor location, so they're the same magnitude as the turbulent fluctuations above.
The red isoline in the figure (right) shows the localities of H-T space where u' at the sensor location is constant.
Where maintaining a constant u' is clearly impossible, I've filled in the gaps with a sweep at constant H which will give us enough data to tie down the variation with T, which is complicated by the two wave regimes (deep water and intermediate)
Hopefully the selection of the isovalue avoids the regions of H-T space which are too energetic for the wave generators to cope with.
Location of the test doesn't really matter - happy for it to be at the load cell or at 0,0, or anywhere else in the central region.
There appear to be a lot of runs - but actually the sensor location doesn't change at all so hopefully they'll go quickly.
JEFF PLEASE CHECK: I don't know what time is involved in setting the wave height for each run. Is my matrix realistic for test 7???

QUESTION FROM PETER: WHAT RIGGING FOR EACH TEST (GANTRY MOUNT OR RIGID FLOOR MOUNT). RIGID FLOOR MOUNT SHOULD GIVE BETTER RESULTS.

TEST MATRIX

Test No	Planned Day	Flow Speed (m/s)	Sensor orientation	Sensor 1 position (mm)			Sensor 2 position (mm)			Frequency (Hz)	Wave Height peak-trough (mm)	Duration (s)	No. Runs
				x	y	z	Dx	Dy	Dz				
1.1		0.8	-x	-1500	0	1000	0	0	0	na	na	600	2
1.2		0.8	-x	-1500	0	100	0	0	0	na	na	600	2
1.3		0.8	-x	-1500	0	1800	0	0	0	na	na	600	2
2.0.		0.8	-x	-1500	0	1000	0	0	-60	na	na	600	2
2.1		0.8	-x	-750	0	1000	0	0	-60	na	na	600	2
2.2		0.8	-x	0	0	1000	0	0	-60	na	na	600	2
2.3		0.8	-x	750	0	1000	0	0	-60	na	na	600	2
2.4		0.8	-x	1500	0	1000	0	0	-60	na	na	600	2
~~3.1~~		~~0.8~~	~~-x~~	~~1500~~	~~0~~	~~1000~~	~~0~~	~~50~~	~~0~~	~~na~~	~~na~~	~~1200~~	~~1~~
~~3.2~~		~~0.8~~	~~-x~~	~~1500~~	~~0~~	~~1000~~	~~0~~	~~75~~	~~0~~	~~na~~	~~na~~	~~1200~~	~~1~~
3.3		0.8	-x	**1500**	0	1000	0	100	0	na	na	**1200**	1
3.4		0.8	-x	**1500**	0	1000	0	175	0	na	na	**1200**	1
3.5		0.8	-x	**1500**	0	1000	0	300	0	na	na	**1200**	1
3.6		0.8	-x	**1500**	0	1000	0	450	0	na	na	**1200**	1
3.7		0.8	-x	**1500**	0	1000	0	600	0	na	na	**1200**	1
3.8		0.8	-x	**1500**	0	1000	0	800	0	na	na	**1200**	1
3.9		**0.8**	**-x**	**1500**	**0**	**1000**	**0**	**1000**	**0**	**na**	**na**	**1200**	**1**
3.10		**0.8**	**-x**	**1500**	**0**	**1000**	**0**	**1300**	**0**	**na**	**na**	**1200**	**1**
3.11		0.8	-x	**1500**	0	1000	0	1600	0	na	na	**1200**	1
3.12		0.8	-x	**1500**	0	1000	0	2300	0	na	na	**1200**	1
~~4.1~~	~~a~~	~~0.8~~	~~-x~~	~~1500~~	~~0~~	~~1000~~	~~0~~	~~0~~	~~-50~~	~~na~~	~~na~~	~~600~~	~~1~~
~~4.2~~	~~b~~	~~0.8~~	~~-x~~	~~1500~~	~~0~~	~~1075~~	~~0~~	~~0~~	~~-75~~	~~na~~	~~na~~	~~600~~	~~1~~
4.3	c	0.8	-x	1500	0	1100	0	0	-100	na	na	**900**	1
4.4	d	0.8	-x	1500	0	1150	0	0	-150	na	na	**900**	1
4.5	e	0.8	-x	1500	0	1250	0	0	-250	na	na	**900**	1
4.6	f	0.8	-x	1500	0	1400	0	0	-400	na	na	**900**	1
4.7	g	0.8	-x	1500	0	1500	0	0	-500	na	na	**900**	1
4.8	h	0.8	-x	1500	0	1600	0	0	-600	na	na	**900**	1
4.9	i	0.8	-x	1500	0	1700	0	0	-700	na	na	**900**	1
4.10	j	0.8	-x	1500	0	1800	0	0	-800	na	na	**900**	1
~~5.1~~	~~a~~	~~0.6~~	~~-x~~	~~-2000~~	~~lc~~	~~profile~~	~~0~~	~~0~~	~~0~~	~~na~~	~~na~~	~~600~~	~~1~~
~~5.2~~	~~b~~	~~0.6~~	~~-x~~	~~0~~	~~lc~~	~~profile~~	~~0~~	~~0~~	~~0~~	~~na~~	~~na~~	~~600~~	~~1~~
~~5.3~~	~~c~~	~~0.6~~	~~-x~~	~~2000~~	~~lc~~	~~profile~~	~~0~~	~~0~~	~~0~~	~~na~~	~~na~~	~~600~~	~~1~~
~~5.4~~	~~d~~	~~0.6~~	~~-x~~	~~4000~~	~~lc~~	~~profile~~	~~0~~	~~0~~	~~0~~	~~na~~	~~na~~	~~600~~	~~1~~
5.5	a	**0.8**	**-x**	**-2000**	**lc**	**profile**	**0**	**0**	**0**	**na**	**na**	**900**	**1**
5.6	b	**0.8**	**-x**	**0**	**lc**	**profile**	**0**	**0**	**0**	**na**	**na**	**900**	**1**
5.7	c	**0.8**	**-x**	**2000**	**lc**	**profile**	**0**	**0**	**0**	**na**	**na**	**900**	**1**
5.8	d	**0.8**	**-x**	**4000**	**lc**	**profile**	**0**	**0**	**0**	**na**	**na**	**900**	**1**
~~5.9~~	~~a~~	~~1~~	~~-x~~	~~-2000~~	~~lc~~	~~profile~~	~~0~~	~~0~~	~~0~~	~~na~~	~~na~~	~~600~~	~~1~~
~~5.10~~	~~b~~	~~1~~	~~-x~~	~~0~~	~~lc~~	~~profile~~	~~0~~	~~0~~	~~0~~	~~na~~	~~na~~	~~600~~	~~1~~
~~5.11~~	~~c~~	~~1~~	~~-x~~	~~2000~~	~~lc~~	~~profile~~	~~0~~	~~0~~	~~0~~	~~na~~	~~na~~	~~600~~	~~1~~
~~5.12~~	~~d~~	~~1~~	~~-x~~	~~4000~~	~~lc~~	~~profile~~	~~0~~	~~0~~	~~0~~	~~na~~	~~na~~	~~600~~	~~1~~
~~5.13~~	~~a~~	~~1.2~~	~~-x~~	~~-2000~~	~~lc~~	~~profile~~	~~0~~	~~0~~	~~0~~	~~na~~	~~na~~	~~600~~	~~1~~
~~5.14~~	~~b~~	~~1.2~~	~~-x~~	~~0~~	~~lc~~	~~profile~~	~~0~~	~~0~~	~~0~~	~~na~~	~~na~~	~~600~~	~~1~~
~~5.15~~	~~c~~	~~1.2~~	~~-x~~	~~2000~~	~~lc~~	~~profile~~	~~0~~	~~0~~	~~0~~	~~na~~	~~na~~	~~600~~	~~1~~
~~5.16~~	~~d~~	~~1.2~~	~~-x~~	~~4000~~	~~lc~~	~~profile~~	~~0~~	~~0~~	~~0~~	~~na~~	~~na~~	~~600~~	~~1~~
6.1	a	0.8	-x	0	0	1000	0	50	0	0.35	0.1057	600	1
6.2	b	0.8	-x	0	0	1000	0	50	0	0.4	0.13	600	1
6.3	c	0.8	-x	0	0	1000	0	50	0	0.45	0.17	600	1
6.4	d	0.8	-x	0	0	1000	0	50	0	0.5	0.24	600	1
6.5	e	0.8	-x	0	0	1000	0	50	0	0.55	0.25	600	1
6.6	f	0.8	-x	0	0	1000	0	50	0	0.6	0.25	600	1
6.7	g	0.8	-x	0	0	1000	0	50	0	0.65	0.1612	600	1
6.8	h	0.8	-x	0	0	1000	0	50	0	0.7	0.2035	600	1
6.9	i	0.8	-x	0	0	1000	0	50	0	0.75	0.25	600	1
6.10	j	0.8	-x	0	0	1000	0	50	0	0.875	0.25	600	1
6.11	k	0.8	-x	0	0	1000	0	50	0	1	0.25	600	1
6.12	a	0.8	45 degrees	0	0	1000	0	50	0	0.35	0.1057	600	1
6.13	b	0.8	45 degrees	0	0	1000	0	50	0	0.4	0.1327	600	1
6.14	c	0.8	45 degrees	0	0	1000	0	50	0	0.45	0.1743	600	1
6.15	d	0.8	45 degrees	0	0	1000	0	50	0	0.5	0.2405	600	1
6.16	e	0.8	45 degrees	0	0	1000	0	50	0	0.55	0.25	600	1
6.17	f	0.8	45 degrees	0	0	1000	0	50	0	0.6	0.25	600	1
6.18	g	0.8	45 degrees	0	0	1000	0	50	0	0.65	0.1612	600	1
6.19	h	0.8	45 degrees	0	0	1000	0	50	0	0.7	0.2035	600	1
6.20	i	0.8	45 degrees	0	0	1000	0	50	0	0.75	0.25	600	1
6.21	j	0.8	45 degrees	0	0	1000	0	50	0	0.875	0.25	600	1
6.22	k	0.8	45 degrees	0	0	1000	0	50	0	1	0.25	600	1
6.23	a	0.8	y	0	0	1000	0	50	0	0.35	0.1057	600	1
6.24	b	0.8	y	0	0	1000	0	50	0	0.4	0.1327	600	1
6.25	c	0.8	y	0	0	1000	0	50	0	0.45	0.1743	600	1
6.26	d	0.8	y	0	0	1000	0	50	0	0.5	0.2405	600	1
6.27	e	0.8	y	0	0	1000	0	50	0	0.55	0.25	600	1
6.28	f	0.8	y	0	0	1000	0	50	0	0.6	0.25	600	1
6.29	g	0.8	y	0	0	1000	0	50	0	0.65	0.1612	600	1
6.30	h	0.8	y	0	0	1000	0	50	0	0.7	0.2035	600	1
6.31	i	0.8	y	0	0	1000	0	50	0	0.75	0.25	600	1
6.32	j	0.8	y	0	0	1000	0	50	0	0.875	0.25	600	1
6.33	k	0.8	y	0	0	1000	0	50	0	1	0.25	600	1

APPENDIX C – Rockland Scientific Internal Note 060

RSI Internal Technical Note 060

InStream Data Processing of Nemo Data by RSI

Rolf Lueck

2017-03-13

Rockland Scientific International Inc.
520 Dupplin Rd
Victoria, BC, CANADA, V8Z 1C1
www.rocklandscientific.com

Contents

List of Figures

List of Tables

1 Introduction

This report summarizes the processing of data, by the author, that were collected by the two Nemo moorings deployed in Minas Passage, Nova Scotia in August of 2016. It provides an overview of the data, a description of the algorithms and methods, and selected results, so that you can process the original raw data files (the p-files) to replicate, and to build on, the results obtained at Rockland Scientific.

2 Nemo Deployments Parameters

The moored instrument system (Figure 1) were deployed in Minas Passage, Nova Scotia, Canada, approximately 2 km west of Black Rock Island. The details of the deployments and recoveries are found in Table 1. Nemo East and Nemo West were separated by approximately 200 m. Nemo East and Nemo West are sometimes denoted as the Dalhousie- and RSI-Nemo, respectively.

Instrument	Parameter	Values
Nemo East	deployment time	2016-08-27 11:43:24 UTC
	recovery time	2016-09-11 10:36:36 UTC
	longitude	64°26.310′ E
	latitude	45°22.149′ N
	water depth	55 m
	height above bottom	14.8 m
	data file names	MP2_XXX.p
	data file, deployment	MP2_002.p
	data file, recovery	MP2_360.p
Nemo West	deployment time	2016-08-28 12:41:16 UTC
	recovery time	2016-09-11 10:19:23 UTC
	longitude	64°26.401′ E
	latitude	45°22.115′ N
	water depth	55 m
	height above bottom	39.8 m
	data file names	MP1_XXX.p
	data file, deployment	MP1_003.p
	data file, recovery	MP1_336.p

Table 1: The basic information of the deployment and recovery of the Nemo systems in Minas Passage. The deployment and recovery times are the the times of anchor release.

The Nemo moorings carried three instrument systems.

- The MicroRider (MR) turbulence package, mounted into the front of Nemo, that carried 4 shear probes, 1 thermistor, a pressure transducer, a two-axis precision inclinometer, and a triplet of three-axis acceleration, rate-of-rotation, and magnetic-field sensors.
- A three-axis ADV (acoustic Doppler velocimeter) that recorded data internally and also sent analog velocity data to the MicroRider.
- An upward looking ADCP (acoustic Doppler current profiler) that recorded its data internally.

Only the data recorded by the MicroRider and the ADVs are discussed here.

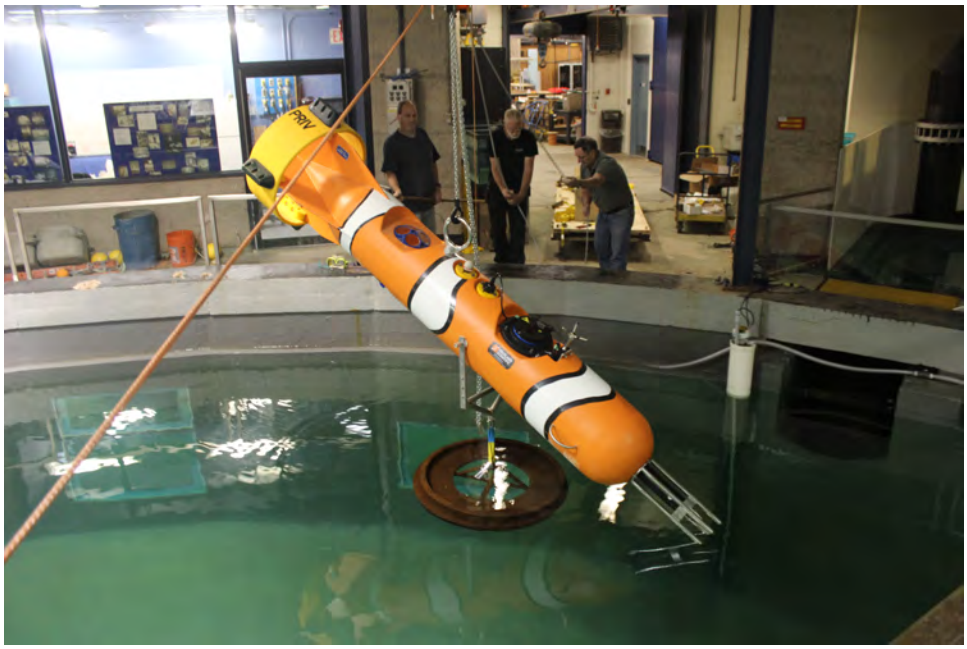

Figure 1: Nemo 'West' about to be tested for static balance in the Dalhousie University Test Tank Facility.

3 Preliminary Processing Scripts

3.1 Background

All data were processed using Matlab (Version 2016b), the ODAS Matlab Library (Version 4.1), and "Vector" functions. All signals measured by Nemo are in the "body frame" that has coordinates denoted by x, y, and z. The x-axis points forward, and into the oncoming stream, along the principle axis of Nemo. The y-axis is directed athwartship to port, and z-axis points nominally upward. The coordinates in the earth frame are denoted by X, Y, and Z and are direct to east, north, and up.

The data are available in `DropBox` and are organized according to Table 2.

Directory	Sub-directory	Contents
Nemo_East_MR_119		raw data, scripts, configuration and `ql_info` files.
Nemo_West_MR_064		raw data, scripts, configuration and `ql_info` files.
Vector_Nemmo_East		ADV raw and processed files.
Vector_Nemmo_West		ADV raw and processed files .
Vector_Nemmo_West	MP_102	ADV data-file runt – nothing useful.
InStream_Nemo_Report		Latex- and pdf-files associated with this report.
InStream_Nemo_Report	Figures	The pdf figures associated with this report.
odas		The latest version of the ODAS Matlab Library.
Vector		Scripts and functions for processing ADV data.

Table 2: The structural organization of the Nemo data.

The approximate chronological order of data processing is described in the following sections.

3.2 ADV data

The ADV data were downloaded from the Nortek Vector using the Windows-based software provided by the Manufacturer. This produces a file with the extension `.vec`, which is a compact binary file. The same software was used to convert the data into a "useable" form. The conversion generates ASCII files with extensions `.dat`, `.hdr`, `.pck`, `.sen`, `.ssl`, and `.bhd`. The main files of interest are the `.dat`-file which contains the velocity, acoustic and pressure data, the `.sen`-file which contains the time stamp, sensor data and error flags, and the `.hdr`-file which contains data on the mechanical, electronic and software configurations, including the sampling rate. The `.dat` file does not contain a time stamp. The function `read_vector` reads these three ASCII files and creates a mat-file of the data, with self-explanatory content.

The function `quick_look_vector_3` plots the data in the ADV mat-file (see appendix A and B). It is not a very sophisticated function and the parameters for the identification

and removal of bad data have to be set manually.

3.2.1 ADV hotel-files

The conversion of Nemo data into physical units requires the speed of profiling. This information is derived from the ADV (Acoustic Doppler Velocimeter) mounted on Nemo. Nemo West used a late model ADV. It was configured to sample at a rate of $16\,\mathrm{s}^{-1}$, to output analog data of the three-components of velocity, and to also record its data internally. A wiring error caused the z-component of the analog output to be suppressed to small values, while the x- and y-components were received correctly. The script `make_nemo_hotel_file` is used to make a Matlab "hotel mat-file" so that the internally recorded data can be subsequently incorporated into a MicroRider Matlab data file.

Methods for creating a hotel file are described in RSI Technical Note 039.

The recording of the analog ADV velocity data on Nemo East was a total failure. The ADV on Nemo East is an older unit that, among other issues, cannot remember its configuration for more than a few minutes after it is disconnected from a source of power. It is likely that power was re-supplied after the ADV lost its configuration information – specifically, to output analog data. This ADV did record data internally (at a rate of $4\,\mathrm{s}^{-1}$), including pressure. From the launch and recovery times, it was possible to align the time base of the internally recorded data with the time base of the MicroRider data collected at Nemo East. This time-base adjustment (involving a shift and stretch of time) was used to create a "hotel file" of velocity data using the script `make_nemo_hotel_file`, at a later stage.

The function `adjust_vector_time` is used to shift and stretch the time base of the ADV data. Repeated shifting and stretching is tracked (placed into the ADV mat-file) so that the adjustments can be done with every increasing finesse, without corrupting the original time stamps.

The scripts `make_nemo_hotel_file` are slightly different for Nemo East and Nemo West, and they are located in their respective directories with the ADV data (Table 2).

3.3 MicroRider configuration corrections

The original MicroRider data files all had errors in their embedded configuration string. This string contains the information that is required for the conversion of the raw data into physical units. Most of the error involve offset and scale adjustments for the GyroCube accelerometers, the PNI magnetometers, and the pre- to post-deployment change of sensitivity of the shear probes. These are not true errors. Rather, they are unavoidable adjustments to account for changes of sensor characteristics. There were real errors in the analog channel assignment of the three components of velocity measured by the ADV, due to wiring errors.

The script `make_1_min_averages_from_P_files` was used to make a data file of one-minute averages of most data in physical units, without the need to create mat-files from the original MicroRider data files. The script `show_big_picture` reads the file of one-minute averages and plots the data in a multitude of figures. A `return` statement must be inserted near line 900 so that the scripts ends there because the remainder of the script uses dissipation estimates, which are not yet available at this stage of the data processing. At this stage, the figures are used to determine the corrections of the configuration string.

The offset and sensitivity of the x- and y-components of the Gyro-Cube accelerometer signals were adjusted so that these signals agreed with the readings by the inclinometers. The z-component of acceleration was offset so that the magnitude of the vector sum of accelerations was close to $9.81\,\mathrm{m\,s^{-2}}$. The x- and y-components of acceleration are then used to derive the Euler angles of rotation in the horizontal plane. That is, these two Euler angles can be used to rotate any vector measured by Nemo into a horizontal plane. A final rotation around the vertical axis (the third Euler angle) can then be used to transform the data into the geographically oriented Earth frame of X, Y, and Z.

The first two Euler angles are used to rotate the magnetometer signals into the horizontal earth plane. The magnetometer parameters are adjusted so that the horizontal components of the magnetic field form a hodograph centred on the origin and of constant radius equal to the true horizontal magnetic field (see Figures 22 and 48). The parameters of the vertical component (in the Nemo frame) of the magnetometer is adjusted so that the vertical component of the magnetic field in the Earth frame is independent of the direction of the Nemo. The adjustment process is iterative.

The pressure transducer offset coefficient was adjusted (by 0.9 dbar) so that the pressure reading was zero while the Nemo was still on the deck of the deployment boat. The pressure transducer still reported zero pressure when the Nemo was hoisted back aboard the recovery boat at the end of the deployment.

The offset coefficients for the rate of rotation sensors were adjusted so that the average rates are zero for the deployment.

No adjustments were made for the analog signals from the ADV, for Nemo West, because these signals agreed closely with the digital data that were recorded internal by the ADV.

The conversion of the raw data into physical units is controlled by the parameters in the configuration string. A new configuration string can be "patched" into a raw data file using the function `patch_setupstr`. The last files that were patched are:

- `setup_119_2017_01_26.cfg` for the files collected at Nemo East, and
- `setup_064_2017_01_11.cfg` for the files collected at Nemo West.

The figures created by the script `show_big_picture` are in Appendix C and D, for Nemo West and East, respectively. This script is slightly different for Nemo West compared to Nemo East because the analog ADV data are meaningless for Nemo East, at this stage of data processing.

4 Processing the Nemo Data

After the configuration string has been corrected and patched into the raw (*.p) data files, and after the creation of the hotel files containing the ADV data (section 3.2), it is possible to conduct the full processing of the MicroRider data files using the function `quick_look_HMP`.

4.1 Processing Nemo West MicroRider data

The MicroRider data from Nemo West was processed using the script `do_it_all`, which processes all files in the range of file numbers 3 to 336, inclusive. The main command in this script is

```
temp_diss = quick_look_HMP(...
    file_name, [], [], ql_info, 'make_figures', false);
```

which places the dissipation structure into `temp_diss`. The data are processed according to the fields in the structure `ql_info`, the rendering of figures is suppressed (to decrease the processing time), and no spectra are displayed for a time range because the start and end values of this range are empty, `[]`.

The value of the fields in the structure `ql_info` are

```
ql_info =
                  HP_cut: 1
                  LP_cut: 80
                    YD_0: 0
               despike_A: [8 0.5000 0.0400]
               despike_C: [10 1 0.0400]
              despike_sh: [10 0.5000 0.0400]
             diss_length: 60
                    f_AA: 392
                 f_limit: 300
              fft_length: 0.5000
               fit_2_isr: 1.5000e-05
               fit_order: 3
                 goodman: 1
            make_figures: 1
                 op_area: 'tidal_ch'
                 overlap: 0
          profile_min_P: 1
          profile_min_W: 0.2000
   profile_min_duration: 20
            profile_num: 1
       MF_extra_points: 20
```

```
           MF_k: 5
        MF_k_mag: 1.7000
          MF_len: 4096
       MF_st_dev: 'st_dev'
     MF_threshold: []
              aoa: []
    constant_speed: []
     constant_temp: []
      gradC_method: 'high_pass'
      gradT_method: 'high_pass'
        hotel_file: 'hotel_nemo'
      speed_cutout: 0.1500
         speed_tau: []
       time_offset: 0
           vehicle: ''
```

Only the fields starting with `aoa` and ending with `vehicle` are used for conversion into physical units. The remainder pertain to data processing. If a mat-file corresponding to a raw data file does not exists, a new one is created. If a mat-file corresponding to a raw data file does exist *and* if it was created using fields different from the ones specified in `ql_info`, then the user is requested to allow its erasure and, if allowed, a new mat-file is created using the specified fields. Otherwise, the existing mat-file is used for data visualization and the estimation of the rate of dissipation of kinetic energy, ϵ.

For Nemo West I specified the hotel file containing the ADV data. These data are incorporated into the mat-file and are interpolated on to the time base of `t_slow` that is used for all slow channels collected by the MicroRider. The recently added fields `gradC_method` and `gradT_method` (which are now the default values) specify the method used to convert the pre-emphasized data into gradients.

The remaining fields in `ql_info` control the processing of the converted data, and the major specifications are:

- high-pass filtering (`HP_cut`) of the shear-probe data at 1 Hz,
- despiking of shear-probe data (`despike_sh`) using a threshold of 10, a neighbourhood, that is the inverse of 0.5 Hz, for comparison of spike magnitude, and a *minimum* replacement window[1] of 0.04 s,
- despiking of piezo-accelerometer data (despike_A) using threshold of 8, and other parameters that are identical to those used for the shear-probe data,
- an upper limit (`f_limit`) of 300 Hz for spectral integration for the estimation of the shear variance,
- a fft-length (`fft_length`) of 0.5 s for the computation of periodgrams, which provides

[1] The width of the window is automatically increased to remove spikes that are wider than the minimum specification.

a frequency resolution of about 2 Hz and a spectral bandwidth of 2.9 Hz (Nuttall, 1971),

- the ensemble averaging (`diss_length`) of the periodograms, derived from each fft-segment, over an interval of 60 s, for an equivalent degrees of freedom of approximately 456 (Nuttall, 1971), and
- the removal of vibration-coherent noise (`goodman`) from the shear-probe data using the method of Goodman et al. (2006).

The script `do_it_all` then changes the name of the structure `temp_diss` to `diss_MP1_XXX` where `XXX` is the data file number, with leading zeros, and appends it to data file `MP1_XXX.mat` for later use.

4.2 ADV data in the MR data files, Nemo West

Channel name	Description
U	Velocity in direction x, recorded by the MR
V	Velocity in direction y, recorded by the MR
W	Velocity in direction z, recorded by the MR
U_internal_slow	Velocity in direction x, recorded internally by the ADV
V_internal_slow	Velocity in direction y, recorded internally by the ADV
W_internal_slow	Velocity in direction z, recorded internally by the ADV
Heading_internal_slow	Heading recorded internally by the ADV
P_internal_slow	Pressure recorded internally by the ADV
Pitch_internal_slow	Pitch recorded internally by the ADV
Roll_internal_slow	Roll recorded internally by the ADV
U_internal_fast	empty
V_internal_fast	empty
W_internal_fast	empty
Heading_internal_fast	empty
P_internal_fast	empty
Pitch_internal_fast	empty
Roll_internal_fast	empty

Table 3: The data in the MicroRider mat-files that are related to the ADV for Nemo West. The analog signal line for W was not properly connected and, therefore, the W signal is meaningless.

The MicroRider in Nemo West successfully recorded the analog data provided by the ADV[2]. The data recorded internally by the ADV was added to the MicroRider data files via the "hotel file" option of the conversion of the MR data into physical units. At the time of this phase of the data processing, the ODAS Matlab Library interpolated the data from a hotel file on to the time bases `t_fast` and `t_slow` used by the fast and slow channels

[2]Note, however, that the analog W component is corrupted.

of the MR data, respectively. The sampling of the fast and slow time bases are 2048 and $256\,s^{-1}$, respectively. The sampling rate of both time bases greatly exceeds the internal ADV sampling rate of $16\,s^{-1}$. For this reason the script `do_it_all` for Nemo West replaces the ADV data interpolated on to the fast time base with empty data, which reduces the size of the mat-files by about 400×10^6 bytes. In addition to the three components of velocity, the hotel file also contains ADV heading, pressure, pitch and roll signals, for a total of 7 signals. The ODAS Matlab Library function `odas_mat`, which does the actual incorporation of a hotel file, has subsequently been modified to only interpolate data on to the time base `t_slow`. The ADV related data in the MicroRider mat-files are listed in Table 3.

Before the hotel file is generated, the time in the mat-file containing the recorded ADV data (`MP_103.mat`) is adjusted using the function `adjust_vector_time`, which can shift and stretch the time tags in the ADV mat-file (section 3.2.1). Best results are obtained for a shift of 0.1250 days (undoubtably due to using local time instead of UTC) and a stretch of 2.4537×10^{-6} days per day. The fluctuations of velocity in the analog and the ADV internally recorded data then coincide within less than 1 s for the entire deployment.

4.3 Processing Nemo East MicroRider data

The MicroRider data from Nemo East was processed using the script `do_it_all`, which processes all files in the range of file numbers 2 to 360, inclusive. The main command in this script is

```
temp_diss = quick_look_HMP(...
    file_name, [], [], ql_info, 'make_figures', false);
```

which places the dissipation structure into `temp_diss`. The data are processed according to the fields in the structure `ql_info`, the rendering of figures is suppressed (to decrease the processing time), and no spectra are displayed for a time range because the start and end values of this range are empty, `[]`.

The value of the fields in the structure `ql_info` are identical to those used for Nemo West (section 4.1), except that the name of the hotel file is `hotel_nemo_east`. Therefore, the processing of the MicroRider data is nearly identical for the two Nemo locations.

4.4 ADV data in the MR data files, Nemo East

The MicroRider in Nemo East did not record meaningful data from the analog output of the ADV because the output was disabled. The ADV at Nemo East did record its data internally, at a rate of $4\,s^{-1}$. The pitch, roll, and heading data did not look sensible (possibly because these signal are not enabled in this older model unit, see Figure 8). The pressure data did look partial sensible – the launch and recovery are clearly evident (Figure 7). However, the pressure transducer in this unit has a full-scale range of $\sim$25 dbar while the deployment depth was seldom less than 40 m. Therefore, the time of the launch

and recovery of Nemo East can be determined, from the pressure signal, to within better than 1 s with respect to the clock internal to the ADV. The same events can be determined to a slightly better accuracy with respect to the internal clock of the MR. The time base of the ADV data was then adjusted using the function `adjust_vector_time`. The shift and stretch that makes the launch and recovery agree to within better than 1 s are 7.4×10^{-5} days and 3.4340×10^{-5} days per day, respectively. Evidently the clock on this ADV was set closely to UTC but its rate-of-drift with respect to the MR clock was 14 times faster than the drift rate at Nemo West.

The data recorded internally by the ADV was added to the MicroRider data files via the "hotel file" option of the conversion of the MR data into physical units. The script `do_it_all` was used to convert the MR data into physical units and to incorporate the ADV in the hotel file.

The ADV related data in the MicroRider mat-files are listed in Table 4.

Channel name	Description
U	Velocity in direction x, recorded by the MR
V	Velocity in direction y, recorded by the MR
W	Velocity in direction z, recorded by the MR
U_slow	Velocity in direction x, recorded internally by the ADV
V_slow	Velocity in direction y, recorded internally by the ADV
W_slow	Velocity in direction z, recorded internally by the ADV
Heading_slow	Heading recorded internally by the ADV
P_slow	Pressure recorded internally by the ADV
Pitch_slow	Pitch recorded internally by the ADV
Roll_slow	Roll recorded internally by the ADV

Table 4: The data in the MicroRider mat-files that are related to the ADV for Nemo East. The data in U, V and W are meaningless because the analog output of the ADV was not enabled.

5 Final creation of one-minute average data

After the data processing described above, the MicroRider mat-files will contain the dissipation structure returned by the function `quick_look_HMP`. The dissipation structure contains one-minute averages of all data, plus the one-minute estimates of the rate of dissipation of kinetic energy, ϵ and the spectra of every minute of shear-probe, vibration and temperature-gradient data.

The function `make_1_min_averages_from_Diss_structure` will extract the information out of each structure and creates a single mat-file of one-minute average data. The function `show_big_picture` can then be used to for data visualization (see Appendix C and D). The `return` statements, that may have been inserted to end processing after the 19^{th} figure, must be removed in order to generate the higher number figures involving the rate of dissipation.

References

Goodman, L., E. R. Levine, and R. G. Lueck, 2006: On measuring the terms of the turbulent kinetic energy budget from an auv. *Journal of Atmospheric and Oceanic Technology*, **23**, 977–990.

Nuttall, A., 1971: Spectral estimation by means of overlapped fast fourier transform processing of windowed data. NUSC Tech. Rep. 4169, [Available online at http://oai.dtic.mil/oai/oai?verb=getRecord&metadataPrefix=html&identifier=AD0739315], Naval Underwater Systems Center.

A ADV figures, Nemo West

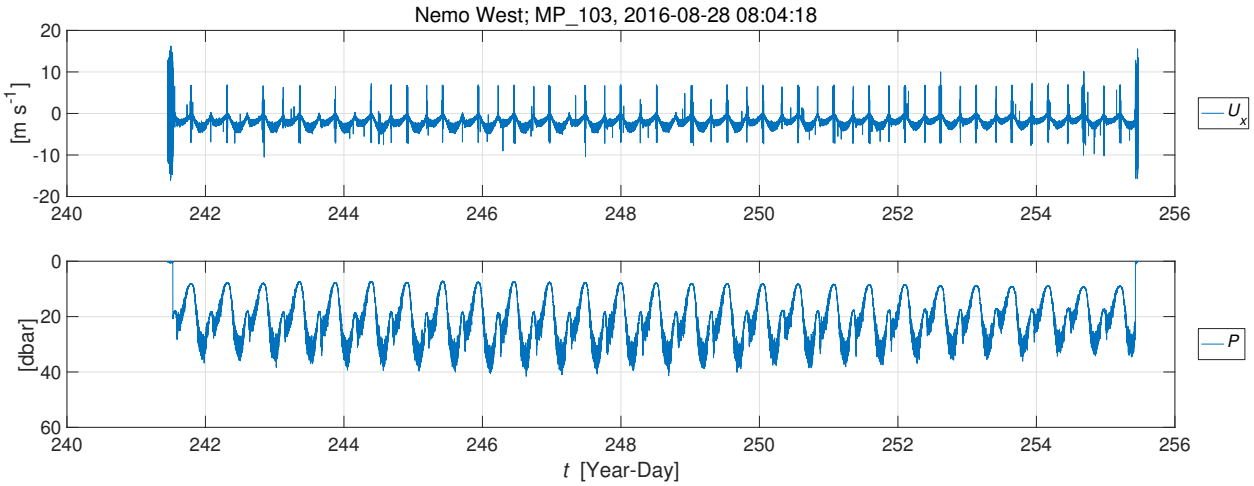

Figure 2: Data recorded internally by ADV; U_x and P data. No median filter.

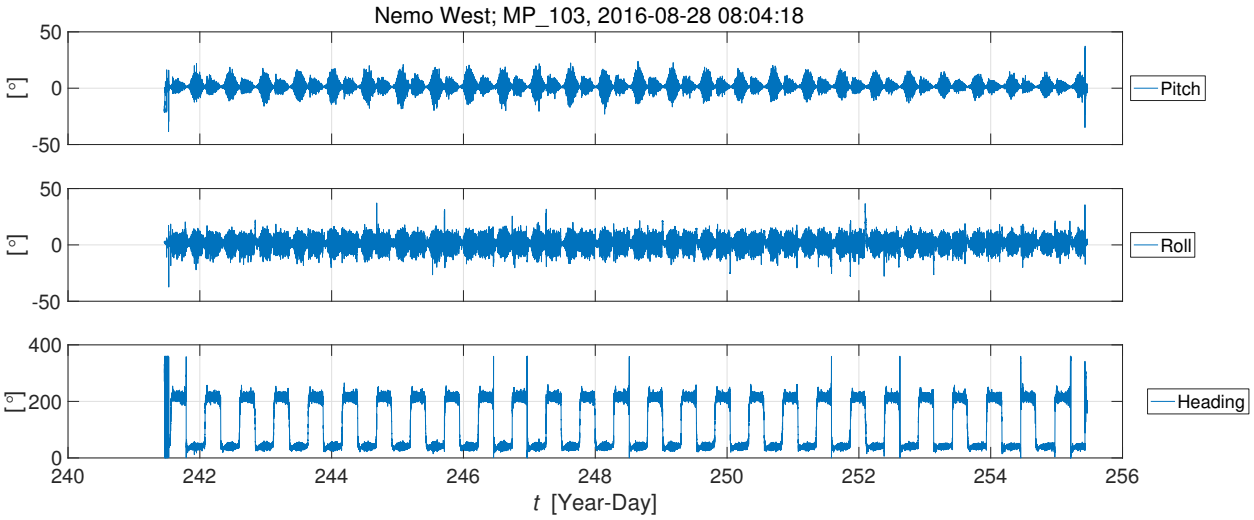

Figure 3: Attitude data recorded internally by the ADV.

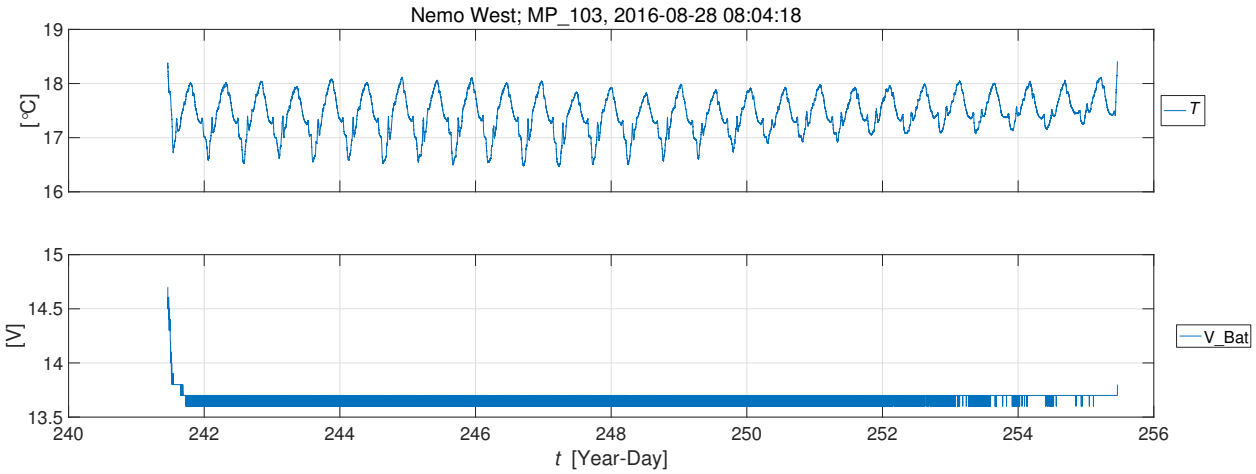

Figure 4: The temperature and battery voltage data recorded internally by the ADV.

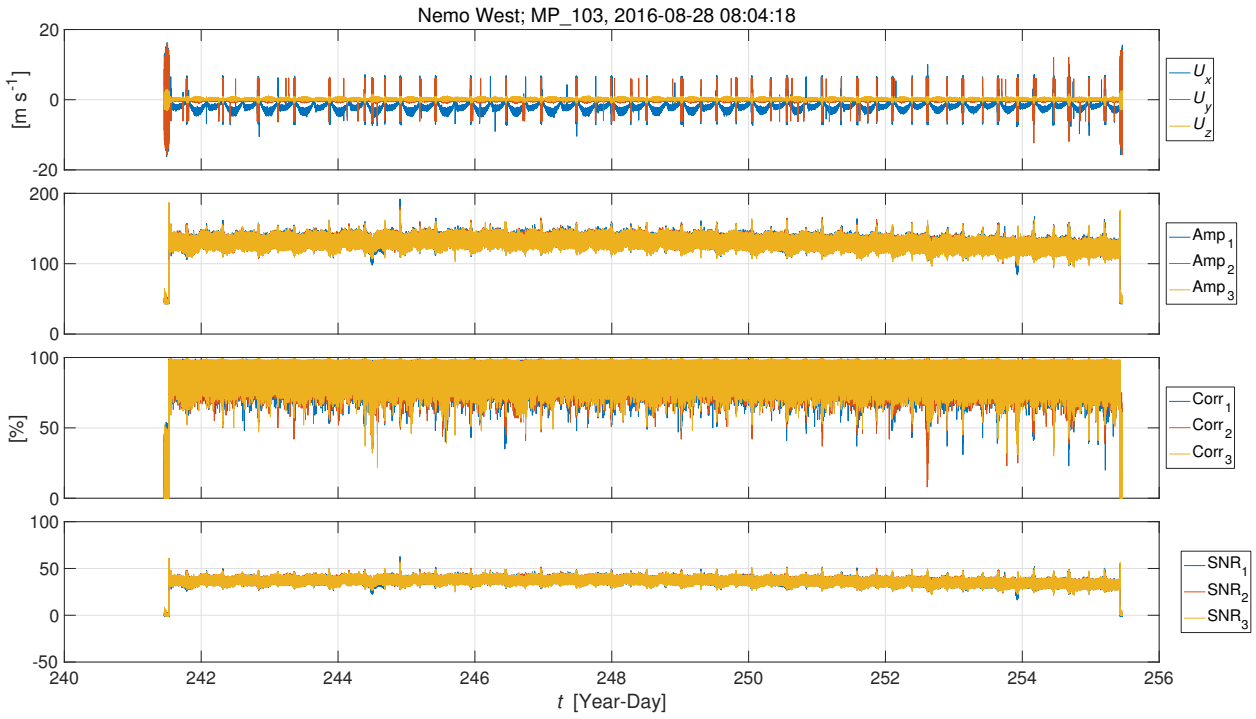

Figure 5: The three components of velocity and the acoustic data recorded internally by ADV.

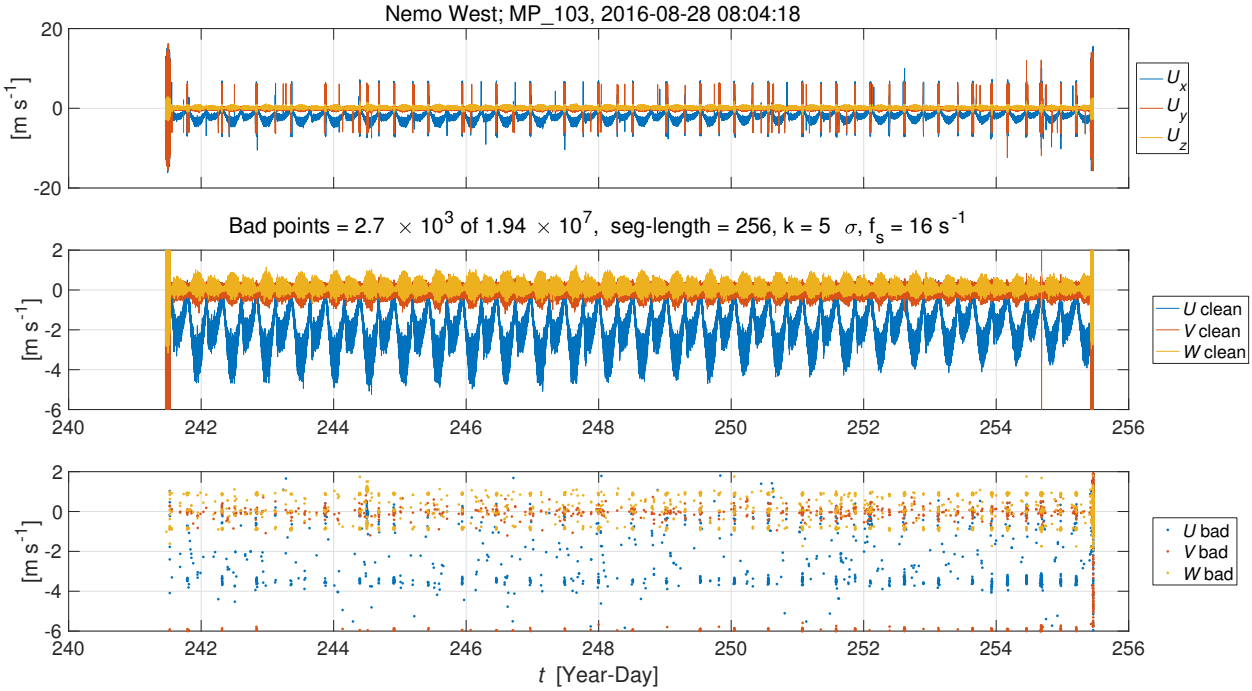

Figure 6: The ADV recorded velocity data. Original (upper panel), after median filtering (middle panel), and the bad data points identified by the median filter (lower panel). Data are examined in segment lengths of 256 points (16 s). Data that deviate more than 5 standard deviations from the median are flagged as bad. All velocity components are flagged bad if any single component is bad. The number of bad samples is 2700. The total number of samples is 1.94×10^7. The fraction of samples flagged to be bad is 1.4×10^{-4}. Most flagged data occur around the turning of the tide.

B ADV figures, Nemo East

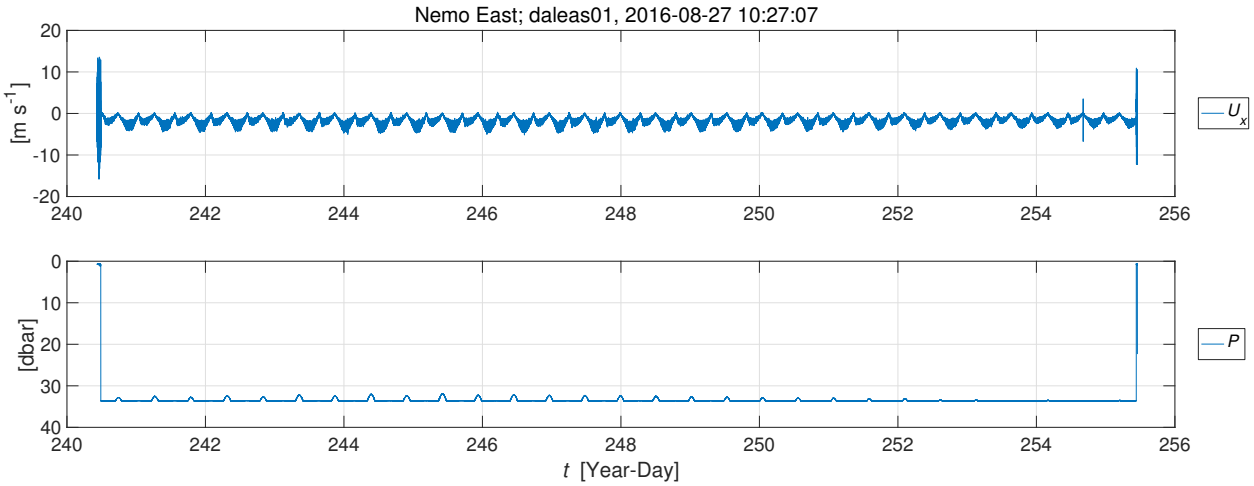

Figure 7: Data recorded internally by ADV; U_x and P data. No median filter. The pressure transducer is almost always off scale during the deployment.

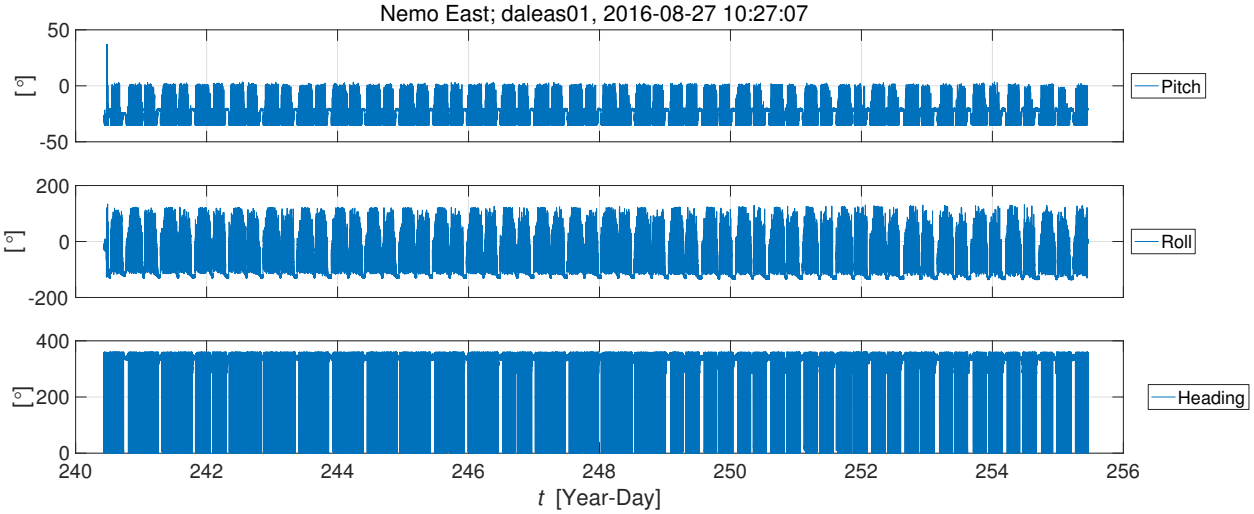

Figure 8: Attitude data recorded internally by the ADV.

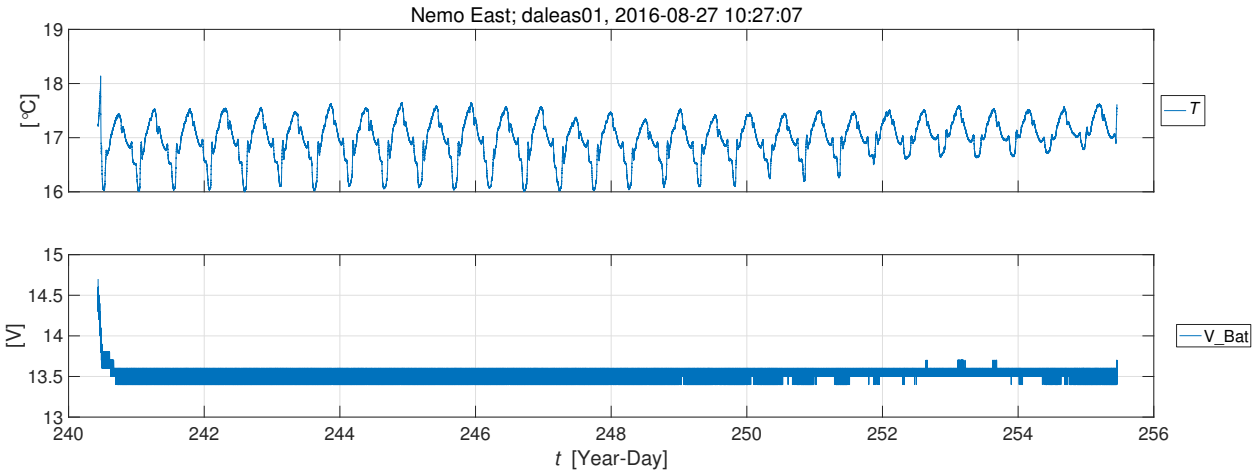

Figure 9: The temperature and battery voltage data recorded internally by the ADV.

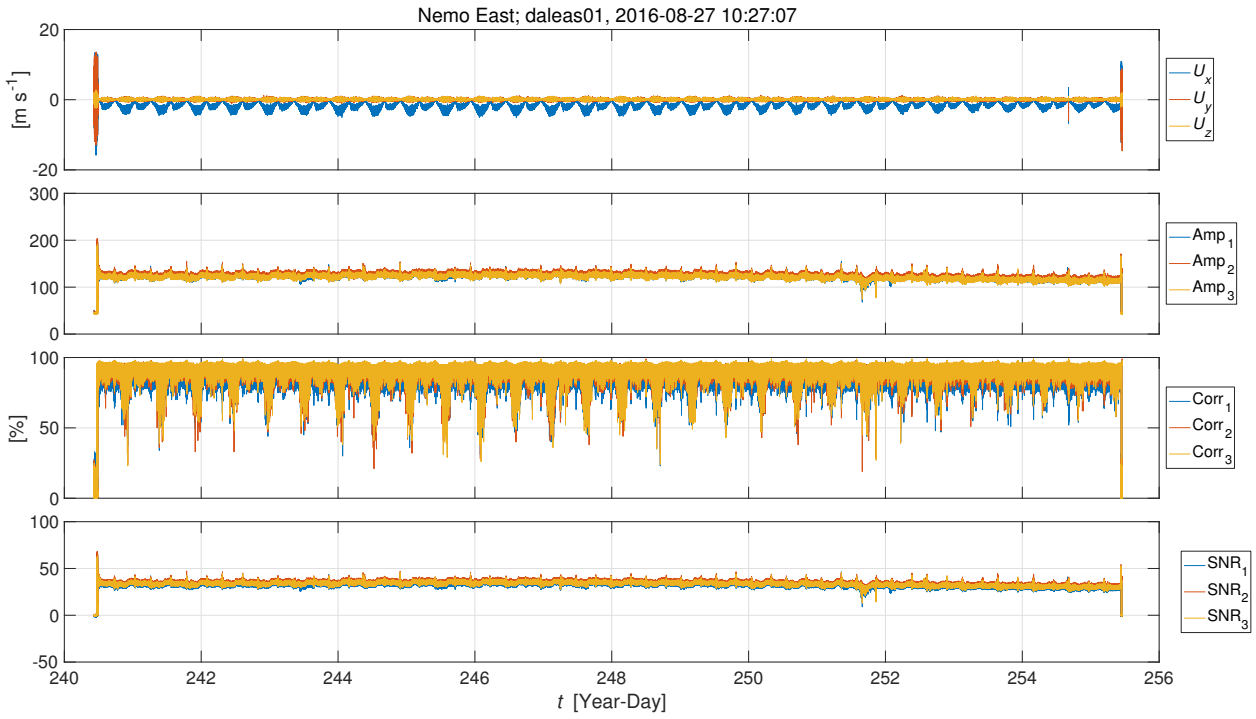

Figure 10: The three components of velocity and the acoustic data recorded internally by ADV.

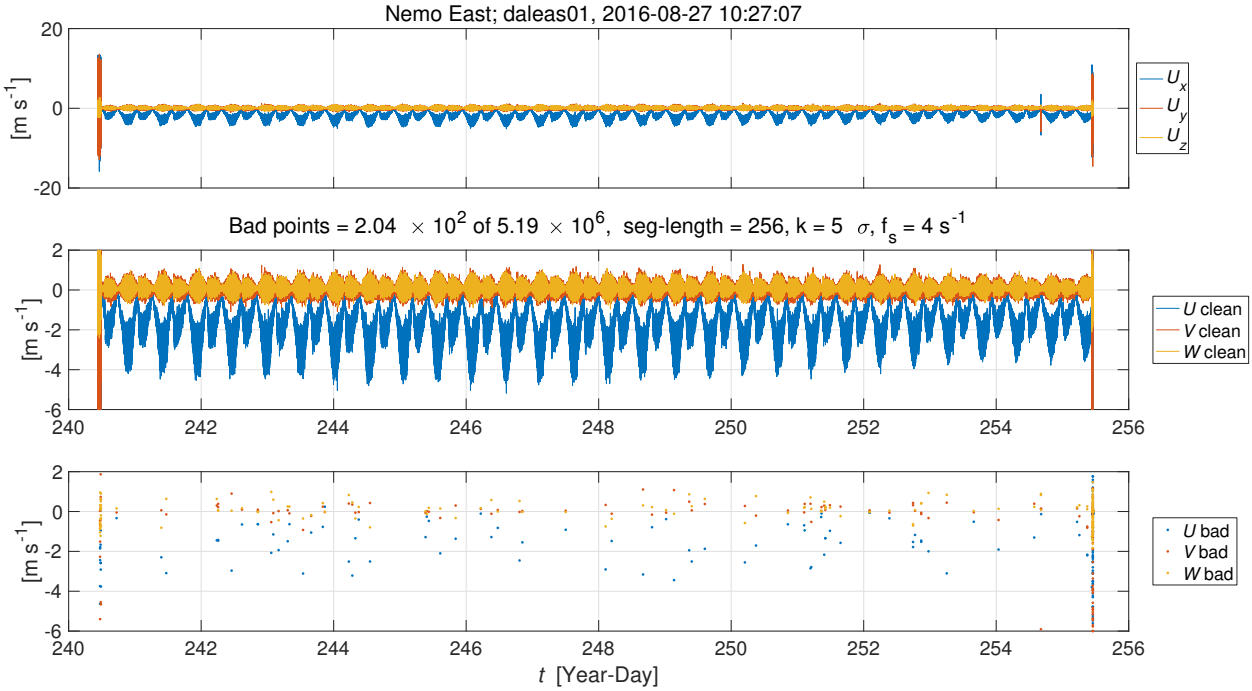

Figure 11: The ADV recorded velocity data. Original (upper panel), after median filtering (middle panel), and the bad data points identified by the median filter (lower panel). Data are examined in segment lengths of 256 points (16 s). Data that deviate more than 5 standard deviations from the median are flagged as bad. All velocity components are flagged bad if any single component is bad. The number of bad samples is 204. The total number of samples is 5.2×10^6. The fraction of samples flagged to be bad is 4×10^{-5}. Most flagged data occur around the turning of the tide, and during deployment and recovery.

C MicroRider 1-min average data – Nemo West

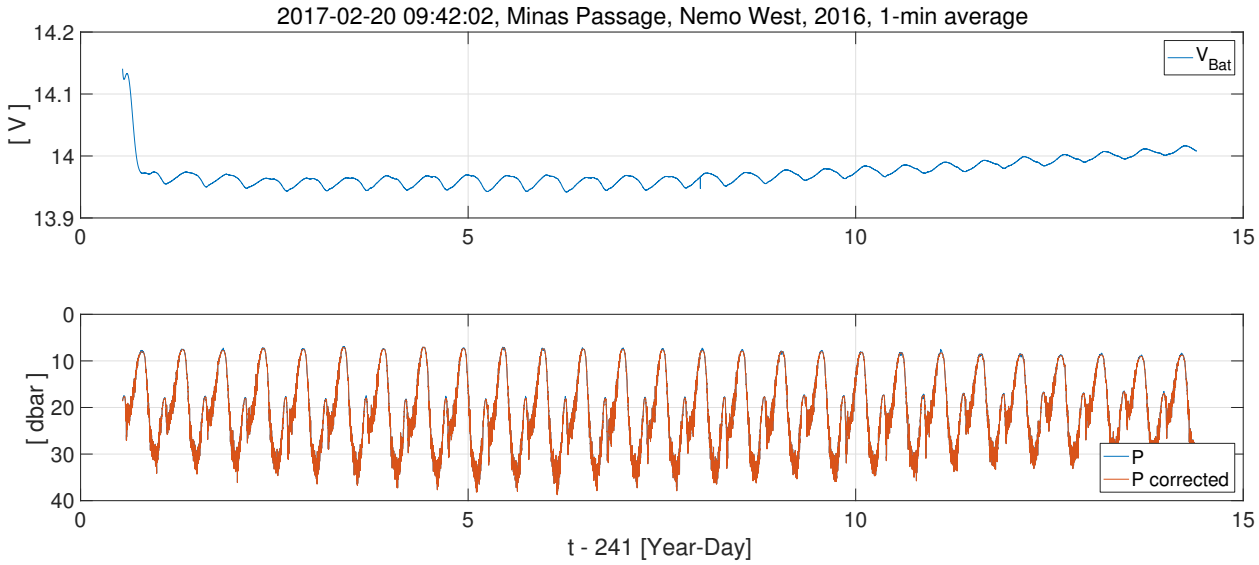

Figure 12: The pressure (lower panel) and battery voltage measured by the MicroRider on Nemo West. The corrected pressure is $P - L_P \sin\theta_y$ where $L_P = 1.36\,\mathrm{m}$ is the distance from the bridle axis to the pressure transducer and θ_y is the rotation around the y-axis (negative pitch).

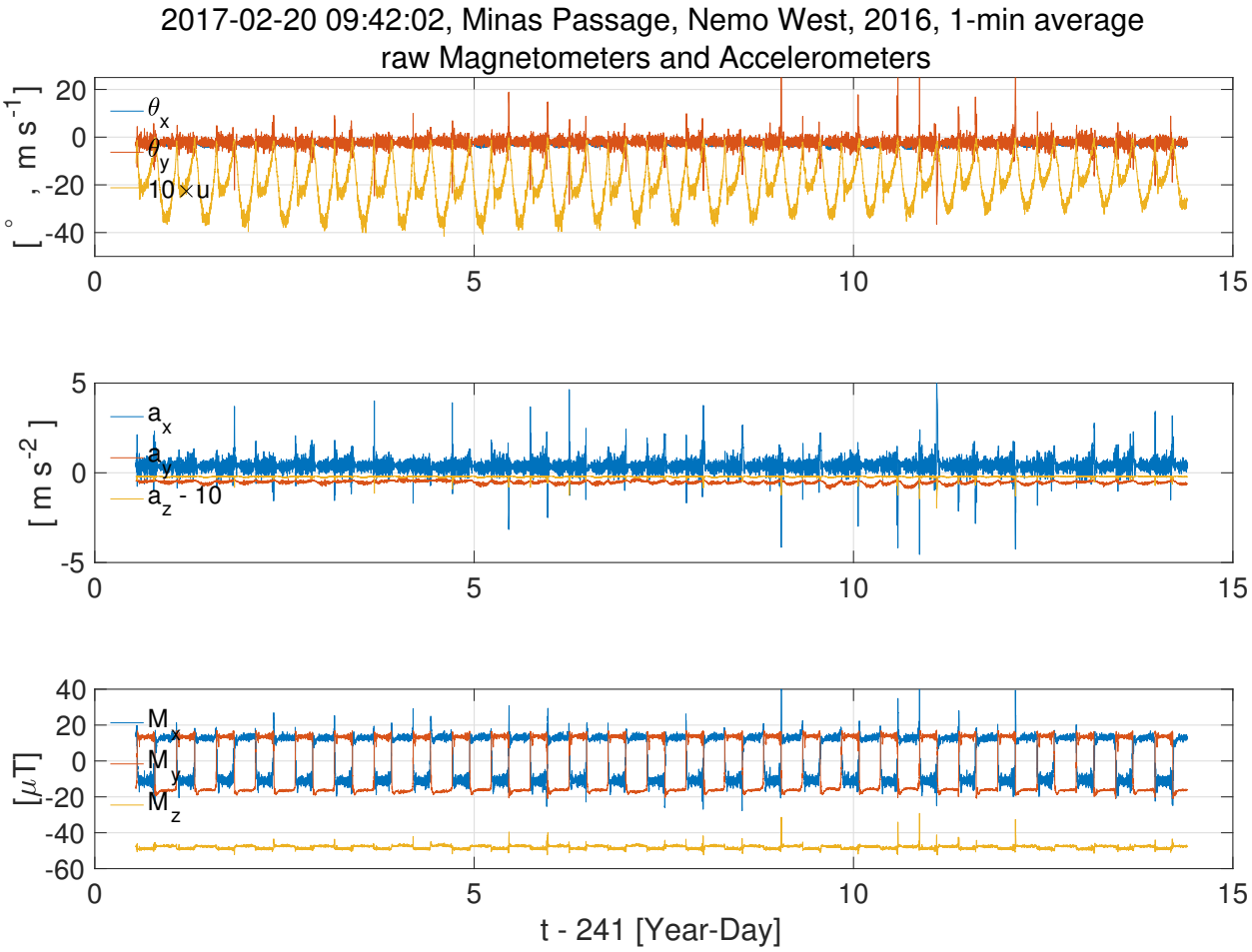

Figure 13: The inclinometer (upper panel), accelerometer (middle panel), and magnetometer (lower panel) data measured by the MicroRider on Nemo West.

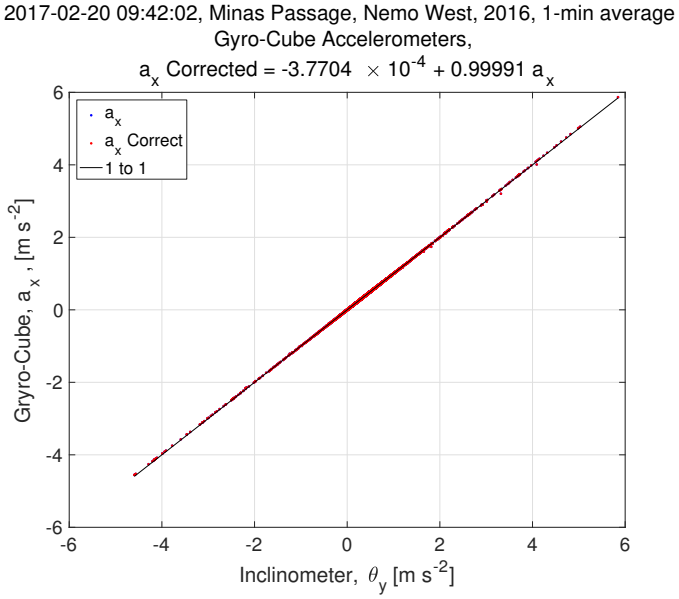

Figure 14: The regression of the Gyro-Cube accelerometer signal a_x against the inclinometer rotation around in the y-axis, measured by the MicroRider on Nemo West.

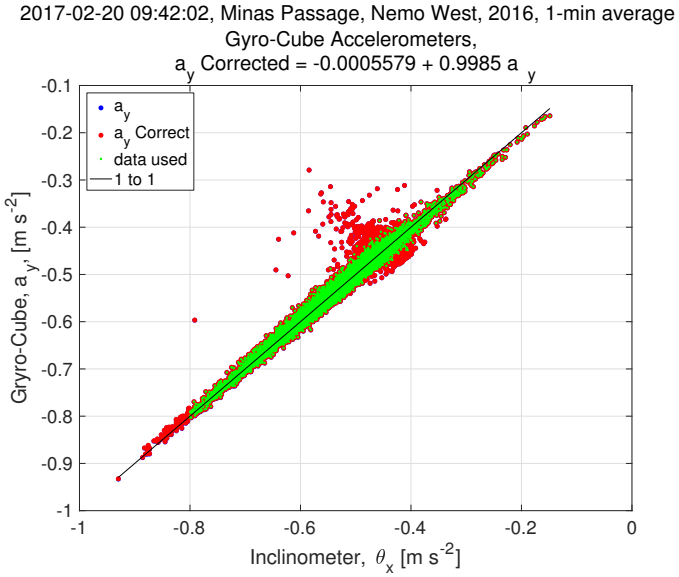

Figure 15: The regression of the Gyro-Cube accelerometer signal a_y against the inclinometer rotation around in the x-axis, measured by the MicroRider on Nemo West. Green points are for speeds greater than $0.5\,\mathrm{m\,s^{-1}}$.

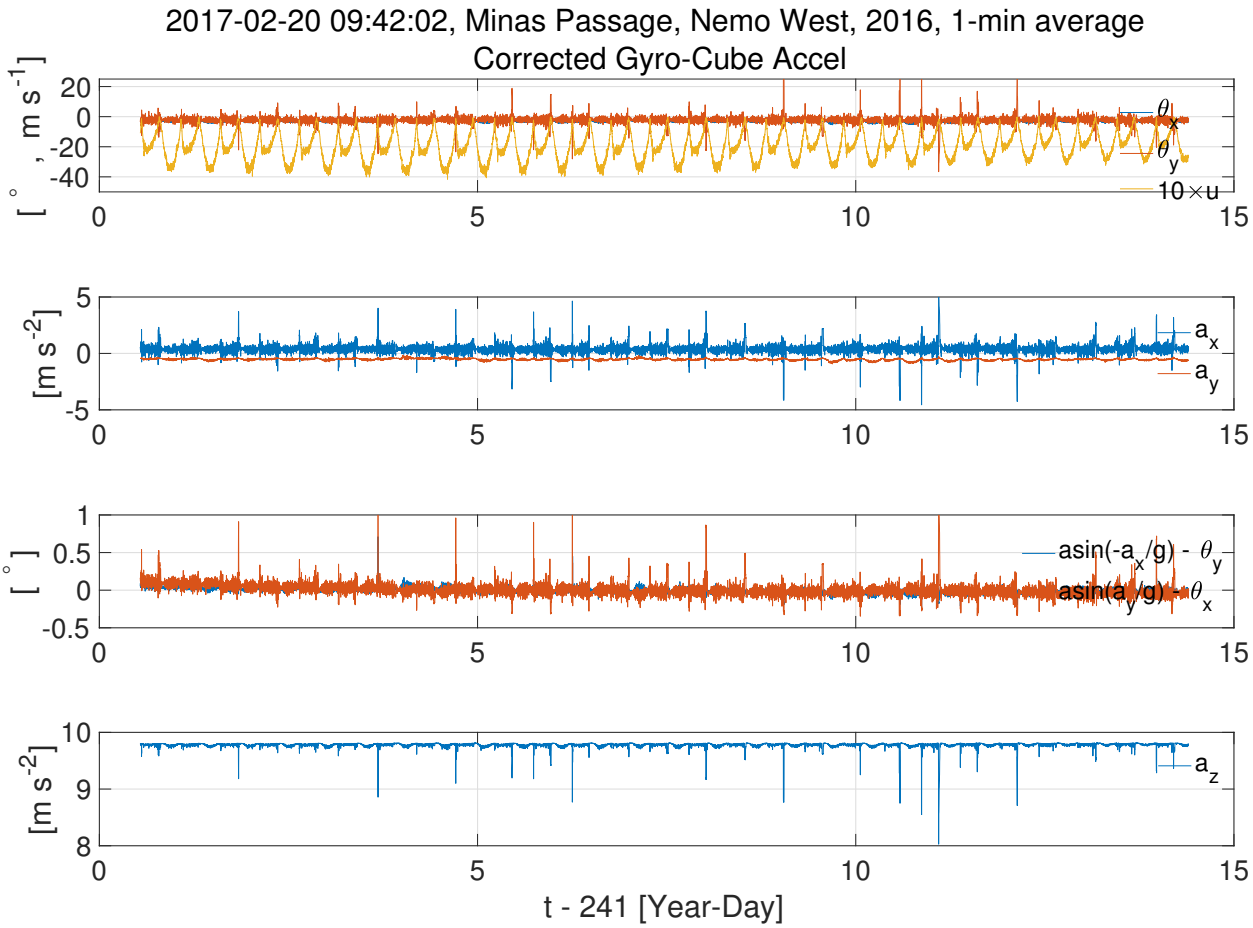

Figure 16: The MicroRider rotation around its x- and y-axes and the velocity in the x-direction determined by the inclinometers (upper panel). The Gyro-Cube a_x and a_y signals (second panel from top). The difference between the rotation around the x- and y-axes determined by the inclinometers and the accelerometers (second panel from bottom). The acceleration in the z-direction (bottom panel).

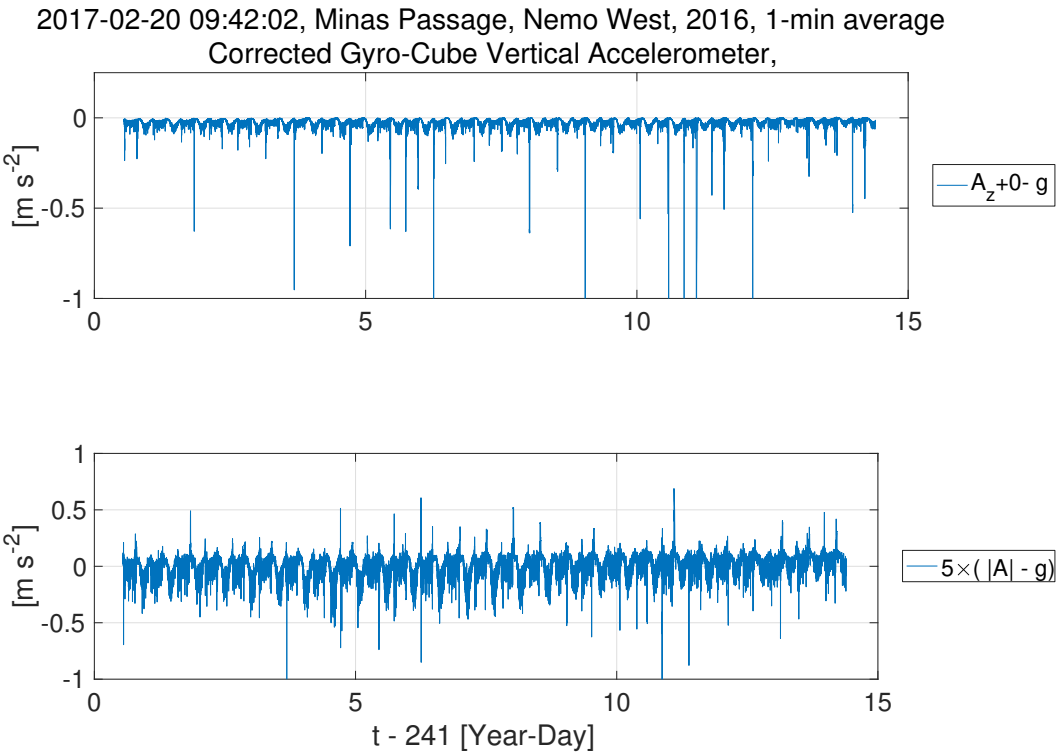

Figure 17: The MicroRider z-accelerometer signal (upper panel), and the magnitude of the vector sum of acceleration (bottom panel).

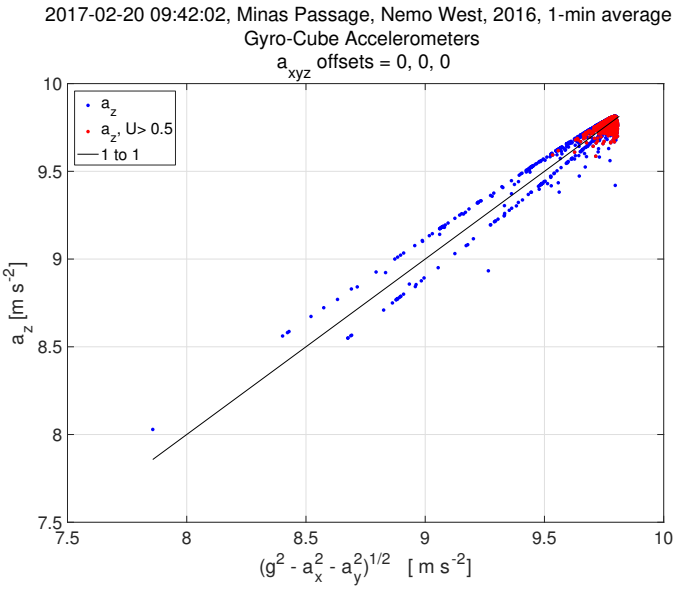

Figure 18: The MicroRider z-accelerometer signal relative to the acceleration inferred by a_x, a_y and gravity.

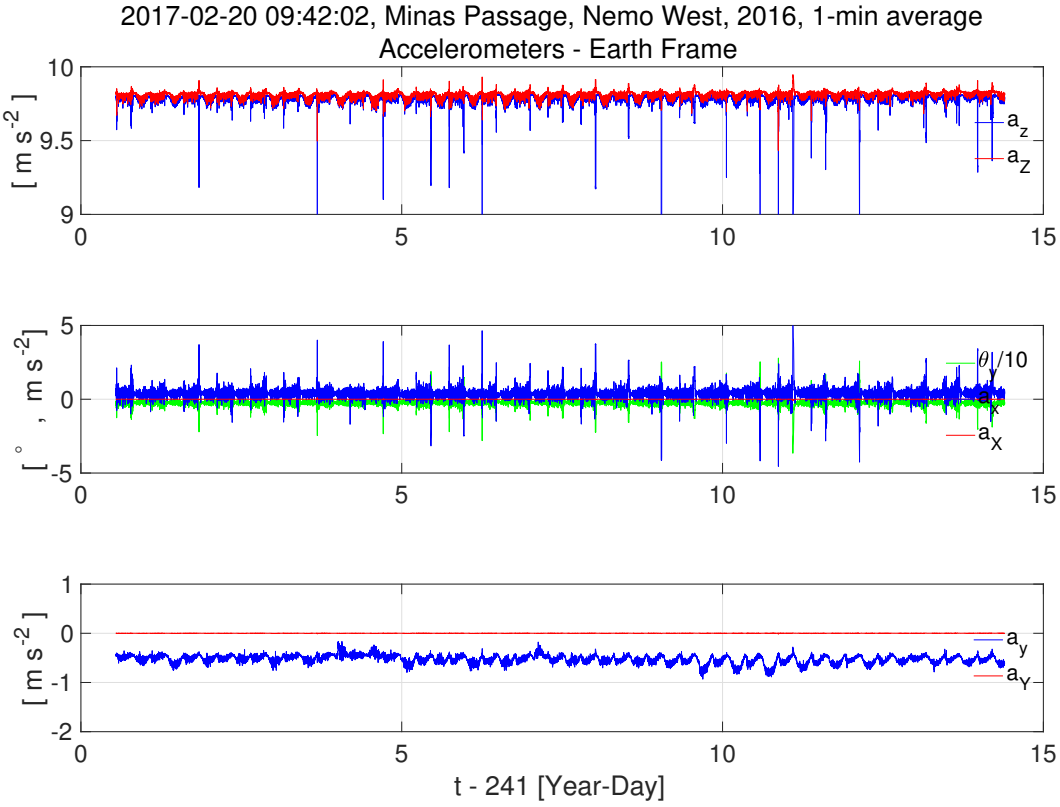

Figure 19: The acceleration signals in the body frame (blue) and a horizontal earth frame (red). Upper panel – vertical acceleration. Middle panel – forward acceleration. Lower panel – athwartship acceleration. The accelerations have been rotated into the earth horizontal plane, but are not rotated around the vertical axis to give them a specific geographic direction.

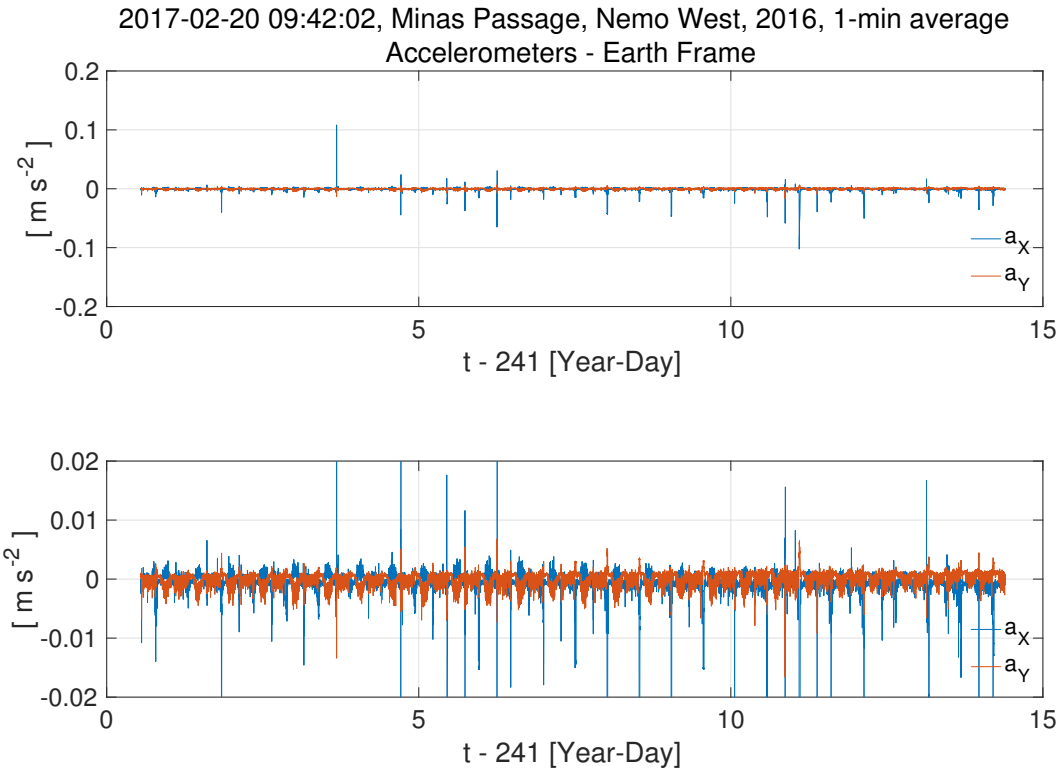

Figure 20: The X- and Y-acceleration signals in a horizontal earth frame (upper panel), and a more zoomed in view (lower panel).

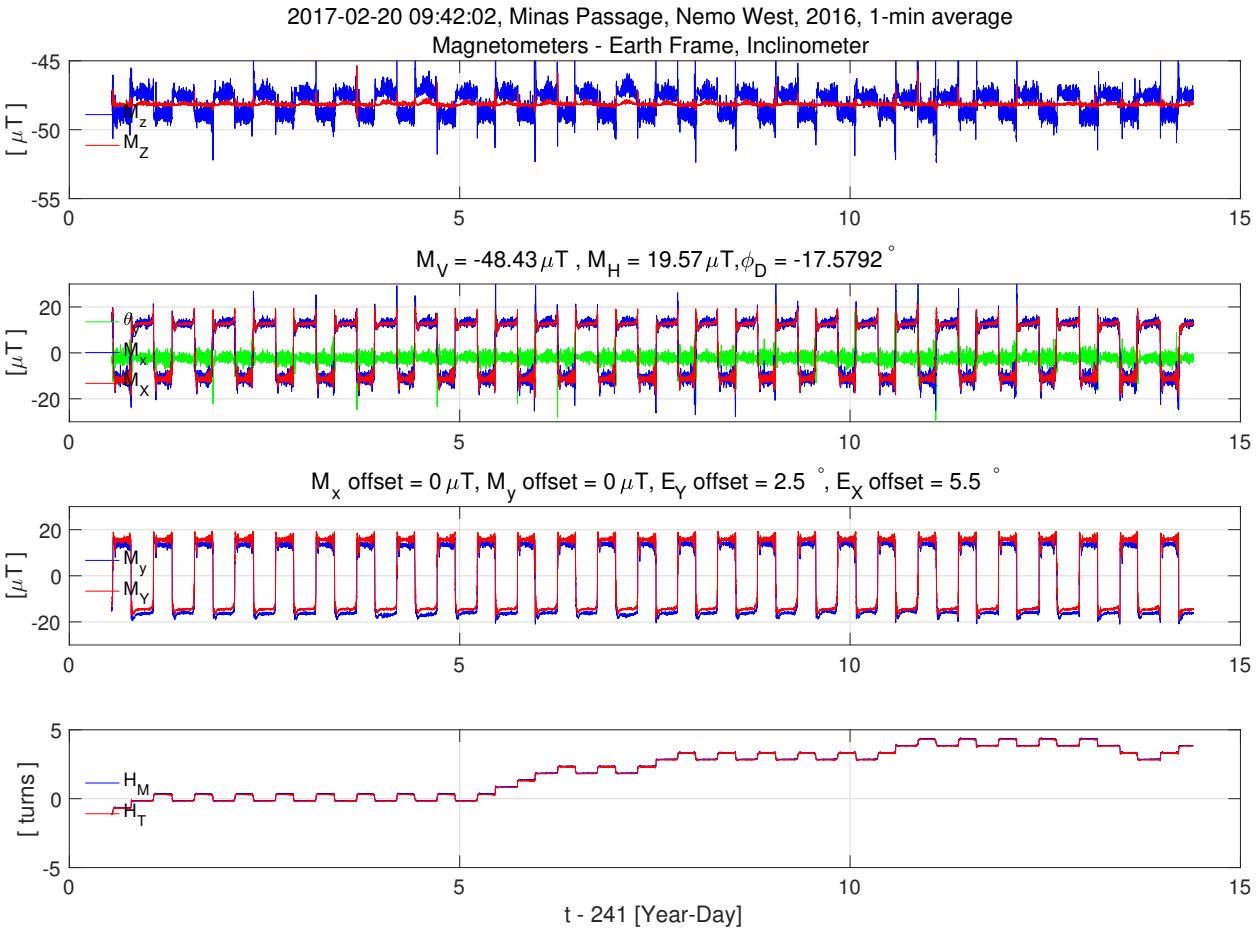

Figure 21: The magnetometer signals in the body (blue) and horizontal earth (red) frames. Upper panel – vertical magnetic field. Second panel from top – forward magnetic field. Third panel from top – athwartship (top port) magnetic field. Lower panel – heading of the Nemo in terms of rotations around the vertical axis.

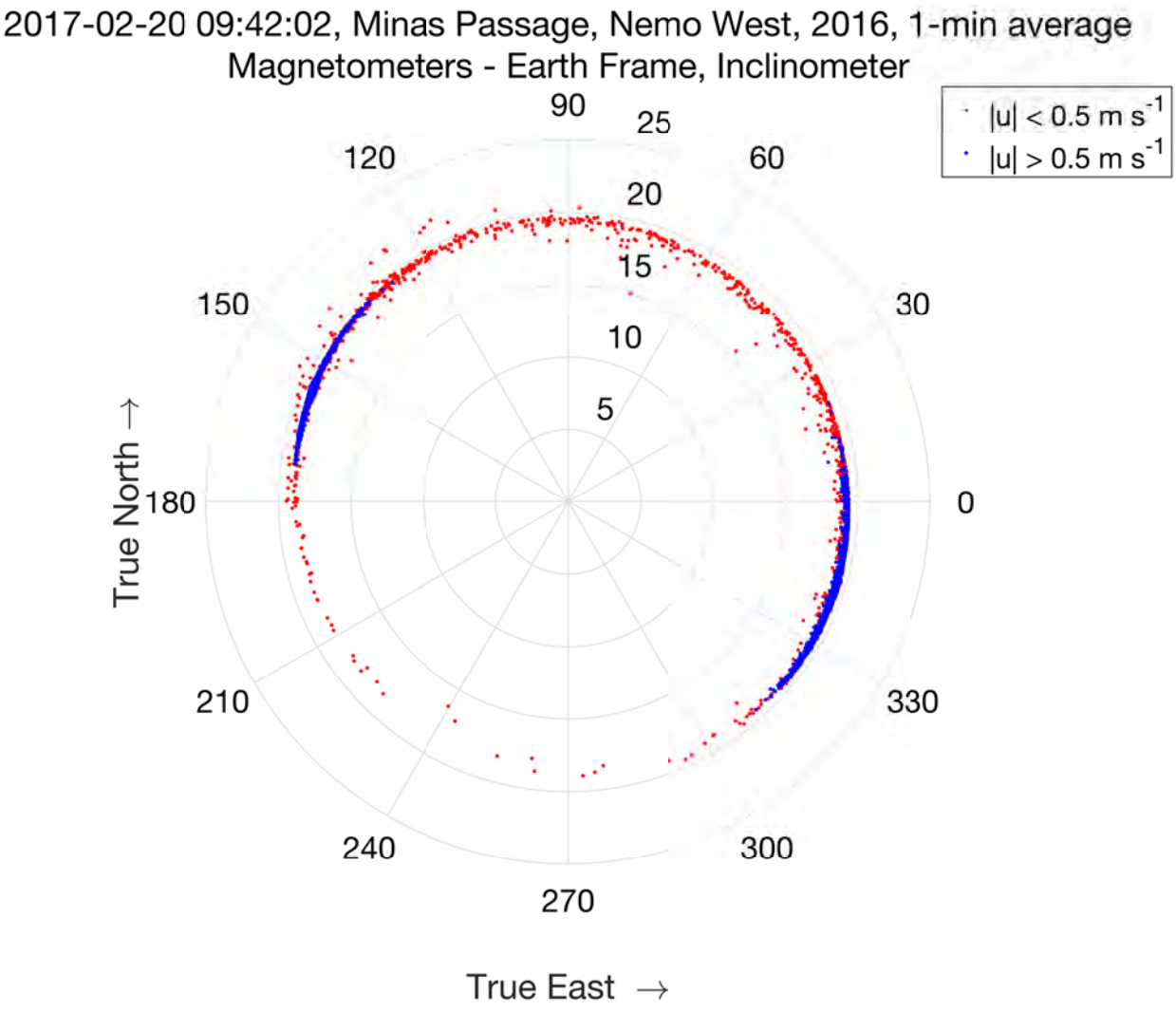

Figure 22: The horizontal magnetic field for speeds more (less) than $0.5\,\mathrm{m\,s^{-1}}$, blue and red dots, respectively.

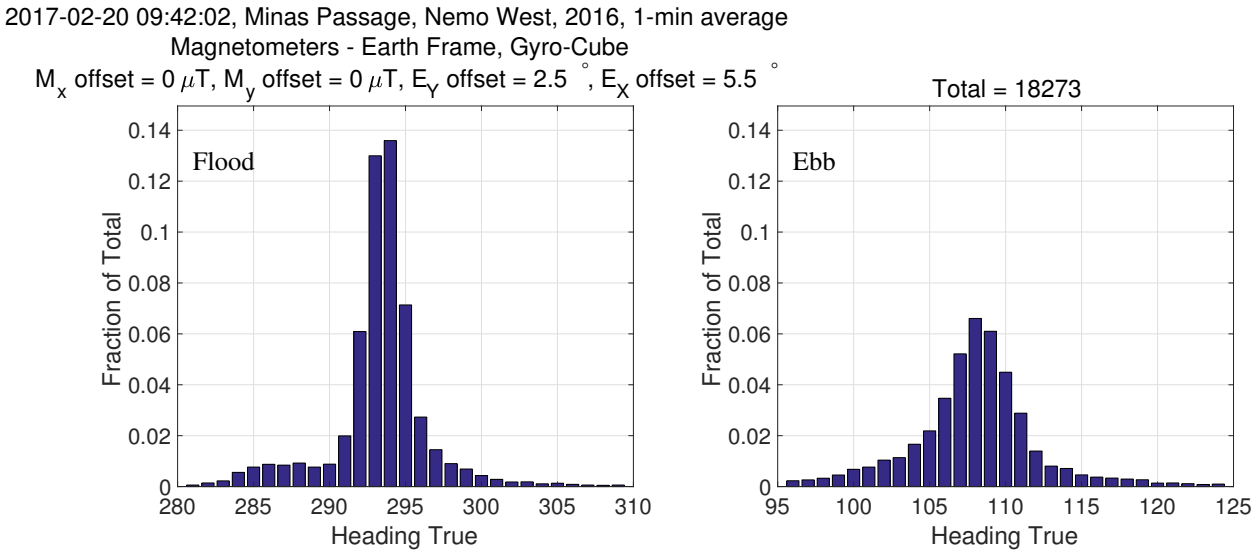

Figure 23: The histogram of heading of Nemo West. More than 90 % of all data are contained by this pair of histograms.

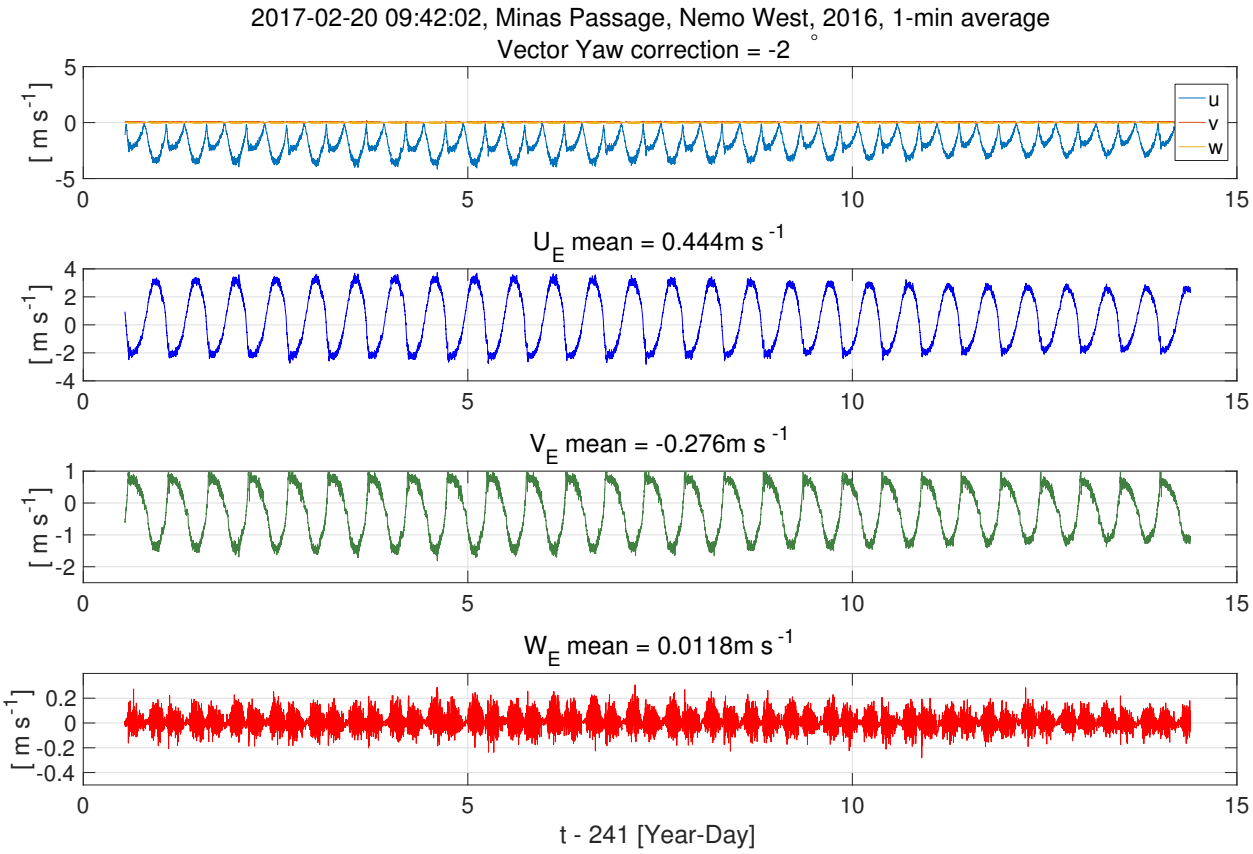

Figure 24: The analog ADV velocity at Nemo West in the Nemo frame (upper panel). The east component (second from top), north component (second from bottom), and the erroneous vertical component (bottom). All data are derived from the analog output of the ADV.

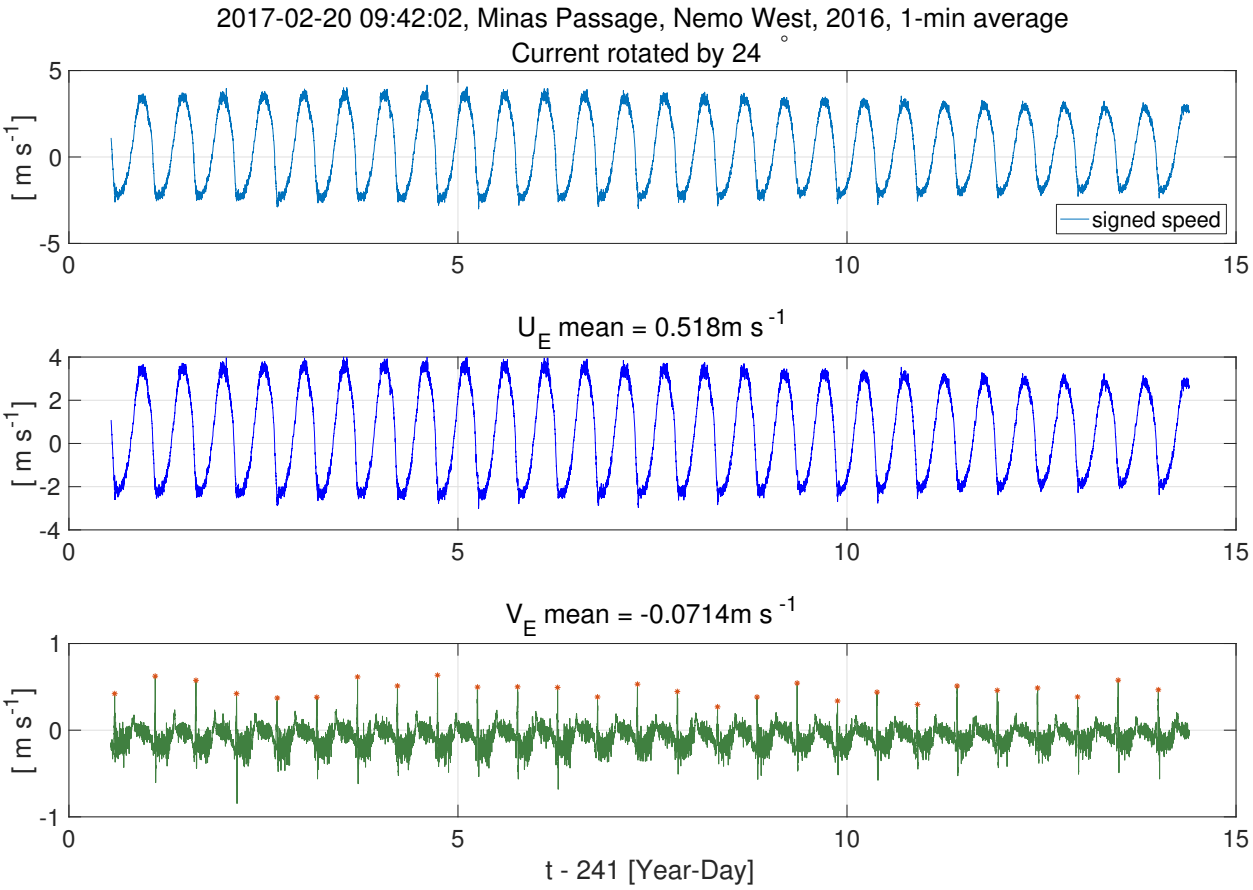

Figure 25: The analog ADV horizontal velocity at Nemo West rotated by 24° to minimize the cross-stream component. Upper panel – speed signed according to flood, with positive to the east and negative to the west. Middle frame – velocity in the direction 24° south of east. Lower panel – the cross-stream component with positive values 24° east of north.

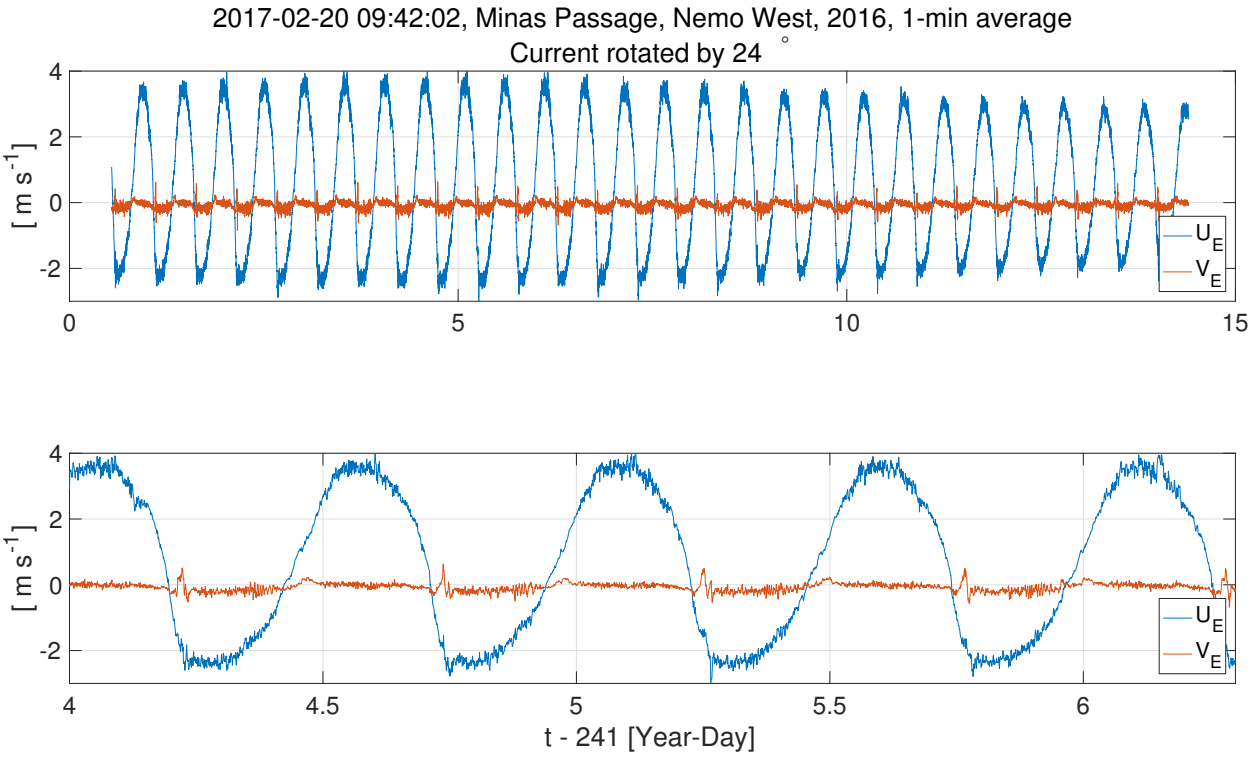

Figure 26: Upper panel – horizontal velocity components rotated 24° counter clockwise. Lower panel – same with zoom in to show the anomalies shortly after the start of each ebb.

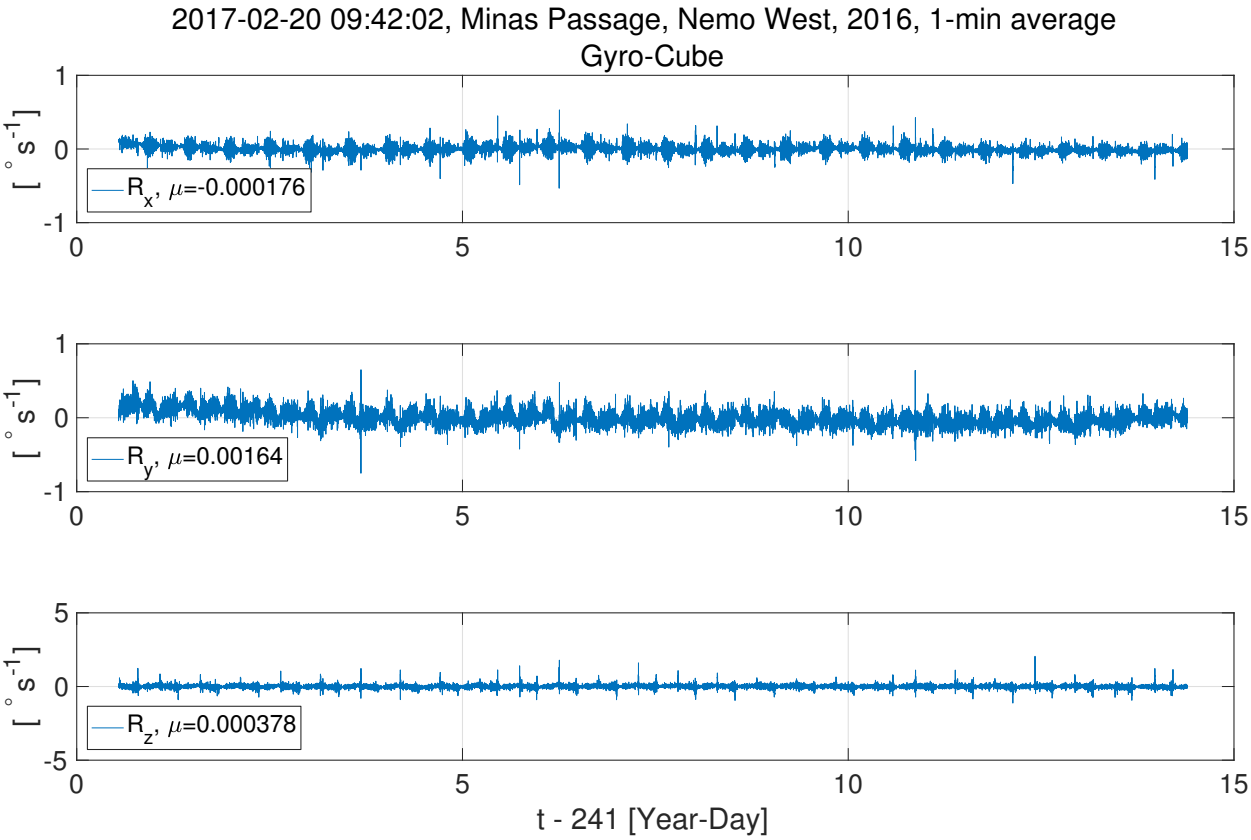

Figure 27: The rates of rotation in the Nemo frame. There is significant drift in the gyroscope data for the x- and y-components during the first 3 days. The mean values are indicated in the legends.

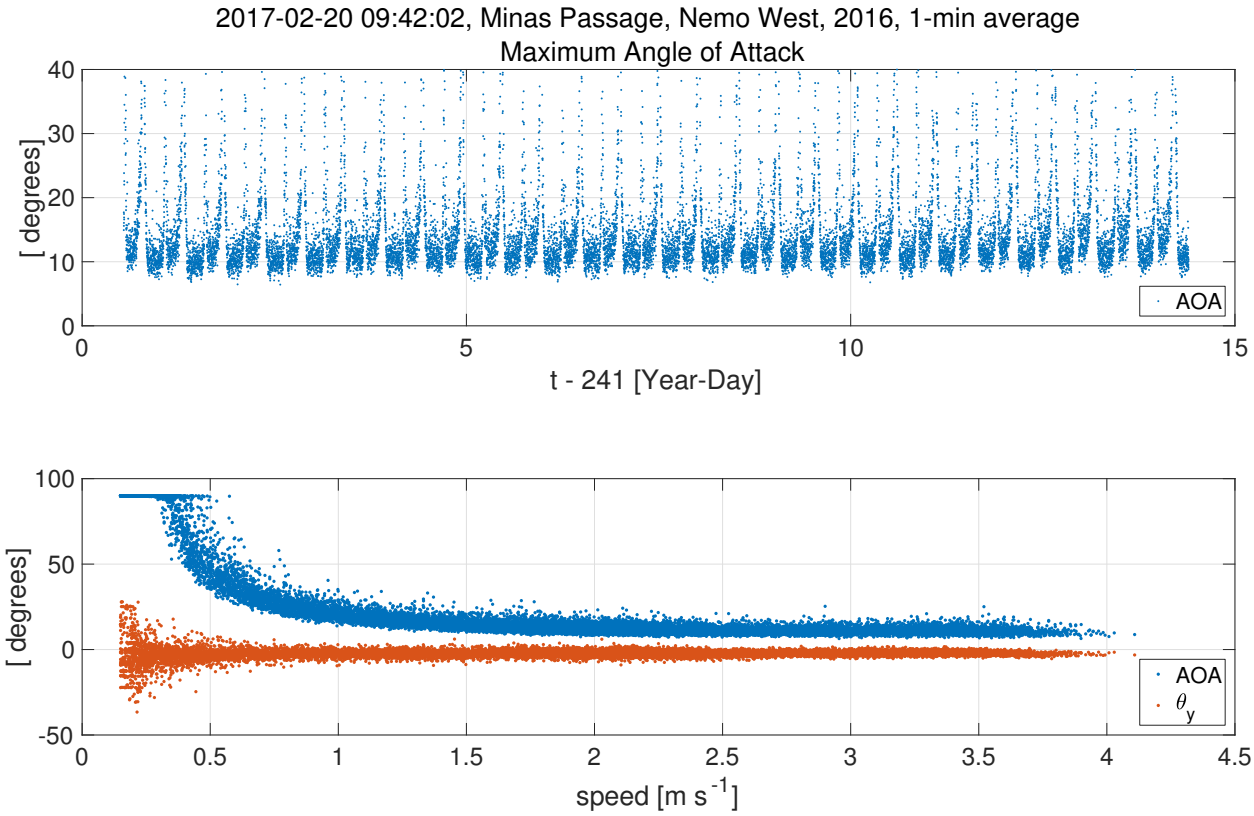

Figure 28: The maximum angle-of-attack for each minute of data (upper panel). The maximum angle-of-attack (blue) and the rotation around the y-axis (red, negative pitch) as a function of speed (lower panel).

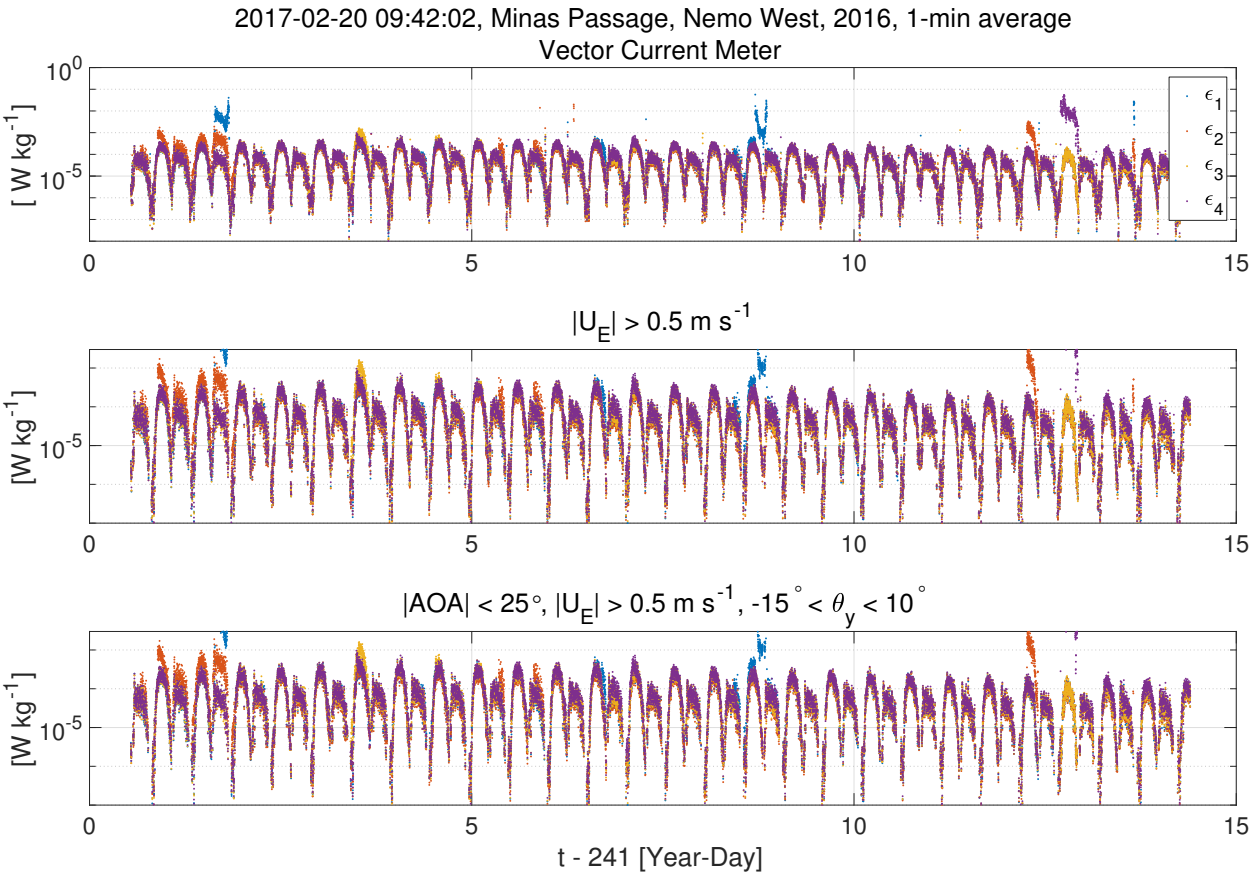

Figure 29: Upper panel – the rate of dissipation of kinetic energy, ϵ, for all four shear probes. Middle panel – Same, but for speeds greater than $0.5\,\mathrm{m\,s^{-1}}$. Lower panel – Same but for speeds greater than $0.5\,\mathrm{m\,s^{-1}}$ and rotations around the y-axis in the range of $-15°$ to $10°$. Anomalously high values are not eliminated by these speed and angle restrictions.

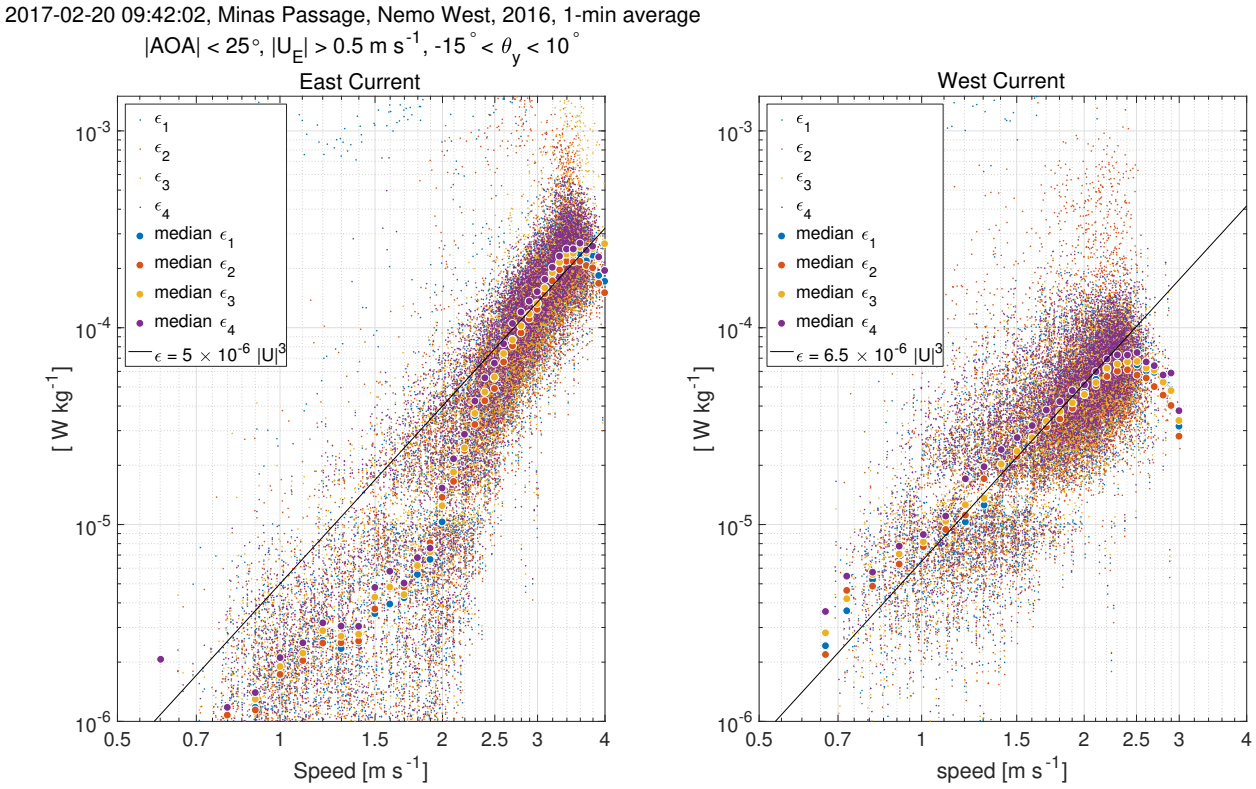

Figure 30: The rate of dissipation of kinetic energy, ϵ, for all four shear probes as a function of speed. Left panel – flood or easterly flow. Right panel – ebb or westerly flow. The wide dots are the median rates in bins of $0.1\,\mathrm{m\,s^{-1}}$. The black line is an approximate regression with respect to speed cubed.

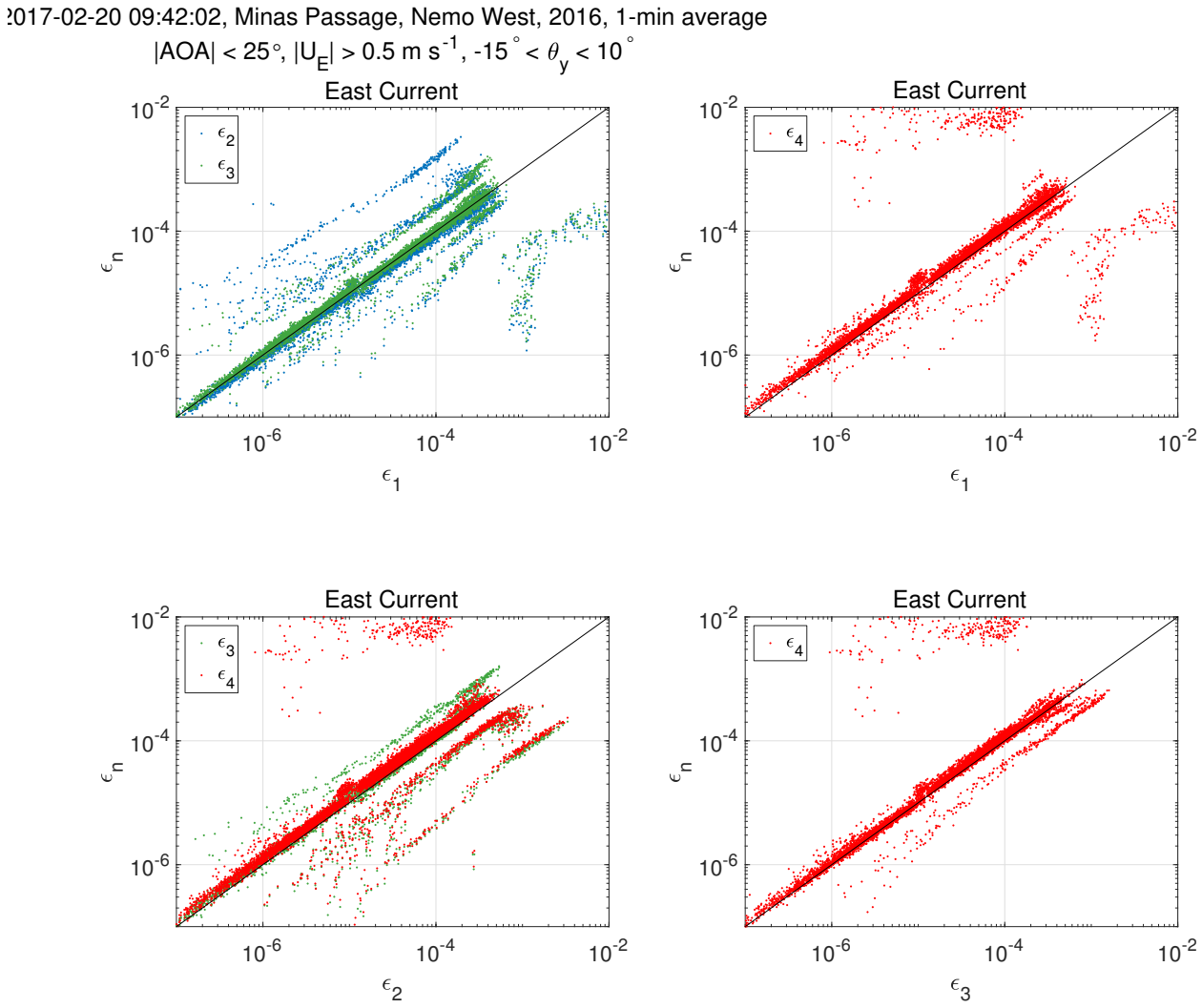

Figure 31: Inter-comparisons of the rates of dissipation of kinetic energy, ϵ, during the floods for all four shear probes. Upper left panel – probes 2 and 3 with respect probe 1. Upper right panel – probe 4 with respect to probe 1. Lower left panel – probes 3 and 4 with respect probe 2. Lower right panel – probe 4 with respect to probe 3.

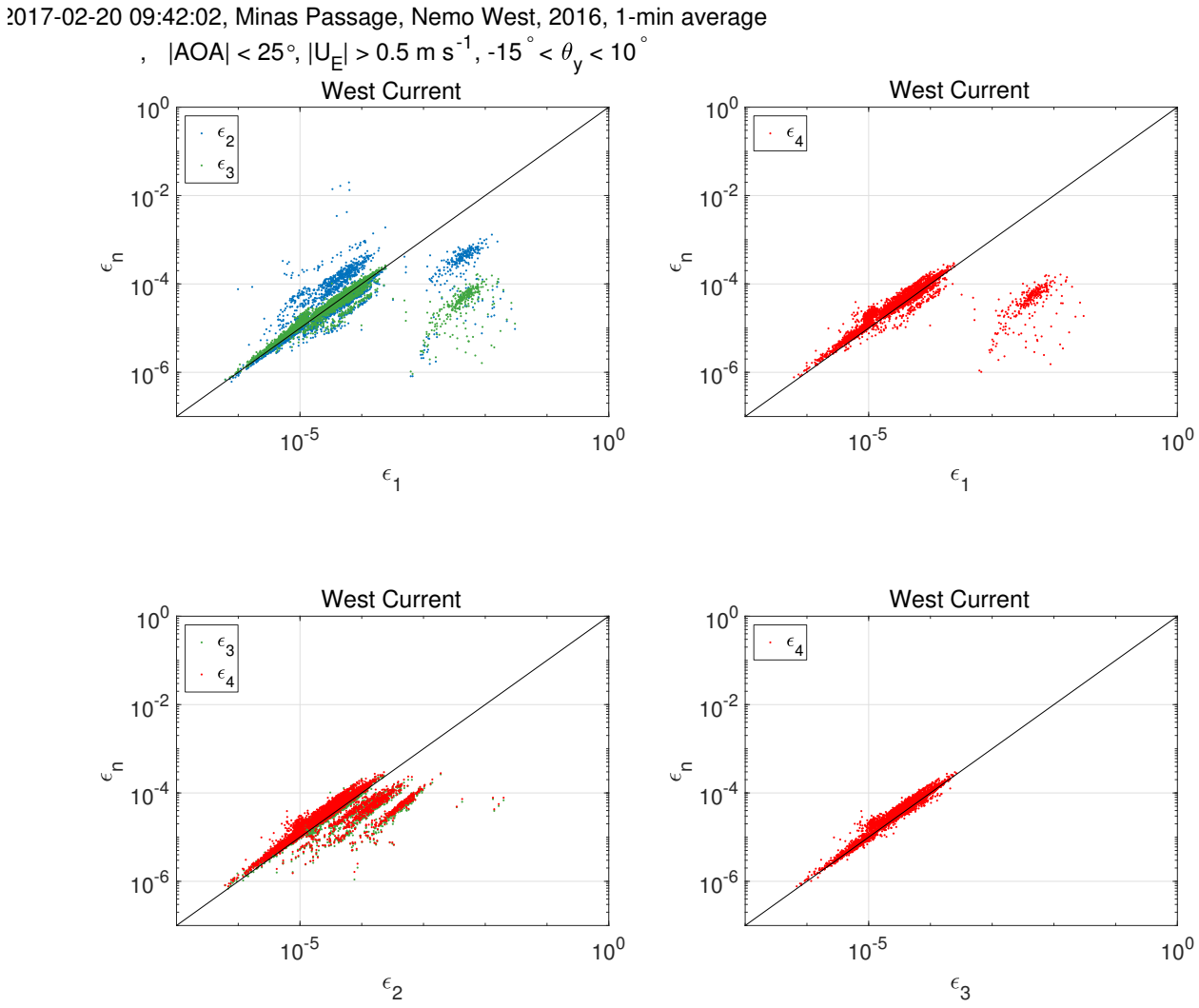

Figure 32: Same as Figure 31 but for the ebbs.

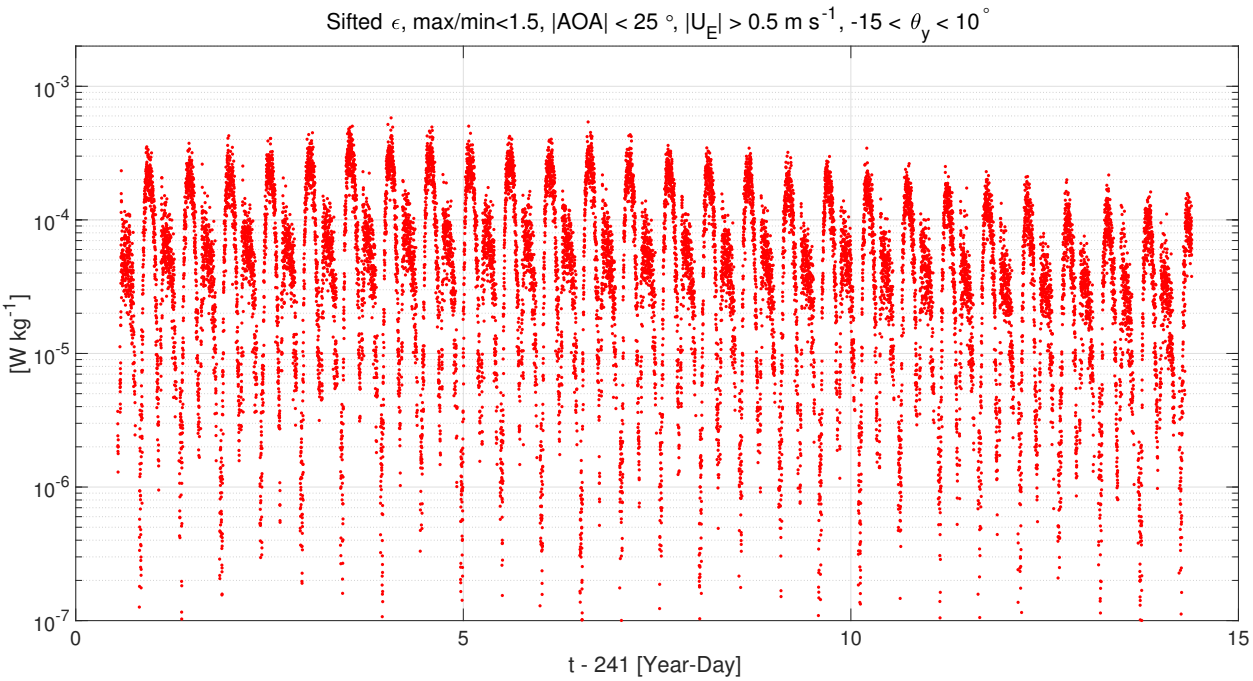

Figure 33: The time series of the sifted rate of dissipation of kinetic energy, ϵ. The values shown are for times when the current speed exceeded $0.5\,\mathrm{m\,s^{-1}}$ and the rotation around the y-axis (negative pitch) was between $-15°$ and $10°$. The sifting process, which is applied to each 1-minute quadruple of ϵ estimates, consists of (i) sorting the four estimates, (ii) eliminating those that are more than 1.5 times larger than the smallest estimate, and (iii) taking the average of the remaining values. This process is intended to eliminate erroneously large estimates.

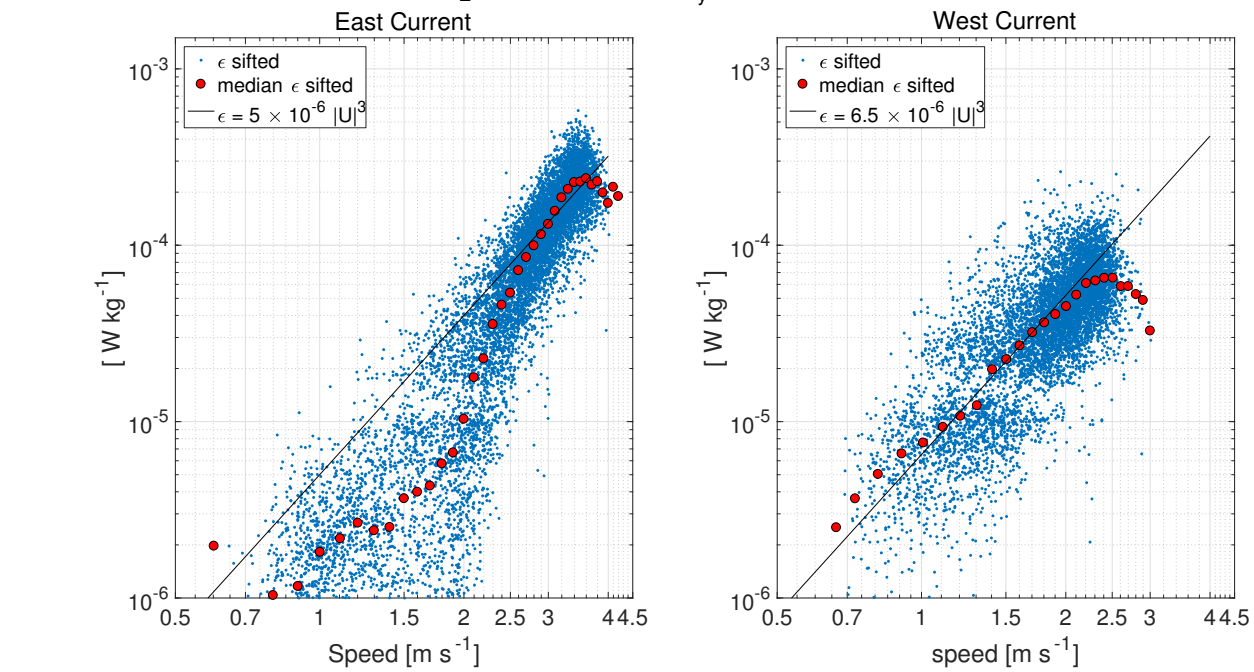

Figure 34: The sifted rate of dissipation of kinetic energy, ϵ, as a function of speed. Left panel – flood or easterly flow. Right panel – ebb or westerly flow. The red dots are the median rates in bins of $0.1\,\mathrm{m\,s^{-1}}$. The black line is an approximate regression with respect to speed cubed.

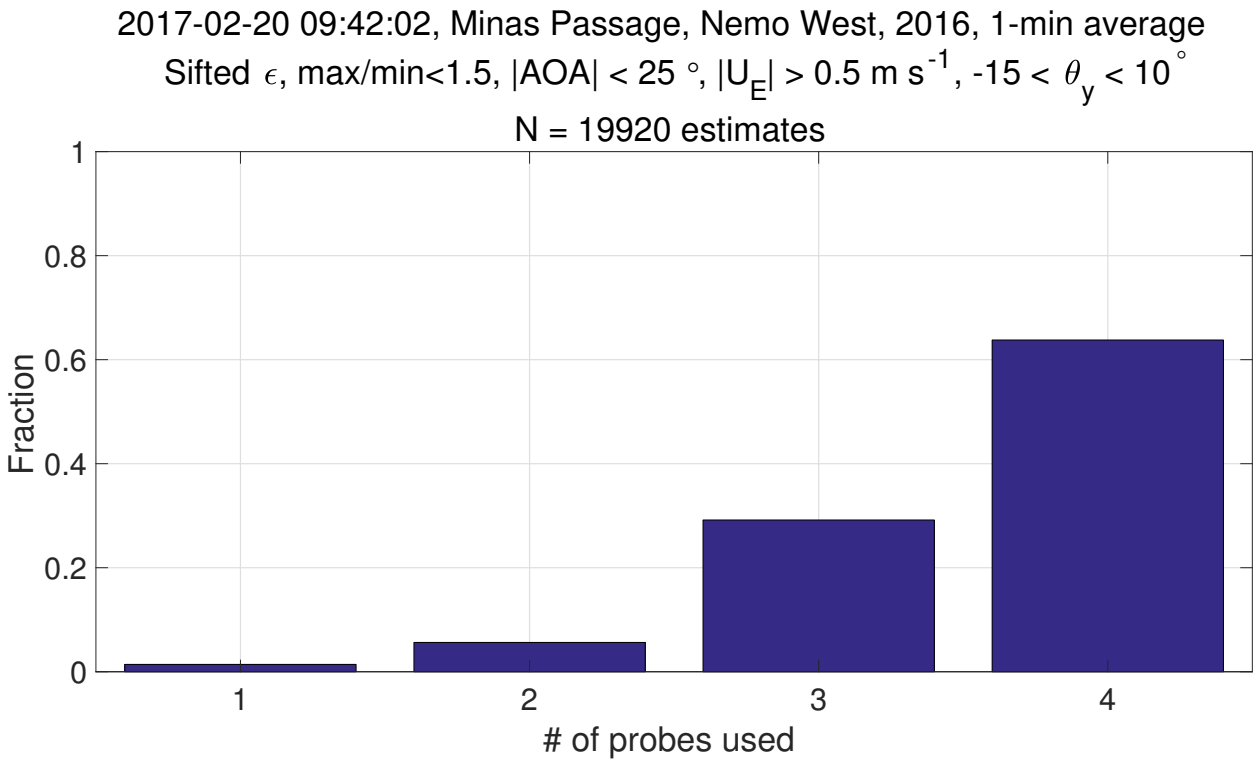

Figure 35: The histogram of the number of probes used in the sifted estimates of the rate of dissipation of kinetic energy, ϵ. More than 90 % of all estimates used 3 or more probes.

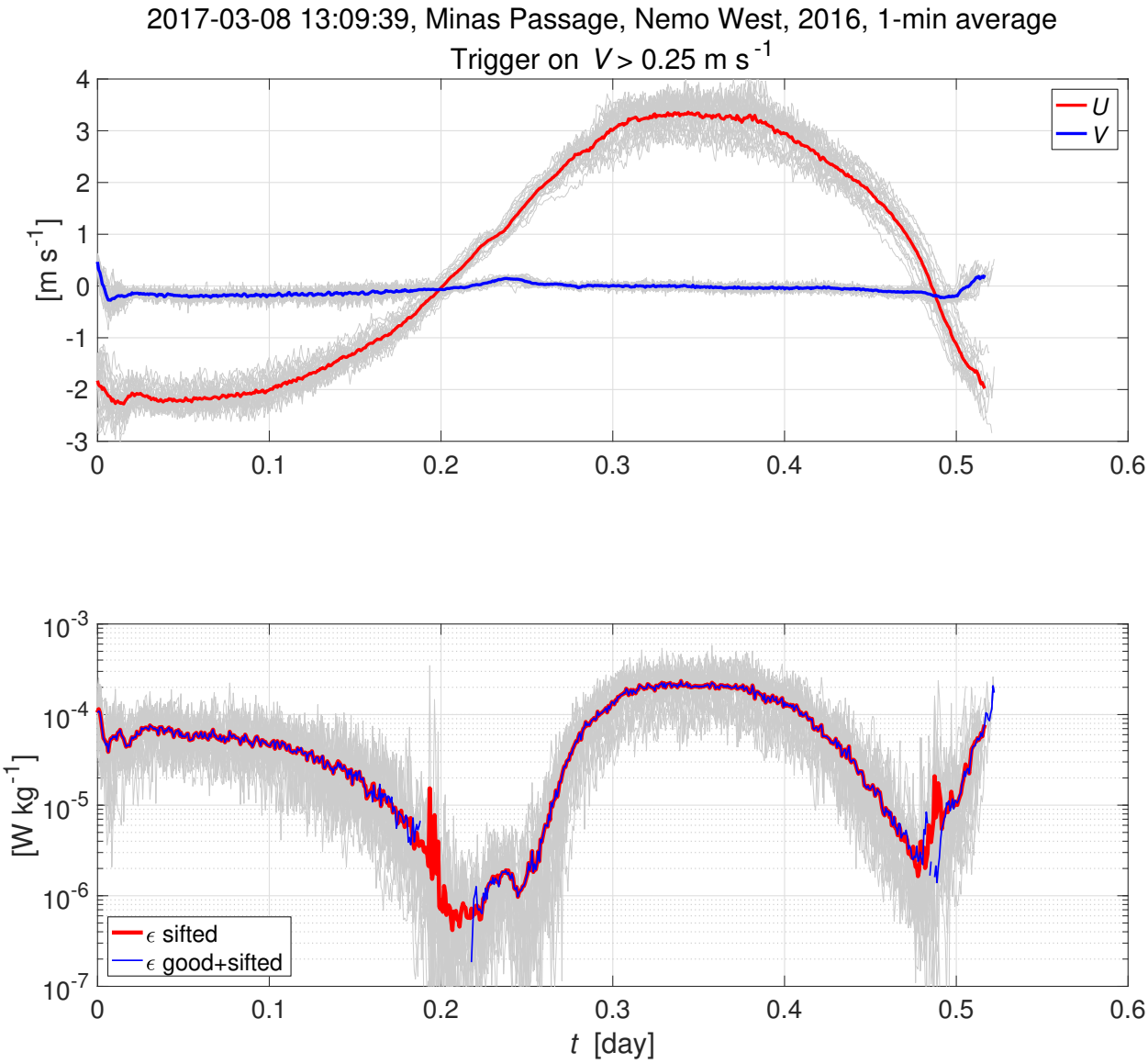

Figure 36: The phase-averaged current (upper panel) and rate of dissipation (lower panel). The trigger point for the phase averaging is a cross-stream current larger than $0.25\,\mathrm{m\,s^{-1}}$ which occurs shortly after the start of ebb. The trigger point is not exactly synchronous with the M_2 tide. The ϵ good+sifted values (blue line, lower panel) are for times that meet the speed ($>0.5\,\mathrm{m\,s^{-1}}$) and θ_y ($-15°$ to $10°$) restrictions. The ϵ sifted values (blue line, lower panel) are for all times.

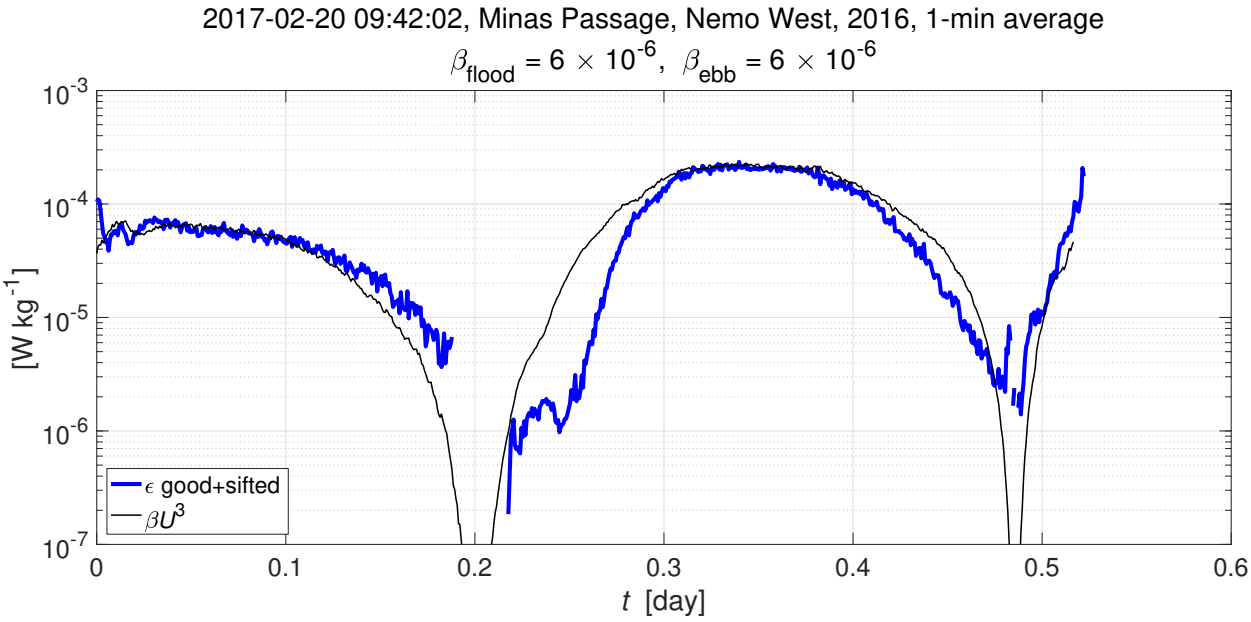

Figure 37: The phase-averaged rate of dissipation (blue) and βU^3 (black). The cubic-speed dependence of ϵ is not tight during the flood and around the turning of the tide.

D MicroRider 1-min average data – Nemo East

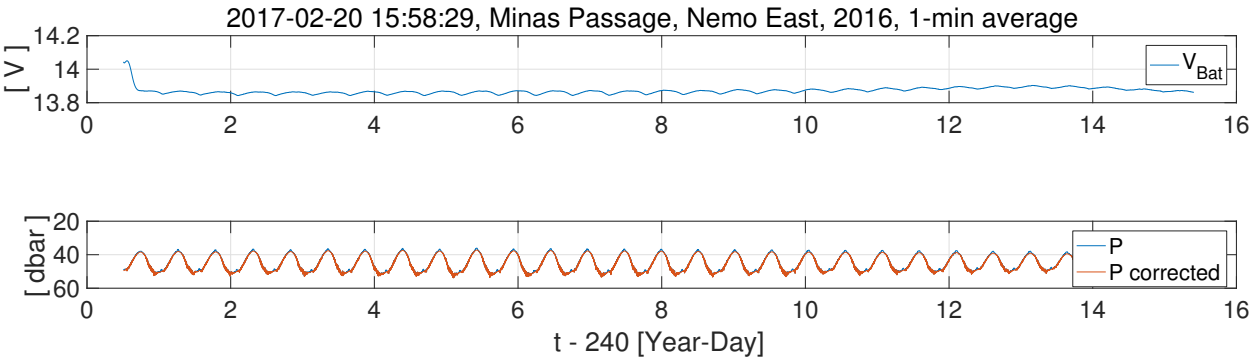

Figure 38: The pressure (lower panel) and battery voltage measured by the MicroRider on Nemo East. The corrected pressure is $P - L_P \sin\theta_y$ where $L_P = 1.68\,\mathrm{m}$ is the distance from the bridle axis to the pressure transducer and θ_y is the rotation around the y-axis (negative pitch).

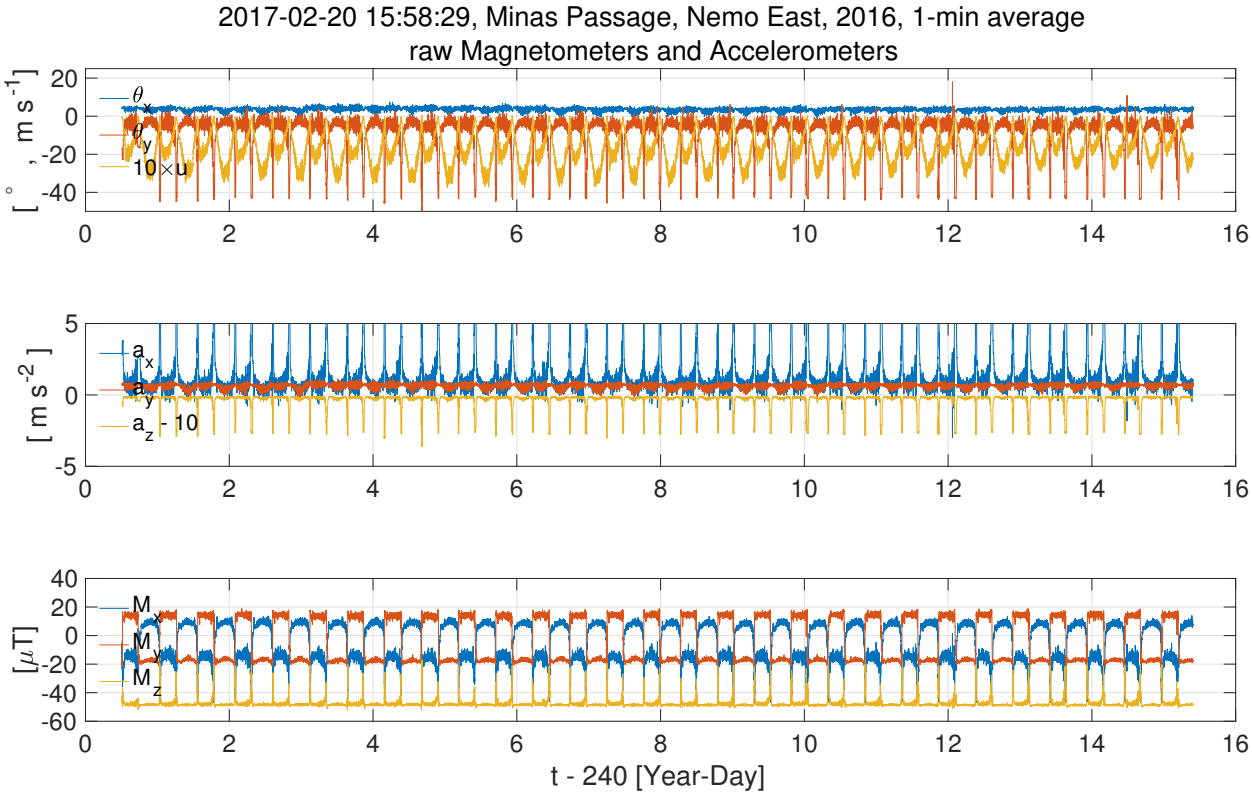

Figure 39: The inclinometer (upper panel), accelerometer (middle panel), and magnetometer (lower panel) data measured by the MicroRider on Nemo East.

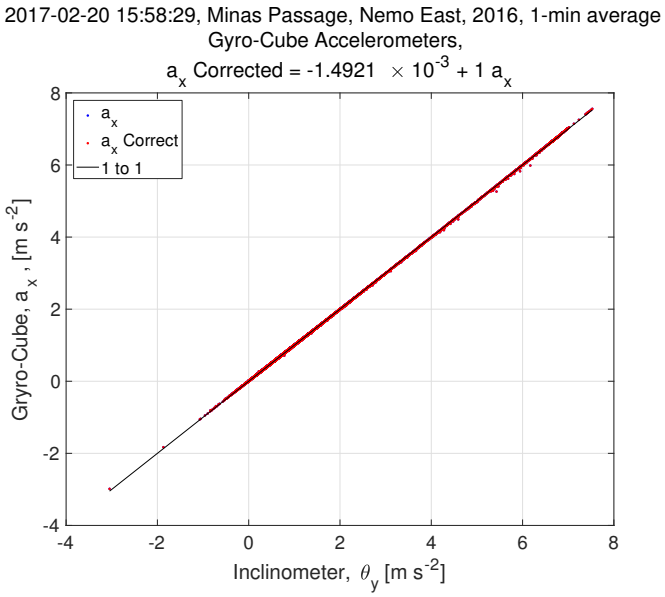

Figure 40: The regression of the Gyro-Cube accelerometer signal a_x against the inclinometer rotation around in the y-axis, measured by the MicroRider on Nemo East.

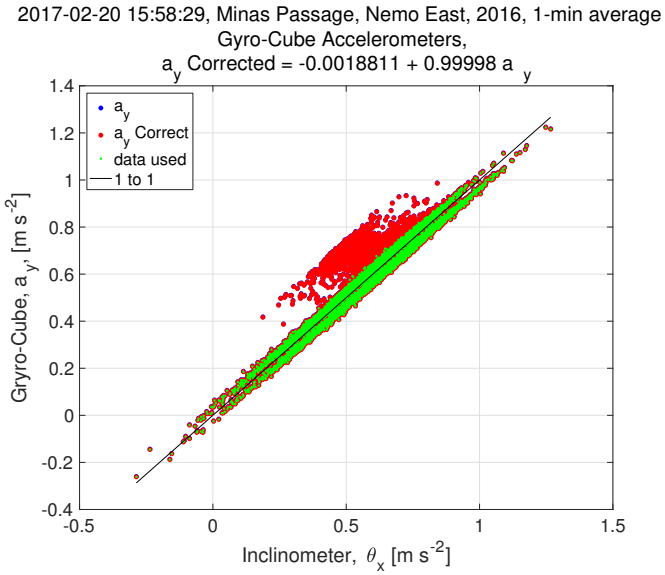

Figure 41: The regression of the Gyro-Cube accelerometer signal a_y against the inclinometer rotation around in the x-axis, measured by the MicroRider on Nemo East. Green points are for speeds greater than $0.5\,\mathrm{m\,s^{-1}}$.

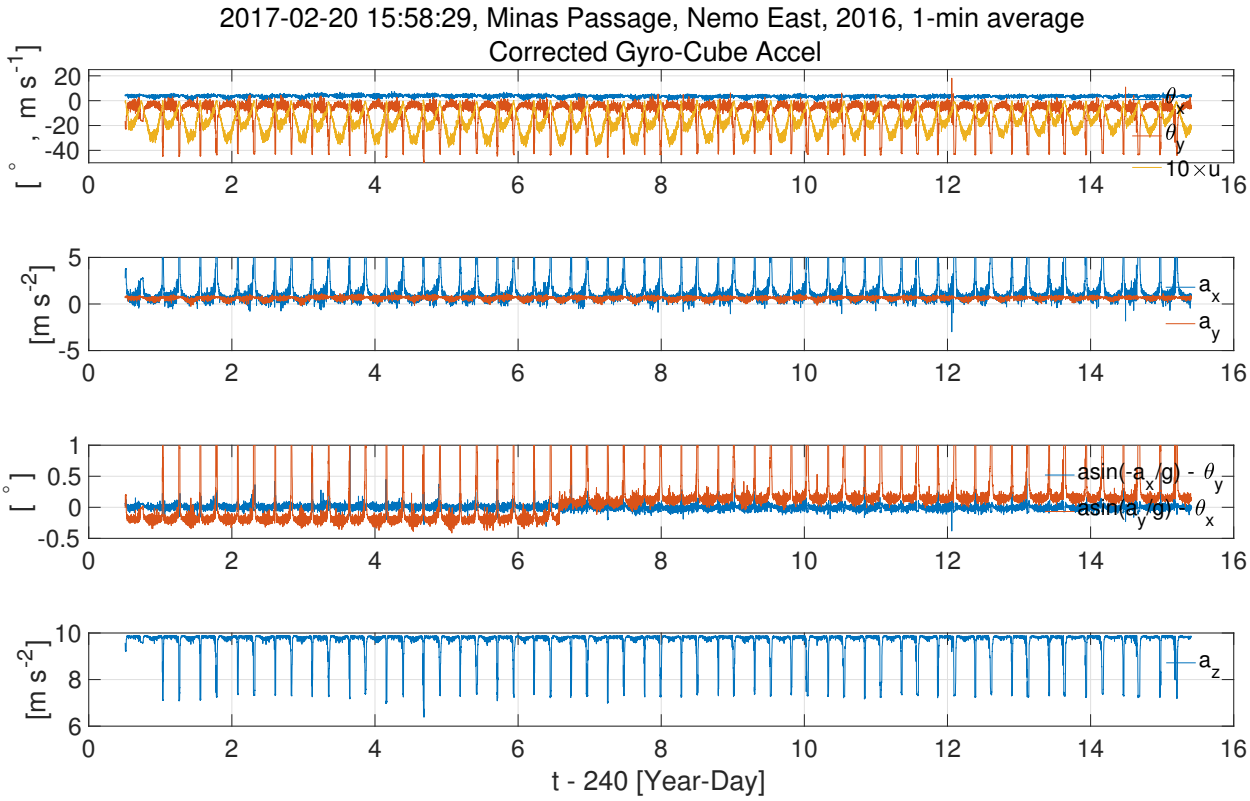

Figure 42: The MicroRider rotation around its x- and y-axes and the velocity in the x-direction determined by the inclinometers (upper panel). The Gyro-Cube a_x and a_y signals (second panel from top). The difference between the rotation around the x- and y-axes determined by the inclinometers and the accelerometers (second panel from bottom). The acceleration in the z-direction (bottom panel). There is a distinct shift of the a_x data relative to the θ_y readings on day 246.5.

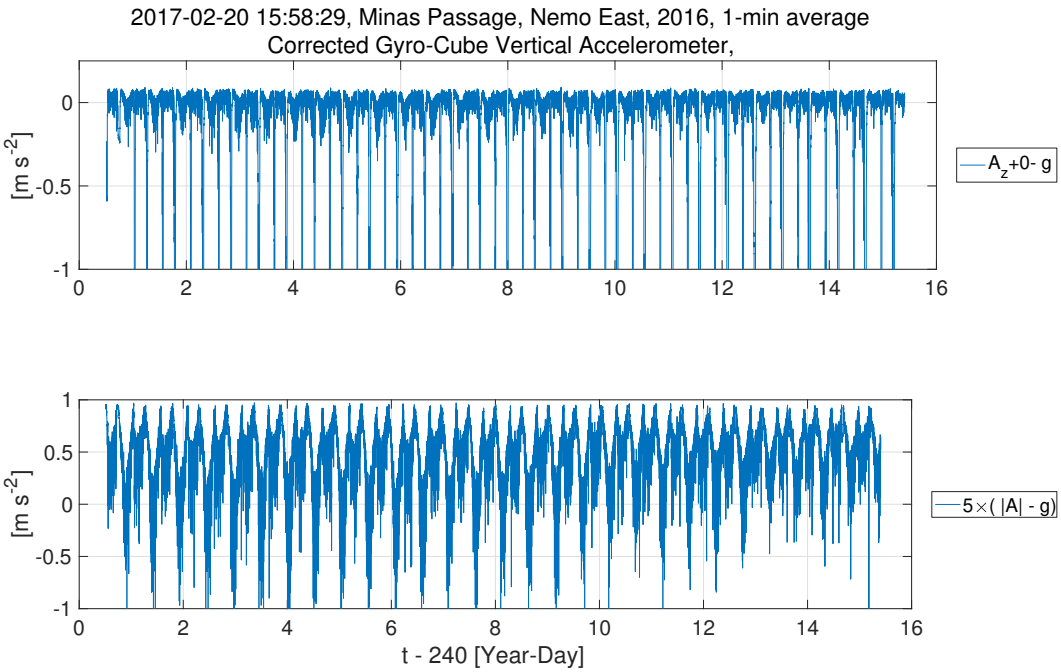

Figure 43: The MicroRider z-accelerometer signal (upper panel), and the magnitude of the vector sum of acceleration (bottom panel).

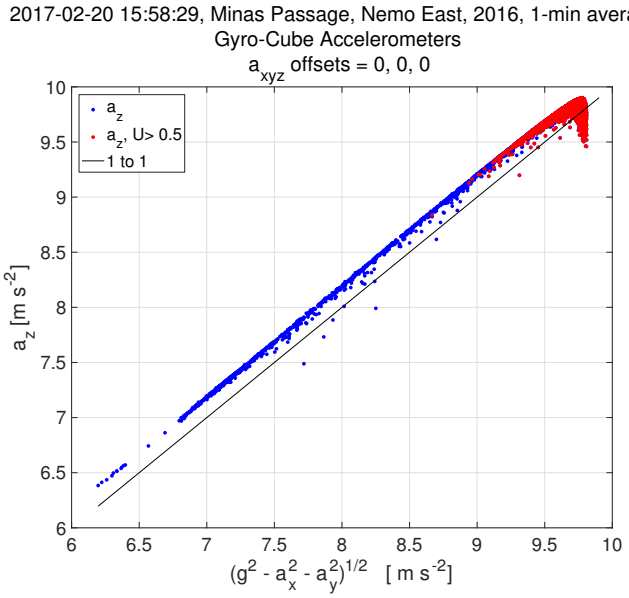

Figure 44: The MicroRider z-accelerometer signal relative to the acceleration inferred by a_x, a_y and gravity.

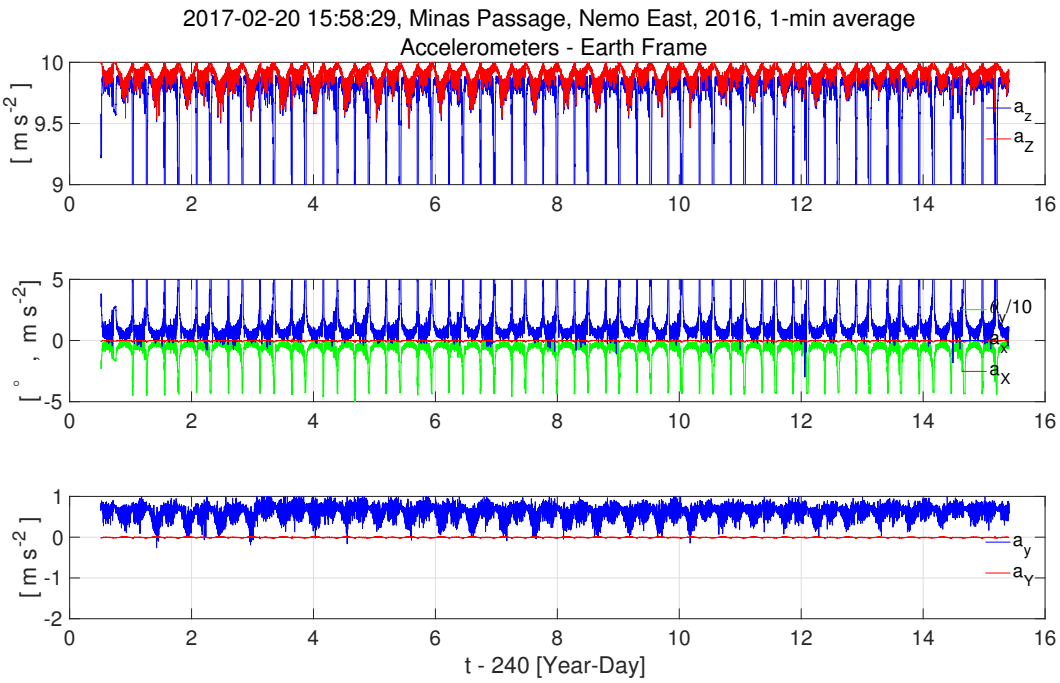

Figure 45: The acceleration signals in the body frame (blue) and a horizontal earth frame (red). Upper panel – vertical acceleration. Middle panel – forward acceleration. Lower panel – athwartship acceleration. The accelerations have been rotated into the earth horizontal plane, but are not rotated around the vertical axis to give them a specific geographic direction.

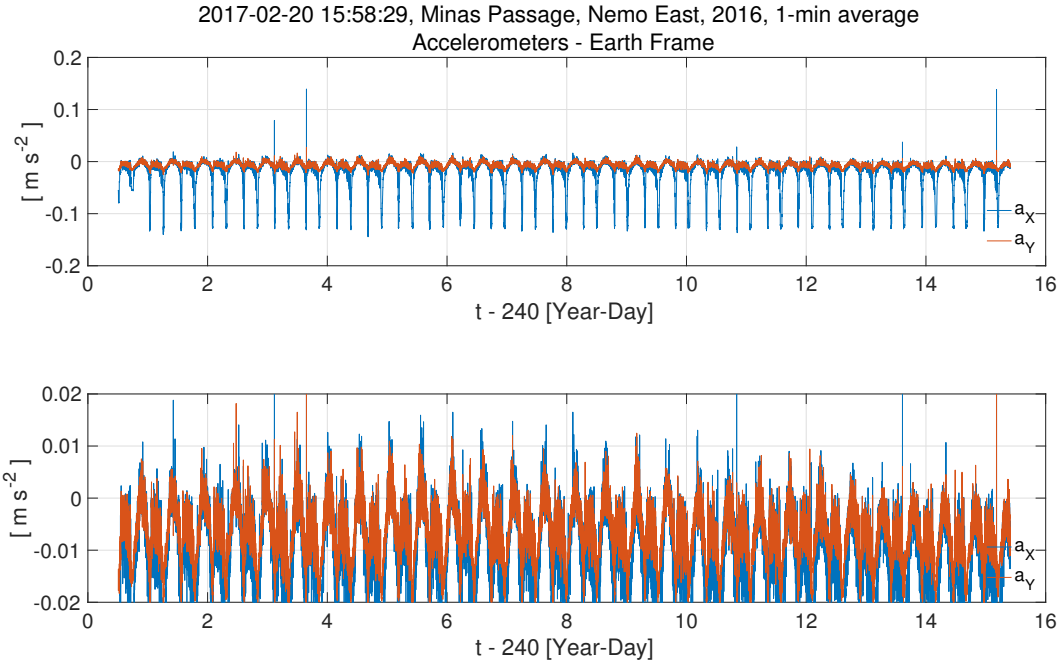

Figure 46: The X- and Y-acceleration signals in a horizontal earth frame (upper panel), and a more zoomed in view (lower panel).

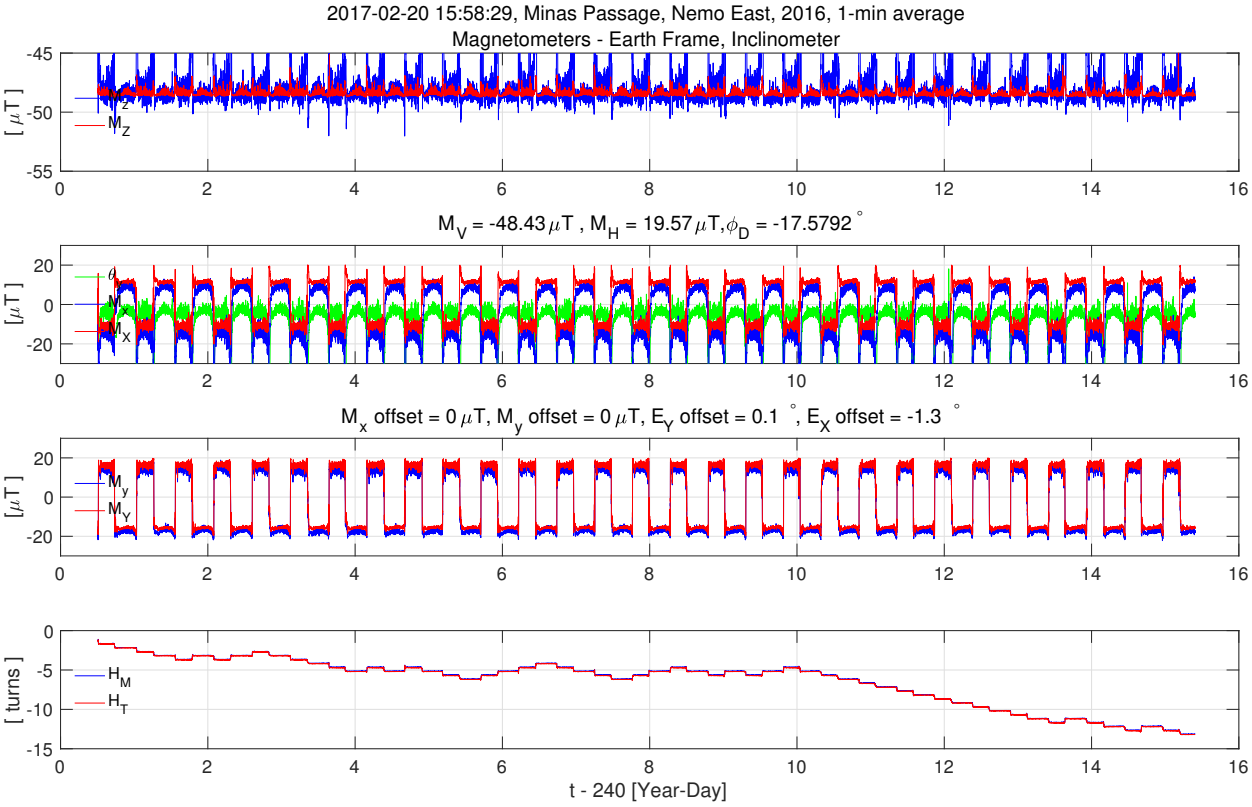

Figure 47: The magnetometer signals in the body (blue) and horizontal earth (red) frames. Upper panel – vertical magnetic field. Second panel from top – forward magnetic field. Third panel from top – athwartship (top port) magnetic field. Lower panel – heading of the Nemo in terms of rotations around the vertical axis.

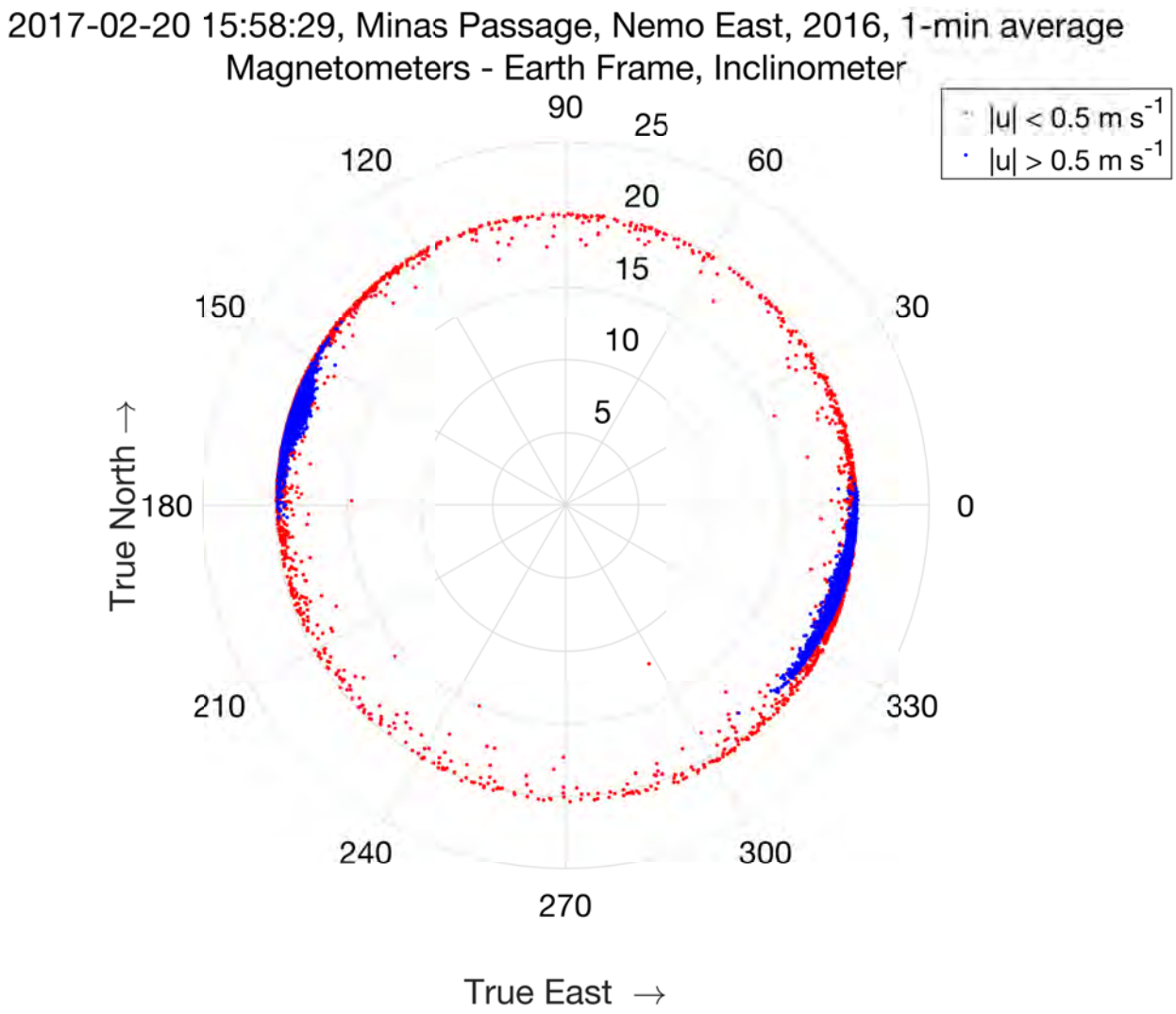

Figure 48: The horizontal magnetic field for speeds more (less) than $0.5\,\mathrm{m\,s^{-1}}$, blue and red dots, respectively.

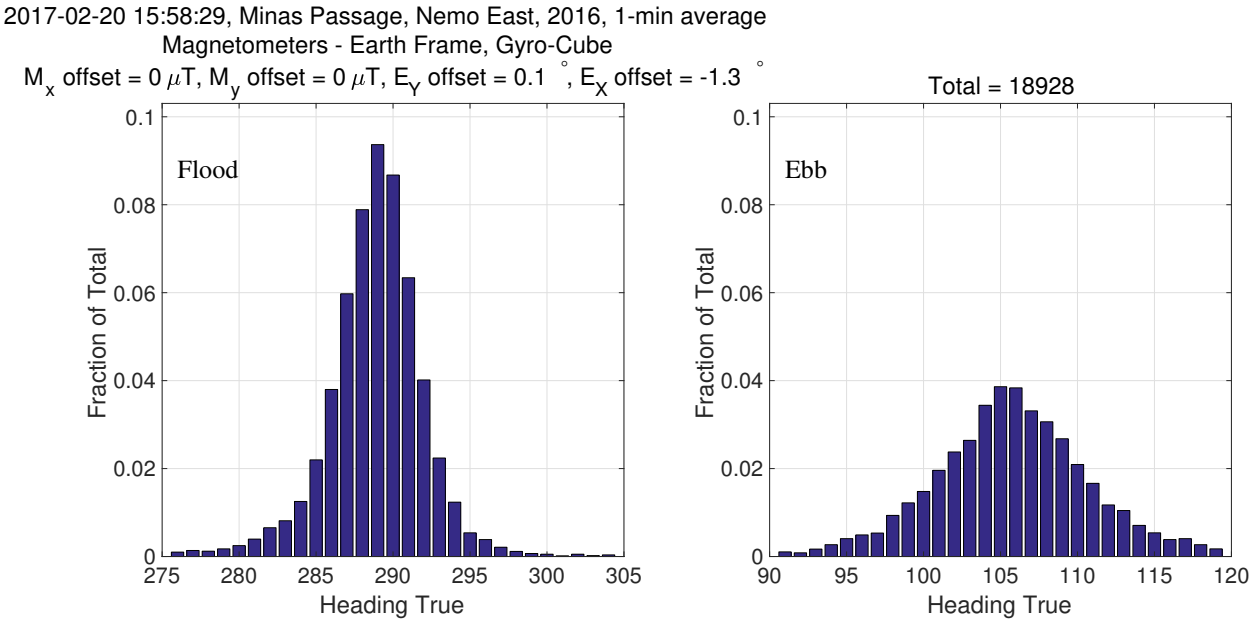

Figure 49: The histogram of heading of Nemo East. More than 90 % of all data are contained by this pair of histograms.

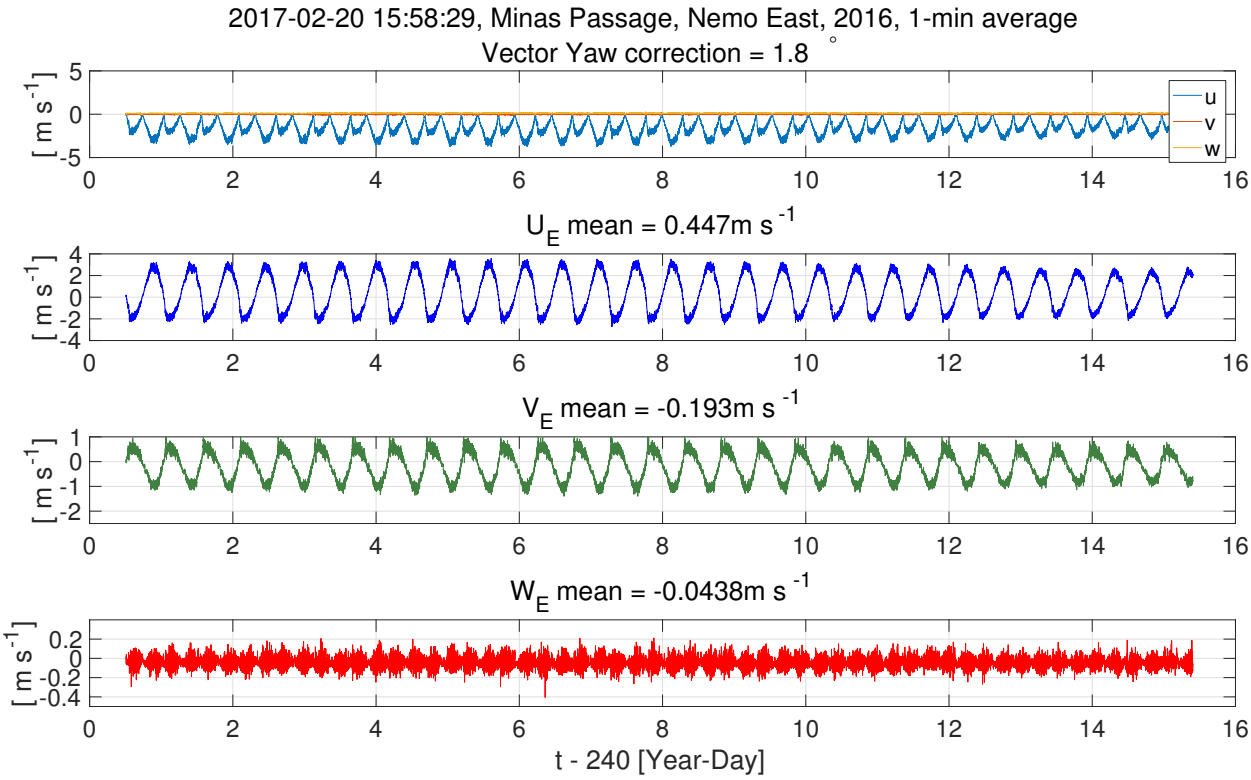

Figure 50: The ADV velocity at Nemo East, recorded internally by the ADV and interpolated on to the time base of the MicroRider data, in the Nemo frame (upper panel). The east component (second from top), north component (second from bottom), and the vertical component (bottom).

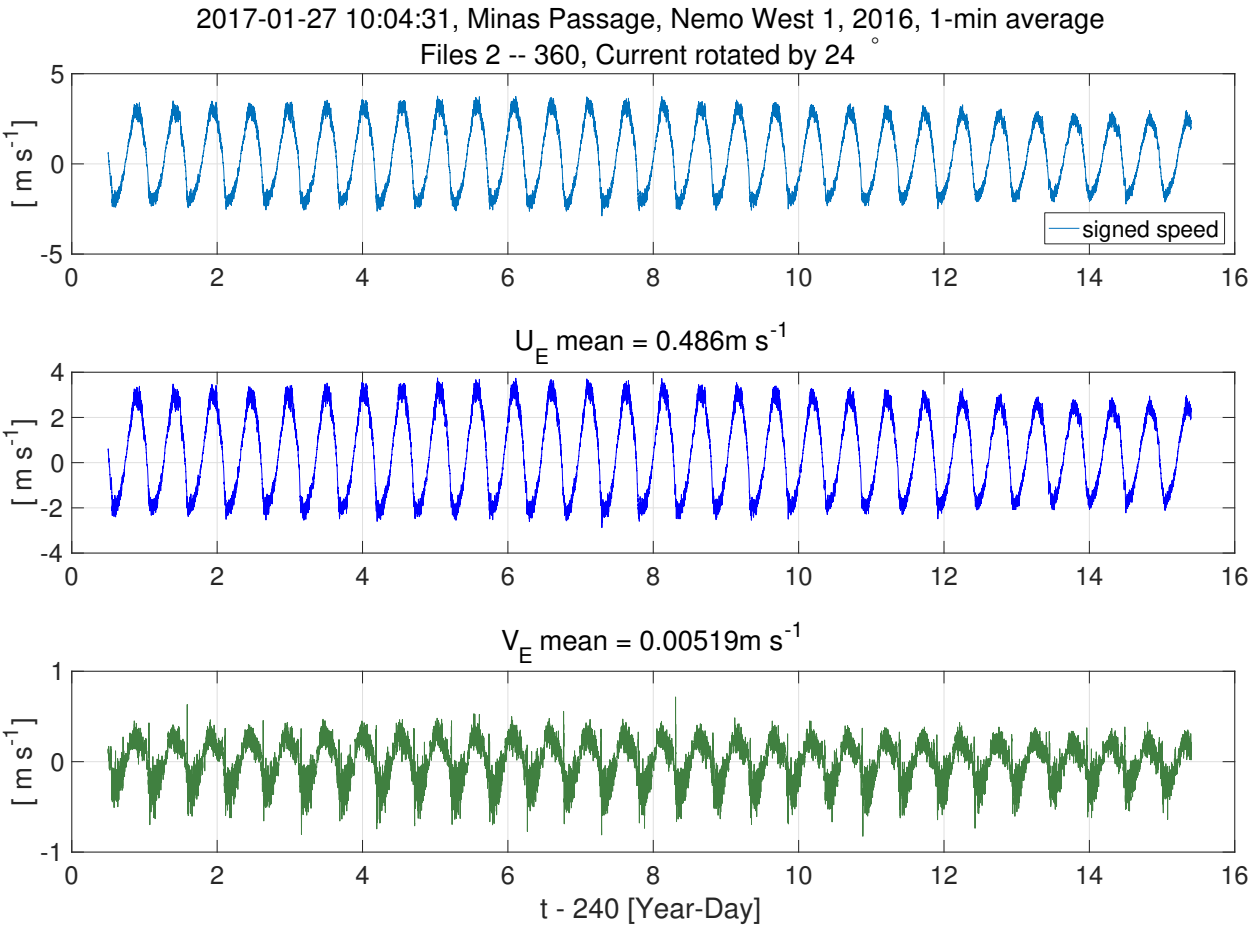

Figure 51: The analog ADV horizontal velocity at Nemo East rotated by 24° to minimize the cross-stream component. Upper panel – speed signed according to flood, with positive to the east and negative to the East. Middle frame – velocity in the direction 24° south of east. Lower panel – the cross-stream component with positive values 24° east of north.

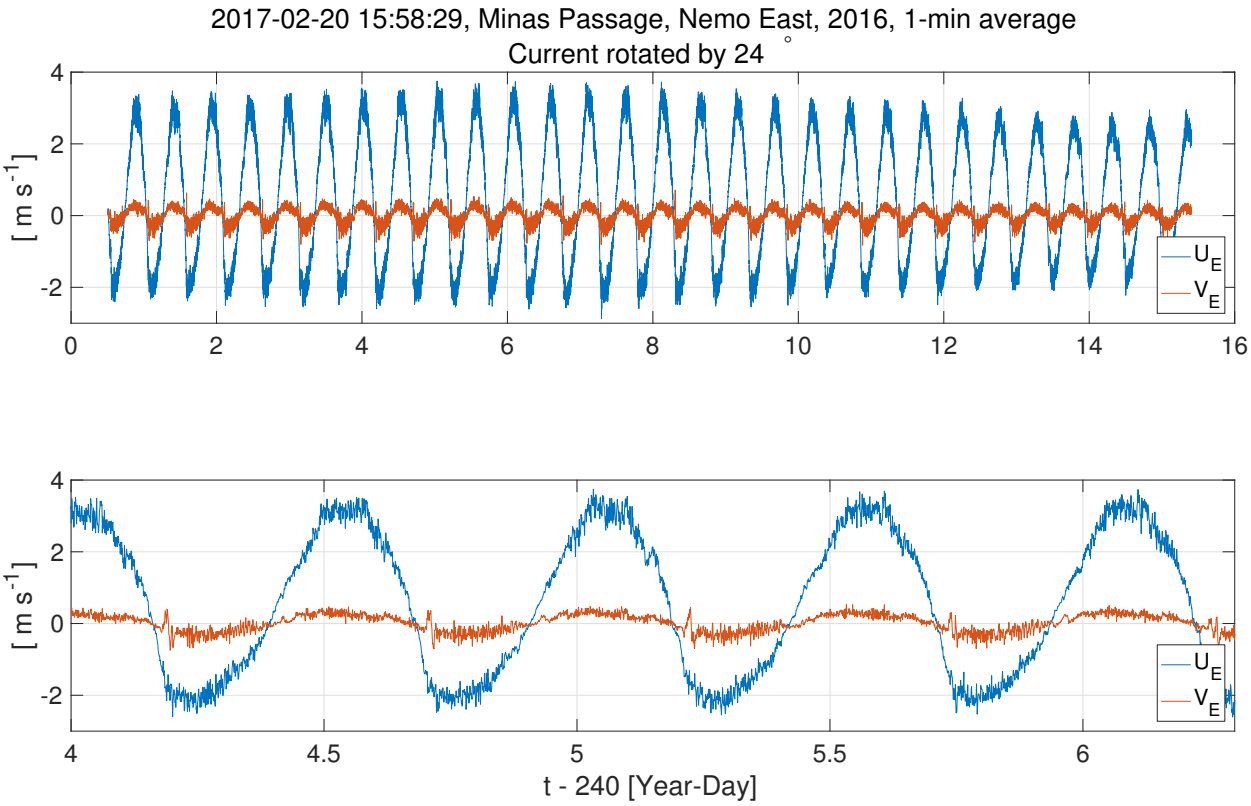

Figure 52: Upper panel – horizontal velocity components rotated 24° counter clockwise. Lower panel – same with zoom in to show the anomalies shortly after the start of each ebb.

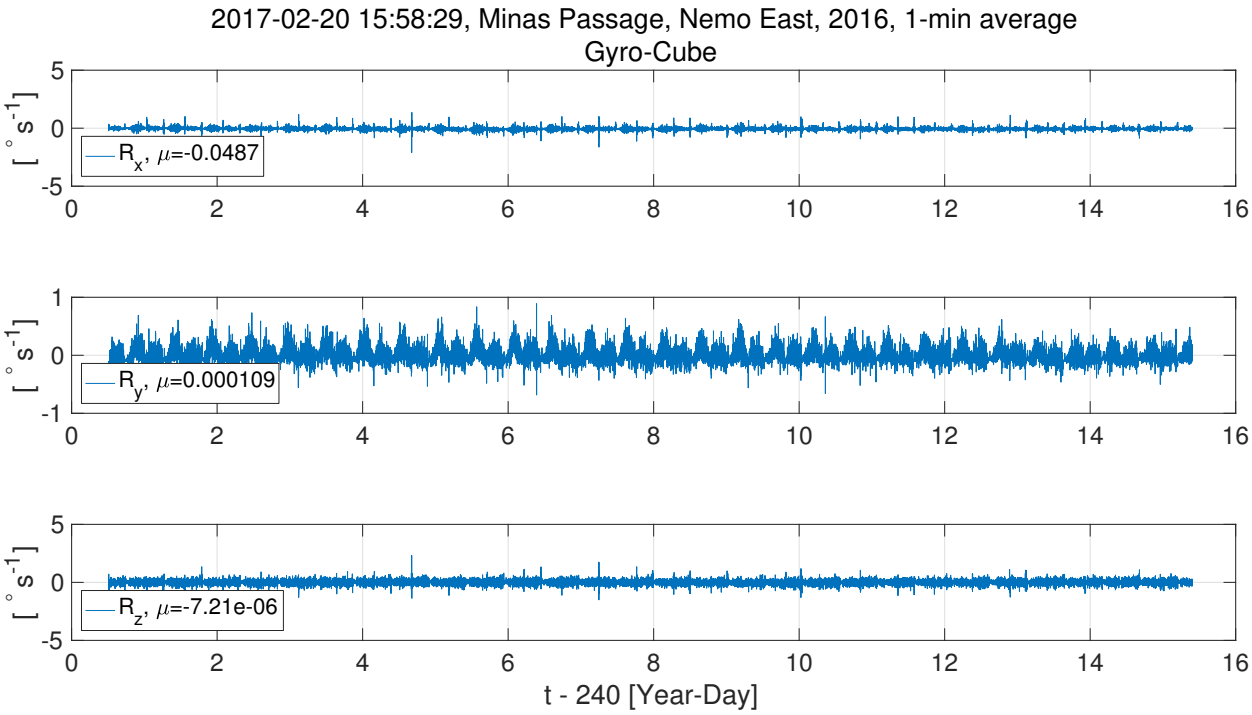

Figure 53: The rates of rotation in the Nemo frame. There is no significant drift in the gyroscope data for the entire deployment. The mean values are indicated in the legends.

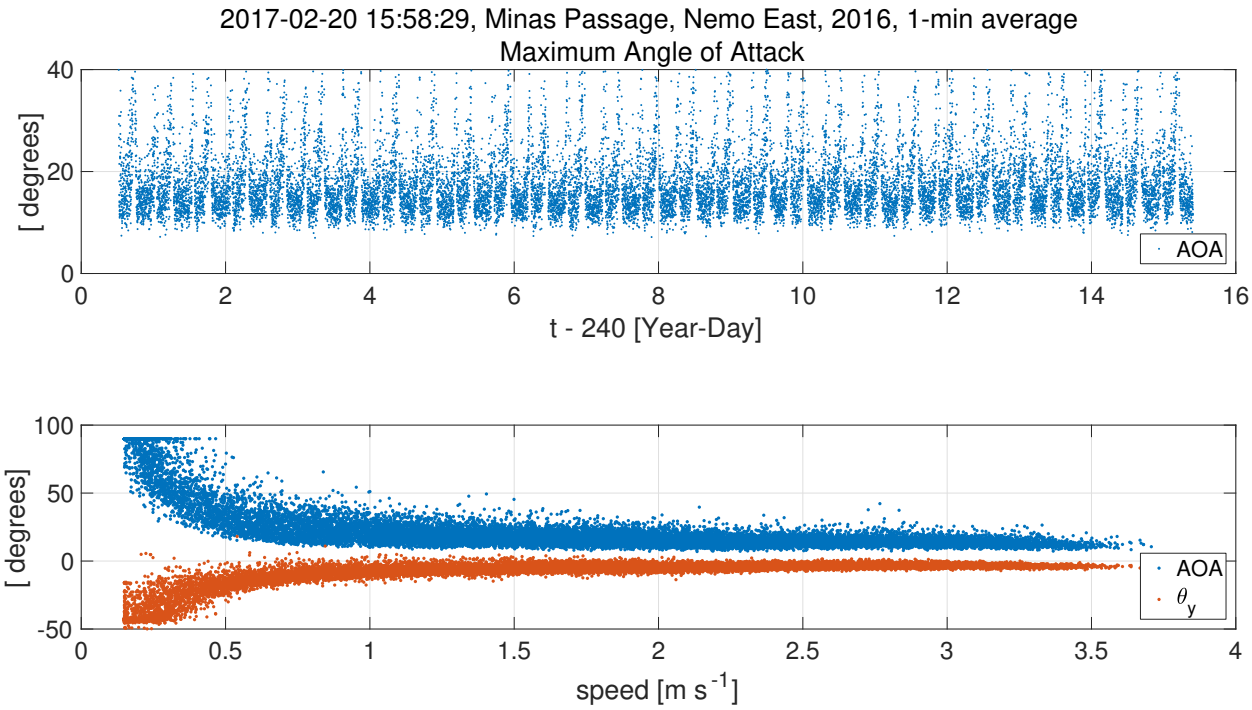

Figure 54: The maximum angle-of-attack for each minute of data (upper panel). The maximum angle-of-attack (blue) and the rotation around the y-axis (red, negative pitch) as a function of speed (lower panel).

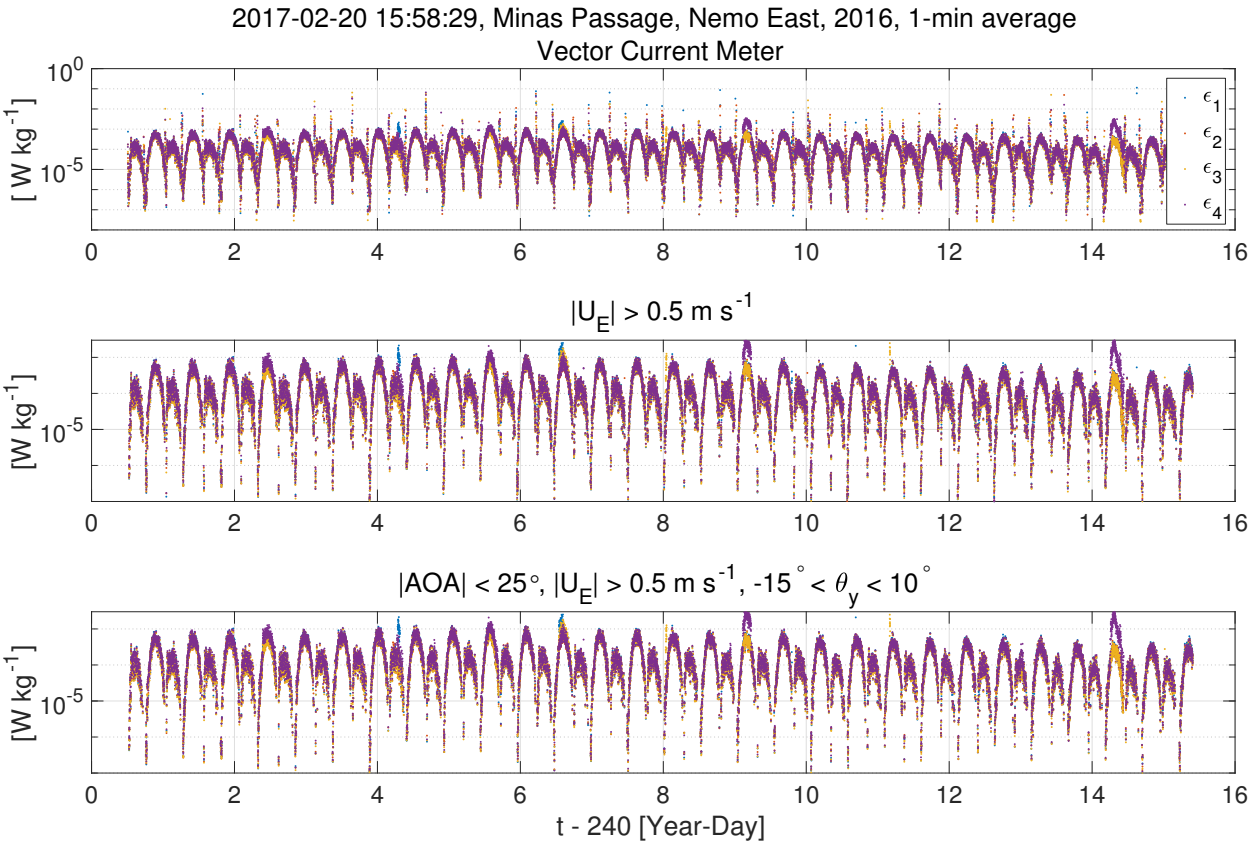

Figure 55: Upper panel – the rate of dissipation of kinetic energy, ϵ, for all four shear probes. Middle panel – Same, but for speeds greater than $0.5\,\mathrm{m\,s^{-1}}$. Lower panel – Same but for speeds greater than $0.5\,\mathrm{m\,s^{-1}}$ and rotations around the y-axis in the range of $-15°$ to $10°$. Anomalously high values are not eliminated by these speed and angle restrictions.

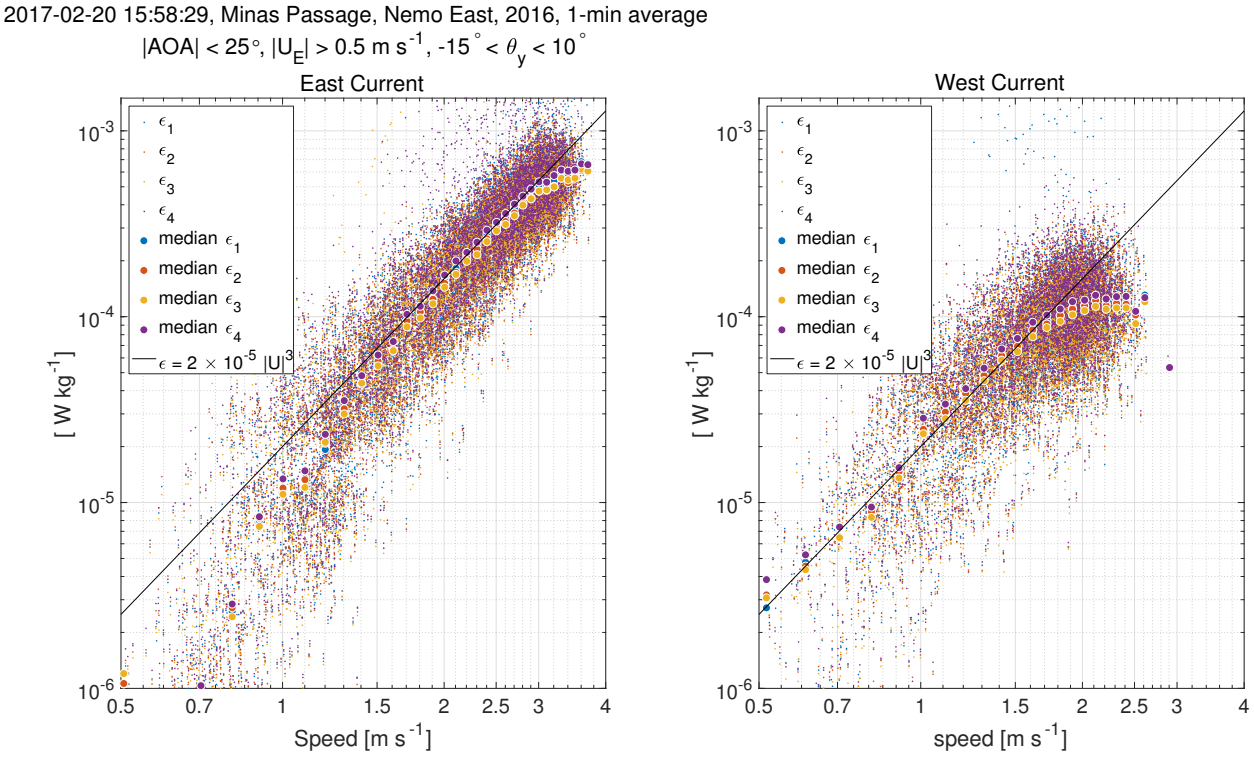

Figure 56: The rate of dissipation of kinetic energy, ϵ, for all four shear probes as a function of speed. Left panel – flood or easterly flow. Right panel – ebb or Easterly flow. The wide dots are the median rates in bins of $0.1\,\mathrm{m\,s^{-1}}$. The black line is an approximate regression with respect to speed cubed.

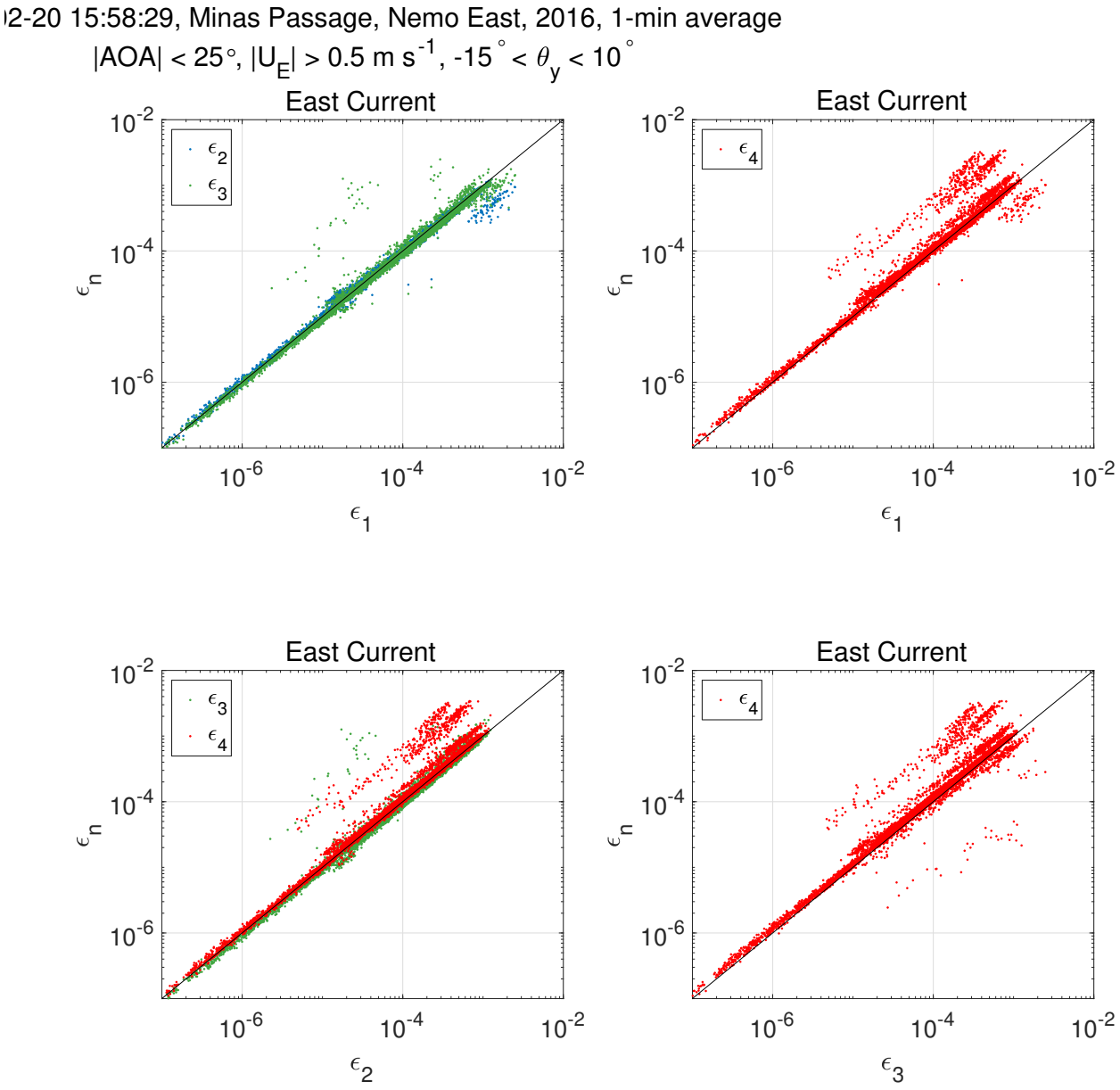

Figure 57: Inter-comparisons of the rates of dissipation of kinetic energy, ϵ, during the floods for all four shear probes. Upper left panel – probes 2 and 3 with respect probe 1. Upper right panel – probe 4 with respect to probe 1. Lower left panel – probes 3 and 4 with respect probe 2. Lower right panel – probe 4 with respect to probe 3.

)2-20 15:58:29, Minas Passage, Nemo East, 2016, 1-min average
, |AOA| < 25°, $|U_E|$ > 0.5 m s^{-1}, -15 ° < θ_y < 10 °

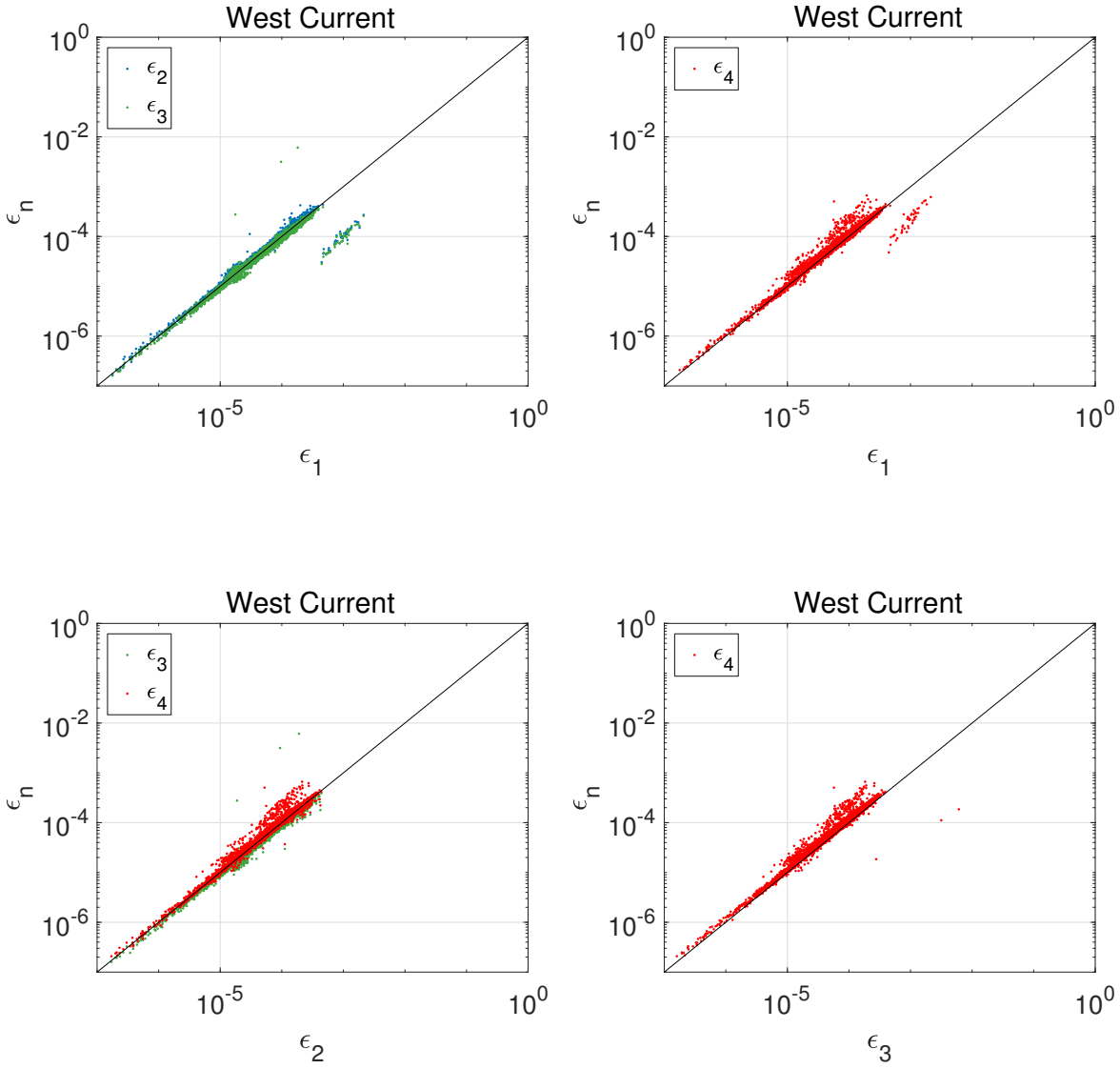

Figure 58: Same as Figure 57 but for the ebbs.

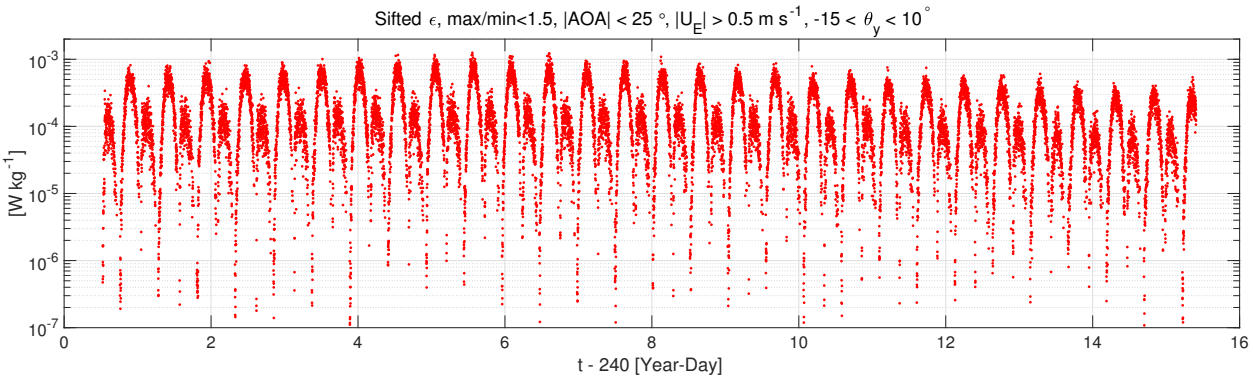

Figure 59: The time series of the sifted rate of dissipation of kinetic energy, ϵ. The values shown are for times when the current speed exceeded $0.5\,\mathrm{m\,s^{-1}}$ and the rotation around the y-axis (negative pitch) was between $-15°$ and $10°$. The sifting process, which is applied to each 1-minute quadruple of ϵ estimates, consists of (i) sorting the four estimates, (ii) eliminating those that are more than 1.5 times larger than the smallest estimate, and (iii) taking the average of the remaining values. This process is intended to eliminate erroneously large estimates.

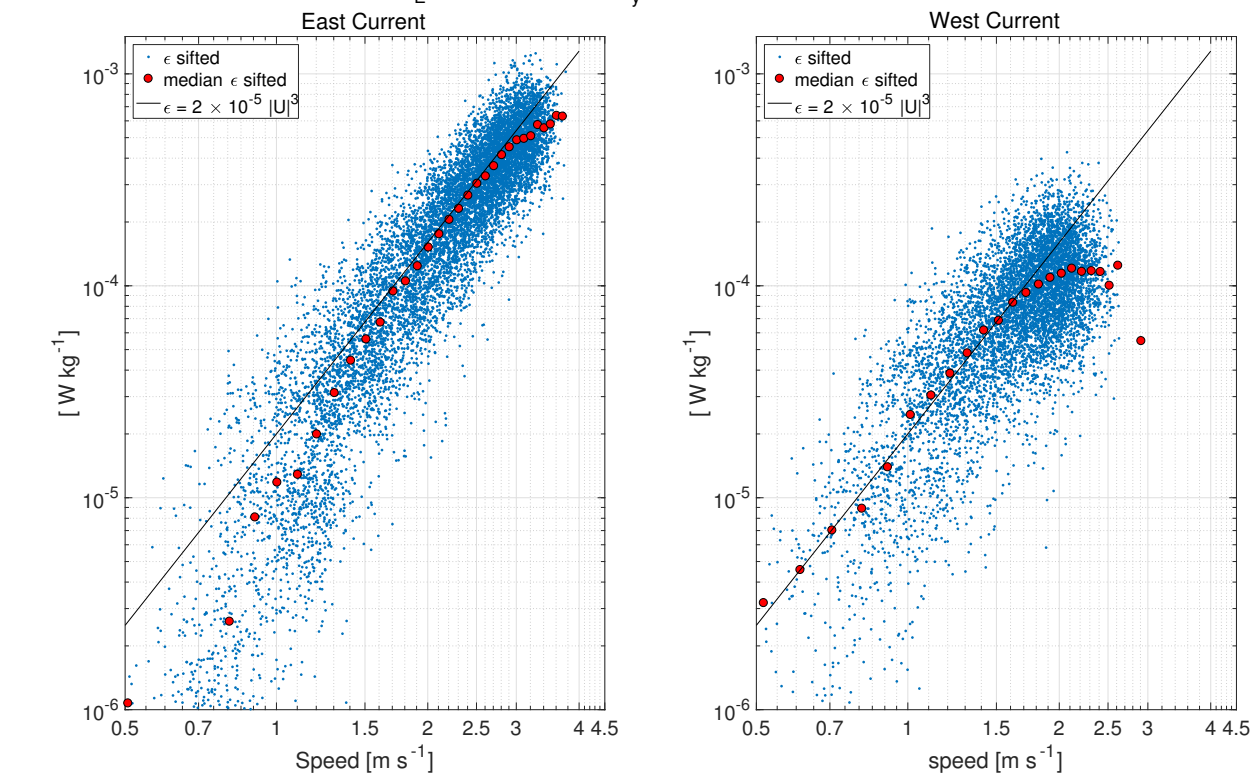

Figure 60: The sifted rate of dissipation of kinetic energy, ϵ, as a function of speed. Left panel – flood or easterly flow. Right panel – ebb or Easterly flow. The red dots are the median rates in bins of $0.1\,\mathrm{m\,s^{-1}}$. The black line is an approximate regression with respect to speed cubed.

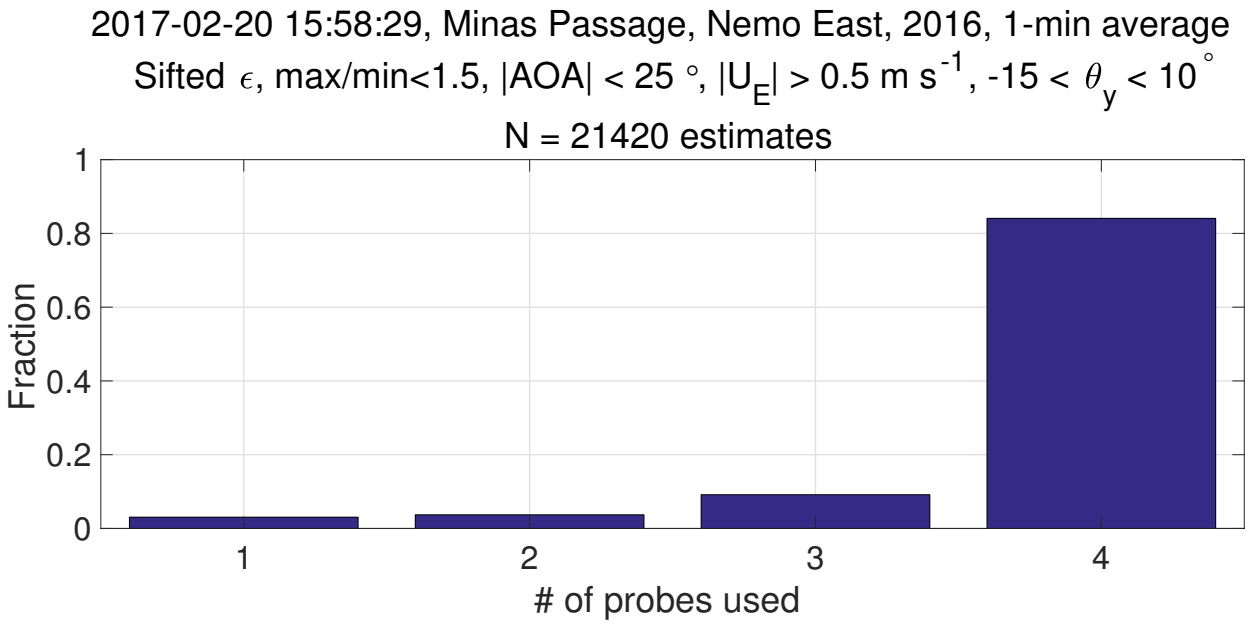

Figure 61: The histogram of the number of probes used in the sifted estimates of the rate of dissipation of kinetic energy, ϵ. More than 90 % of all estimates used 3 or more probes.

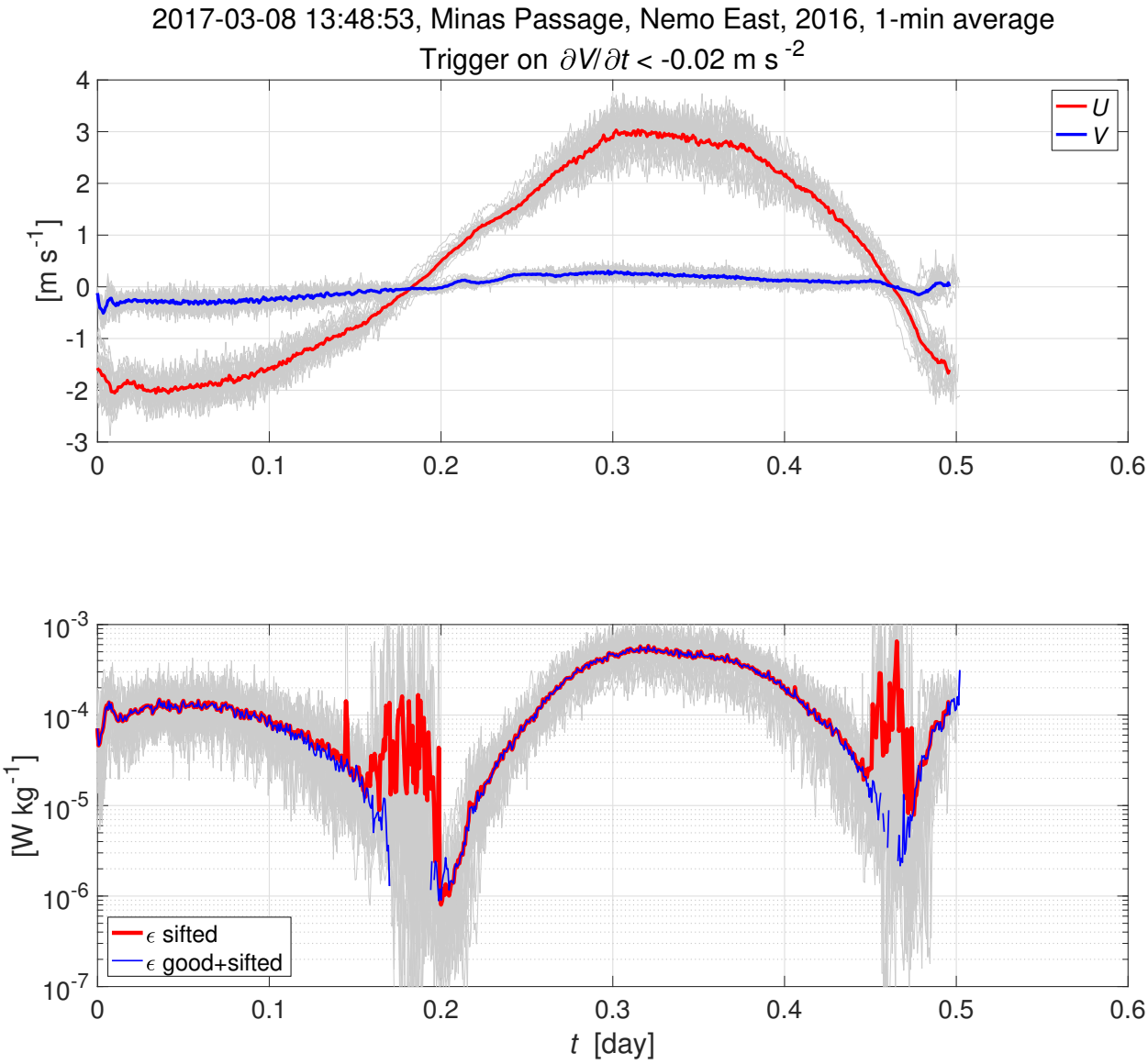

Figure 62: The phase-averaged current (upper panel) and rate of dissipation (lower panel). The trigger point for the phase averaging is $\partial V/\partial t < 0.02\,\mathrm{m\,s^{-2}}$ which occurs shortly after the start of ebb. The trigger point is not exactly synchronous with the M_2 tide. The ϵ good+sifted values (blue line, lower panel) are for times that meet the speed ($>0.5\,\mathrm{m\,s^{-1}}$) and θ_y ($-15°$ to $10°$) restrictions. The ϵ sifted values (blue line, lower panel) are for all times.

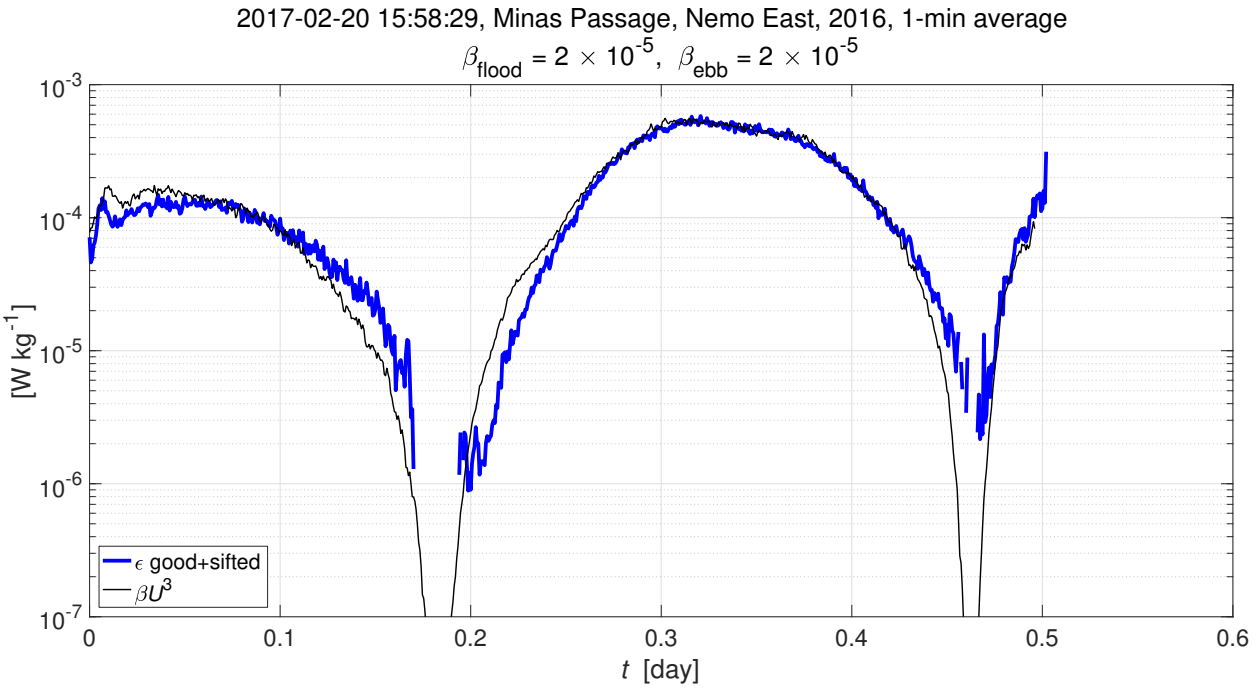

Figure 63: The phase-averaged rate of dissipation (blue) and βU^3 (black). The cubic-speed dependence of ϵ is much tighter compared to Nemo West (Figure 37), and β is three times larger.

End of Document

APPENDIX D – OAS/Octue InSTREAM Final Report

InSTREAM Final Report

An overview of the InSTREAM project outcomes, with especial focus on WP5 - Numerical Analysis

Date January 29, 2018

Author T. H. Clark, PhD, MEng.
Technical Director, Octue Ltd.

Check 1 _____

Check 2 _____

Using:

tg-engine-version:	none
tg-flow-version:	none
tg-clients-version:	none

3 Charles Babbage Road, Cambridge, CB3 0GT, UK

Contents

List of Figures

1 Introduction and Aims

The aim of this report is to provide a summary of the numerical analysis (scaling relations and simulations) undertaken by Octue Ltd (formerly Ocean Array Systems Ltd) as part of the InSTREAM project

3 Charles Babbage Road, Cambridge, CB3 0GT, UK

2 WP5 - Numerical Analysis

2.1 Turbulence characterisation

Turbulence characterisation is predominantly covered in academic conference / journal papers delivered as part of the InSTREAM project [5, 6].

2.1.1 *Selection of metric*

However, it is worth noting the selection of characterisation metric used for the process demonstration here.

The TiME project [4] concluded that lengthscale l and intensity I are generally **not** sufficient to characterise the detailed shape of the load spectrum applied to a turbine. But, it did note their use for early investigations of behaviour and visualisations - and existing literature [1, 2, 8] uses these metrics, so it forms a useful basis of comparison.

For the purpose of demonstrating the process, then, (since the engineering simulations are a proof-of-concept rather than a detailed prediction) the I, l values determined in post-processing were used to create load cases for the scaling investigation.

This is also extremely convenient in our case, since the lengthscale parameter (of course) has units m and thus any scaling adjustment is intuitive to understand.

2.1.2 *Lengthscale at FLOWAVE*

One aspect of post-processing not reported in other parts of InSTREAM project literature is with respect to the lengthscale of turbulence in the FLOWAVE facility. An verification of lengthscale at FLOWAVE was undertaken by Octue (Dalhousie having already computed the same metric for the FORCE site from ADCP data). Octue post-processed velocity data from the Acoustic Doppler Velocimeter (ADV) to verify that the lengthscale was of the expected order ($O(1m)$). As shown in figure **??**, autocorrelation in the flow drops off above $2m$ as expected, since the tank is $2m$ deep, which constrains the turbulent motion.

From this distribution (corrected for baseline noise threshold), the integral lengthscale was calculated at $l = 0.7m$.

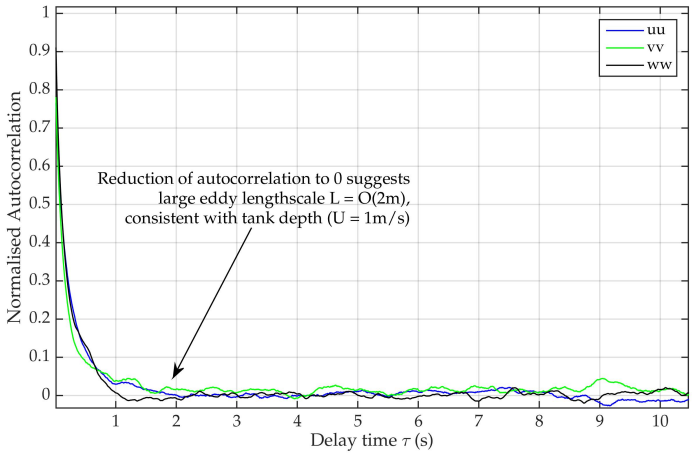

FIGURE 2.1 Autocorrelation of velocity fluctuations varying with time delay τ, showing the largest possible eddy turnover size L is at $O(2m)$, thus initial estimations of integral lengthscale at $l = O(1m)$ were reasonable.

2.2 SCALING

The lengthscale parameter was selected in section 2.1.1 as a turbulent metric to allow us to consistently scale between tank and site.

Whilst it is possible to manipulate the artificially generated turbulent field 2.3.2 to see the effect of different length scales, in providing translation between test tank and field we also have to account for Reynolds Number effects (tank models being much smaller than real turbines).

This is a *considerable obfuscation*, since Reynolds number effects are highly nonlinear - especially affecting the C_l, C_d curves of the aerofoil sections for small models (due to low-Re instabilities). This is way out of scope of the InSTREAM programme, as we wish to isolate turbulent effects.

To overcome this in simulation, rather than scaling the full-size scenario to model scale, we **linearly scale the test tank scenario to match a full scale turbine**.

By doing so, we achieve a simulation in which **all parameters are held constant between the full-scale simulation and the tank simulation**, except turbulent lengthscale and position of the turbine relative to the boundaries.

To do so, we must upscale the tank turbulence. It was theorised that the critical nondimensional number would be ratio of turbine diameter to turbulent lengthscale, since the TiME project [4] found that the dominant effect of chang-

3 Charles Babbage Road, Cambridge, CB3 0GT, UK

ing turbulent lengthscale related to wake structure (and therefore turbine induction).

The following relation was suggested in [5]:

$$\frac{l_{model}}{R_{model}} = \frac{l_{site}}{R_{site}}, \tag{2.1}$$

where l represents integral length scale, R represents tip radius, subscript *model* represents a tank environment and model scale turbine, subscript *site* represents a real environment and full scale turbine. We therefore calculate these metrics for the sites and tanks as well as representative turbine installations.

The scaling used to generate our example load cases is shown in table 2.2.

Scales (m)	FLOWAVE	FORCE	FLOWAVE (SCALED)
Water depth D	2	55	16
Profile height $Z\_\{ref\}$	1	27.5	8
Turbine hub height h	1	27.5	8
Turbine tip radius R_{tip}	0.25	2	2
Turbulent Lengthscale l	0.7	19.3	5.6

TABLE 2.1 Scaling parameters used to adjust a typical experimental setup at FLOWAVE to a configuration with consistent boundary placing and turbulent lengthscale, but a turbine size equivalent to the full scale case

2.3 SIMULATION

2.3.1 *Turbines*

The Schottel Hydro turbine model, pictured in figure 2.2 and expected to be installed as part of a commercial development at the Black Rock site in FORCE, was used as the base turbine:

- Turbine geometry previously supplied to Octue by Schottel was used to build a representative model.
- No blade deflection was accounted for, to reduce computational costs in this proof-of-concept study. However, such behaviour can be trivially incorporated by switch of a control parameter if necessary.
- No platform motion was accounted for, as no details of platform dynamics were available.
- Blade section shapes were pre-computed into C_l, C_d curves by Octue, using a proprietary process that accounts not only for Reynolds Number

3 Charles Babbage Road, Cambridge, CB3 0GT, UK

FIGURE 2.2 Schottel Hydro turbine, used as the base device for the simulations.

Re and Angle-of-attack α, but also the local turbulent intensity I, which affects stall behaviour of aerofoils.

2.3.2 *Turbulent Field Generation*

The artificial turbulent fields used for simulation were generated using the Mann method [7], consistent with the approach used in the TiME project [3]. Like the TiME project, these fields were generated spatially, covering the domain of the simulation, then advected through the domain throughout 10 minute load cases following the mean velocity.

These fields were computed directly from the integral lengthscales determined from measurement with the NEMO platform at FORCE and the microstructure profiler placed in Flowave, providing a completely integrated process for the InSTREAM methodology.

3 Charles Babbage Road, Cambridge, CB3 0GT, UK

2.3.3 *Mean velocity shear*

A logarithmic velocity profile was used for the example simulations, based on an average of a 10-minute window from the FORCE ADCP data, at which the average velocity at the reference height was $1.2m/s$ used as reference for all cases to keep as many variables consistent as possible.

The velocity profile was set with a linearly scaled reference height, which slightly alters the relative shapes of the profile. To avoid bias, the power-weighted, area-averaged mass flux through the turbine disc in the FORCE load case is chosen to match the power-weighted, area-averaged mass flux through the disc in the FLOWAVE case. This ensures that the only effect on power coefficient must be from turbulent effects, not shear.

2.4 Results

Results are captured as videos, displayed he video depicts two different simulations shown together. In each, the wake helix of the turbine is shown as it evolves over time from the simulation start.

2.4.1 *Simulation 1*

See https://vimeo.com/253207151

In the upper part of the video, evolution of the turbine wake is shown in the conditions found at the FORCE eastern site.

A smooth floor and level sea surface (i.e. no waves, and neglecting large scale bathymetric effects) is chosen, both for simplicity and to provide best comparison with the Flowave simulation.

In the results, we clearly see a dramatic difference in wake evolution, power coefficient Cp and thrust coefficient Ct (figure 2.3) between the Flowave and FORCE sites, with all variables other than turbulent effects held constant.

- Turbulent Kinetic Energy at the FORCE site exists at much longer length-scales than the turbine diameter. This leads to a significant off-axis meandering of the wake, having considerable impact on any downstream turbines placed in an array arrangement.
- At the Flowave site, Turbulent Kinetic Energy is concentrated at length-scales of a similar order to the turbine diameter. This leads to rapid breakdown in the wake of the turbine in the bottom of the video, (decreasing the turbine blockage, due to a reduced self-induction) and much less meandering in the wake.

3 Charles Babbage Road, Cambridge, CB3 0GT, UK

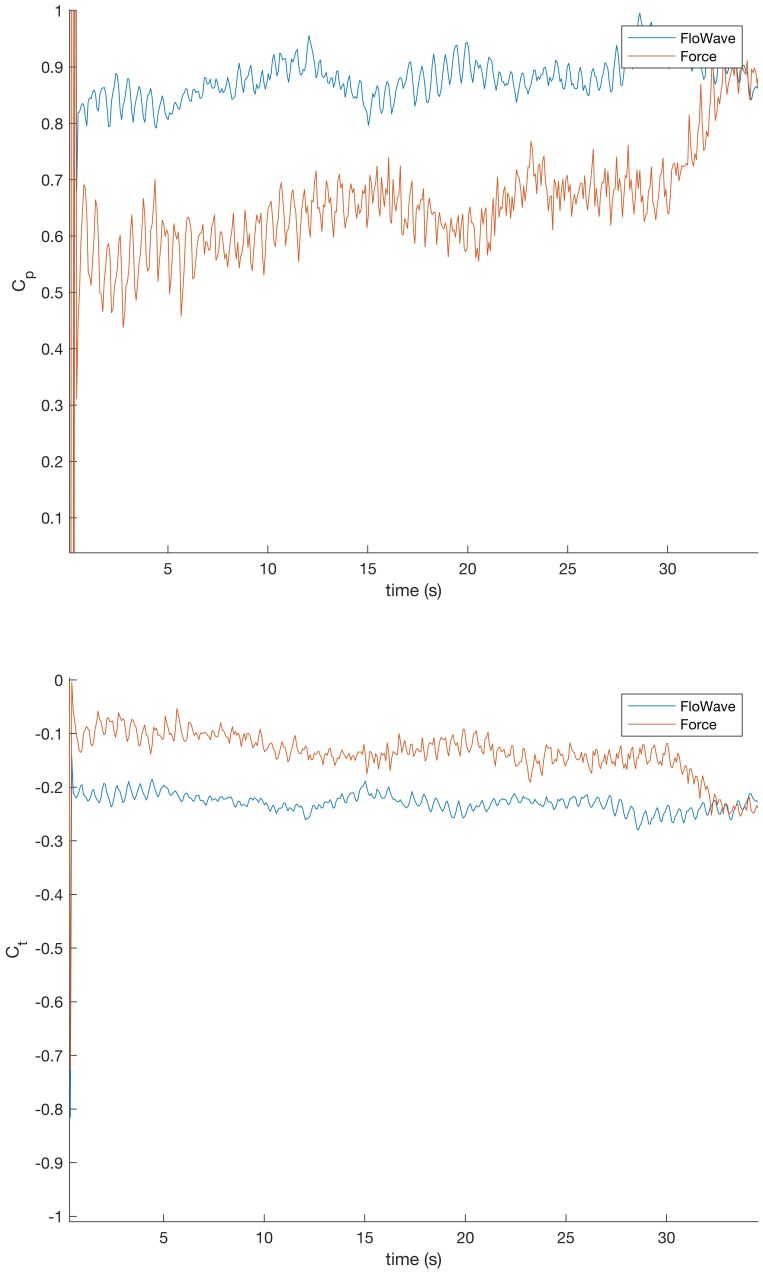

FIGURE 2.3 Significant discrepancy in Power coefficient C_p (top) and thrust coefficient C_t (bottom) resulting from turbulent lengthscales representative of FLOWAVE and FORCE, all other variables held constant.

3 Charles Babbage Road, Cambridge, CB3 0GT, UK

2.4.2 *Simulation 2*

See https://vimeo.com/253204915

In this simulation, additional turbines were spaced at intervals of 8 turbine diameters in the streamwise direction, offset by two turbine diameters in the cross-stream direction. Parameters were otherwise identical to Simulation 1 above.

Clearly, the different wake cone caused by the change in turbulent lengthscale has a large impact on downstream turbines, leading us tentatively to the following advice:

> Experiments with arrays in Flowave may not replicate wake interaction effects, where a meandering wake from an upstream turbine intermittently impinges on downstream turbines. This is critical both for fatigue-load design and ultimate power performance of arrays.

3 Charles Babbage Road, Cambridge, CB3 0GT, UK

3 Data Processing Platform

A related project which ran during the course of the InSTREAM work (the UK's Global Co-Operation fund) partially funded the development of a data analytics platform by Octue, allowing for quick and easy generation of analysis 'apps' in the cloud, from existing engineering analysis codes. Screenshots are shown in figures 3.1 and 3.2.

The InSTREAM programme was chosen as a showcase for the platform, which is approaching an open Beta version at the time of writing. Within InSTREAM, the platform was used to manage the diverse range of data sources, and to host execution of the numerical analyses discussed in the previous chapter.

This provided a mutual benefit to both projects - particularly since the platform provides a route to exploitation of the analysis tools (such as RSI's Ocean Data Acquisition System, ODASlib) refined during InSTREAM.

InSTREAM project partners will be invited as collaborators on the platform once it is general release - serving as a permanent repository of the heavyweight datasets and associated metadata generated during the project.

3 Charles Babbage Road, Cambridge, CB3 0GT, UK

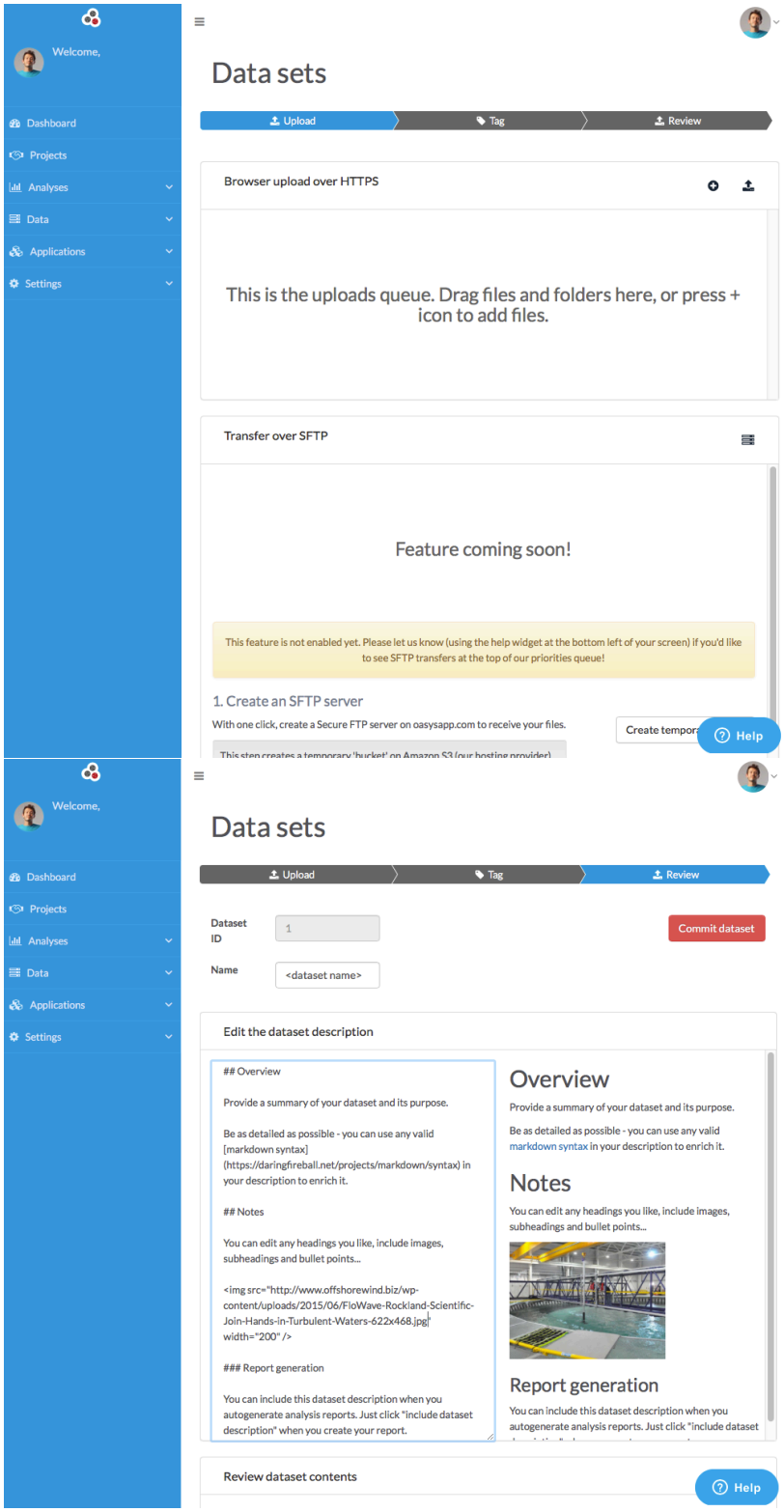

FIGURE 3.1 Screenshots from the data processing platform. Top: file uploader, Bottom: dataset creation tool

3 Charles Babbage Road, Cambridge, CB3 0GT, UK

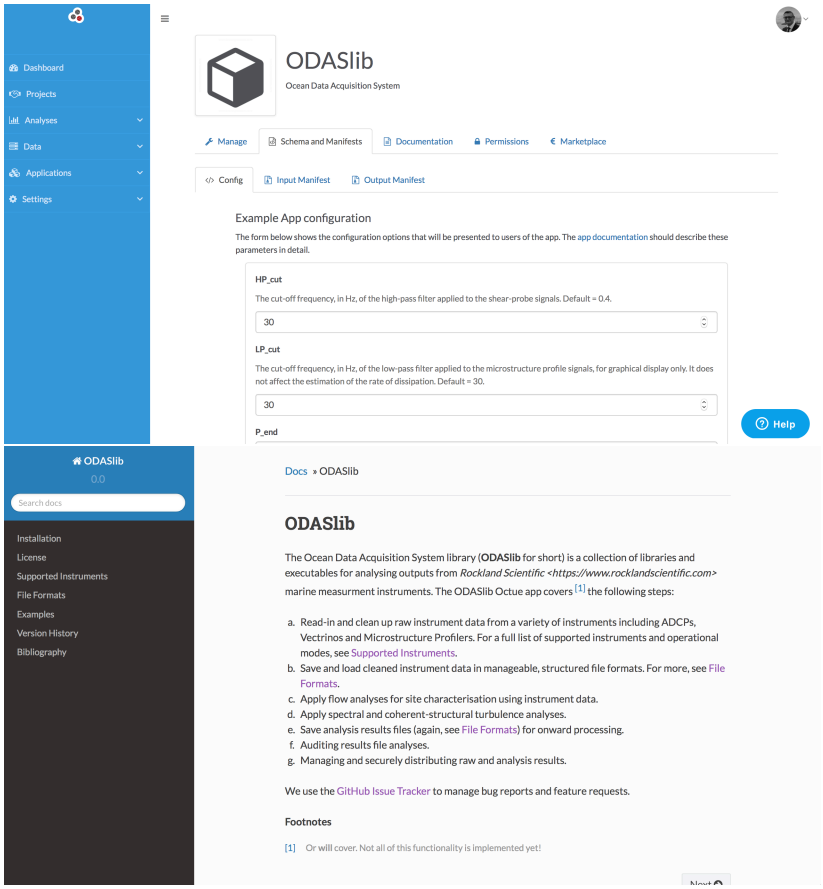

FIGURE 3.2 Screenshots from the data processing platform. Top: Ocean Data Acquisition System app configuration, auto-generated from the data schema specification used in the InSTREAM programme, Bottom: app documentation, auto-generated from same.

3 Charles Babbage Road, Cambridge, CB3 0GT, UK

4 Key Outcomes

4.1 Commercial Outcomes

The global market for tidal power is not experiencing the surge expected at the beginning of the InSTREAM programme. However, whilst market traction of tidal power has been disappointing, installations are still being planned and built out in multiple countries globally. From Octue's perspective, the key commercial outcomes of the InSTREAM project include:

- A process has been developed which extended the TiME methodology to demonstrate it at test sites and in an experimental facility - this process is is now tested and saleable, ready for the tidal market to develop.
- Project partners gained deep experience working at to design experimental / test programmes, and fostered pre-existing collaborative relationships leading to further projects.
- InSTREAM mutually benefited another project to develop a platform for cloud data processing, which will provide RSI with a route to exploit their processing codes as a cloud software service.

4.2 Technical Outcomes

The numerical analyses discussed above formed the final steps in the technical arc of the InSTREAM programme, which demonstrated a complete, joined-up process for characterising turbulence in-tank, at-site, and running simulations allowing translation between them.

With respect to the original project aims:

- Data sets from all three environments (FLOWAVE, FORCE and EMEC) have been secured[1].
- Instrument settings were successfully specified to provide a consistent view of the flow between the different sites, i.e. *data sets are comparable between sites*.
- Hypotheses that the nature of turbulence would vary significantly between tank and site were confirmed.

[1] Although data from the EMEC site was somewhat limited in time period due to technical difficulties with the pod

3 Charles Babbage Road, Cambridge, CB3 0GT, UK

- Data from tank and site was post-processed successfully [5, 6], to characterise turbulence using the TIME methodology. This allows data to be used in engineering simulation software.
- A scaling method was developed (see section 2.2), allowing direct comparison / translation between tank and site.
- Engineering simulations were run as a proof-of-concept, highlighting important differences between tank and site turbulence, especially **considerable differences in power production and fatigue loading** from the different turbulent conditions.

Additional to the original project goals, the consortium:

- Showcased these differences by animation of the engineering simulation results. See comparisons of turbine wake behaviour at `https://vimeo.com/253204915` and `https://vimeo.com/253207151`.
- Secured additional 'nice-to-have' datasets from the FLOWAVE tests, allowing future parametric investigations of wave-turbulence interaction.

One original project aim was a comparison of turbulent spectrum between the two tidal sites. Unfortunately data from EMEC arrived too late in the programme (due to inclement weather) to be investigated fully. However, the primary goal of providing a full process for characterisation and simulation, with a translation tool between tank and site, was nevertheless achieved.

That process consisted of the following steps[2]:

1. Planned multi-instrument test campaigns for measurement and characterisation of two tidal sites and a test tank
2. Executed said campaigns.
3. Post-processed measurements from ADCPs and shear probes.
4. Simulated both a single turbine and a small array, each in two conditions derived from the post-processed measurements: one representative of the FORCE site and one representative of FLOWAVE, highlighting the key differences between the two (see section 2.3).

[2] see final project reports from RSI and FLOWAVE for details of steps 1-4.

3 Charles Babbage Road, Cambridge, CB3 0GT, UK

Key take-away: Scaling

The ratio of integral lengthscale to turbine diameter is critical, as this ratio dominates the wake structure (therefore power performance and unsteady loading).

Engineering simulations attempting to scale results between tank and test should take account of this scaling, keeping the following nondimensional ratio constant where possible:

$$\frac{l_{environment}}{R_{turbine}}, \tag{4.1}$$

3 Charles Babbage Road, Cambridge, CB3 0GT, UK

References

[1] T. Blackmore, W. M. J. Batten, G. U. Muller, and A. S. Bahaj. Influence of turbulence on the drag of solid discs and turbine simulators in a water current. *Experiments in Fluids*, 55(1):1637, dec 2014. ISSN 07234864. doi: 10.1007/s00348-013-1637-9. URL http://link.springer.com/10.1007/s00348-013-1637-9. 2

[2] T. Blackmore, B. Gaurier, L. Myers, G. Gernmain, and A. S. Bahaj. The Effect of Freestream Tubulence on Tidal Turbines. In *Proceedings of the 11th European Wave and Tidal Energy Conference*, Nantes, France, 2015. 2

[3] T. H. Clark. Turbulence in Marine Environments (TiME): A framework for understanding turbulence and its effects on tidal devices. In *Proceedings of the 11th European Wave and Tidal Energy Conference*, Nantes, France, 2015. 5

[4] T. H. Clark, T. Roc, S. Fisher, and N. Minns. MRCF-TiME-KS10 Turbulence and turbulent effects in turbine and array engineering. A guide for the tidal power industry. Technical report, 2015. 2, 3

[5] T. H. E. Clark, R. G. Lueck, A. E. Hay, T. Davey, P. Stern, R. Horwitz, and N. Pearson. InSTREAM : Measurement , Characterisation and Simulation of Turbulence from Test Tank to Ocean . *Proc. of the 12th European Wave and Tidal Energy Conference*, page 7, 2017. 2, 4, 13

[6] R. M. Horwitz and A. E. Hay. Turbulence dissipation rates from horizontal velocity profiles at mid-depth in fast tidal flows. *Renewable Energy*, 2017. ISSN 0960-1481. doi: http://doi.org/10.1016/j.renene.2017.03.062. URL http://www.sciencedirect.com/science/article/pii/S0960148117302483. 2, 13

[7] J. Mann. Wind field simulation. *Probabilistic Engineering Mechanics*, 13(4): 269–282, oct 1998. 5

[8] K. Shah, T. Blackmore, L. Blunden, L. Myers, and A. Bahaj. From Lab to Field: Deployment of a Scale Turbine in a Tidal Estuary. In *Proceedings of the 11th European Wave and Tidal Energy Conference*, Nantes, France, 2015. 2

3 Charles Babbage Road, Cambridge, CB3 0GT, UK

APPENDIX E – Financial Summary

INSTREAM Project

Financial Accounting for full project from 01-SEP-2015 to 30-JAN-2018

COMBINED CANADIAN PROJECT		Actual Cost Incurred for Reporting Period					Total Acutual	Suplus (Deficit)
	Work Package:	WP1, WP2	WP2, WP3	WP4, WP5	WP5	WP6		
Eligible Cost	**Budgeted Amount**	**31. Oct'15 - 31. Mar'16**	**1. Apr - 1. Aug 2016**	**1. Sept'16 - 1. Feb'17**	**1. Mar - 1. Aug 2017**	**1. Sep'17 - 1. Feb'18**		
Labour	$ 205,000	$ 21,410	$ 59,588	$ 56,335	$ 50,896	$ 17,308	$ 205,537	$ (537)
Equipment	$ 25,000	$ -	$ 24,000	$ -	$ (6,753)	$ 2,139	$ 19,387	$ 5,613
Materials and Supplies	$ 181,500	$ 7,643	$ 142,770	$ 12,903	$ -	$ 25,900	$ 189,216	$ (7,716)
Travel	$ 45,400	$ 7,241	$ 14,529	$ 23,296	$ 2,882	$ -	$ 47,947	$ (2,547)
Other	$ 111,100	$ 1,418	$ 6,381	$ 35,604	$ 609	$ 8,000	$ 52,012	$ 59,088
TOTAL	**$ 568,000**	**$ 37,712**	**$ 247,267**	**$ 128,138**	**$ 47,635**	**$ 53,347**	**$ 514,099**	**$ 53,901**

Subject to revision to actuals, as of final claims.